Rockefeller University
Digital Commons @ RU

Student Theses and Dissertations

2008

Cracking the Odor Code: Molecular and Cellular Deconstruction of the Olfactory Circuit of Drosophila Larvae

Kenta Asahina

Follow this and additional works at: http://digitalcommons.rockefeller.edu/student_theses_and_dissertations

 Part of the Life Sciences Commons

Recommended Citation
Asahina, Kenta, "Cracking the Odor Code: Molecular and Cellular Deconstruction of the Olfactory Circuit of Drosophila Larvae" (2008). *Student Theses and Dissertations.* Paper 196.

This Thesis is brought to you for free and open access by Digital Commons @ RU. It has been accepted for inclusion in Student Theses and Dissertations by an authorized administrator of Digital Commons @ RU. For more information, please contact mcsweej@mail.rockefeller.edu.

Cracking the Odor Code: Molecular and Cellular Deconstruction of the Olfactory Circuit of *Drosophila* Larvae

A Thesis Presented to the Faculty of

The Rockefeller University

in Partial Fulfillment of the Requirements for

the degree of Doctor of Philosophy

By

Kenta Asahina

June 2008

© Copyright by Kenta Asahina 2008

CRACKING THE ODOR CODE: MOLECULAR AND CELLULAR DECONSTRUCTION OF THE OLFACTORY CIRCUIT OF *DROSOPHILA* LARVAE

Kenta Asahina, Ph.D.

The Rockefeller University 2008

The *Drosophila* larva offers a powerful model system to investigate the general principles by which the olfactory system processes behaviorally relevant sensory stimuli. The numerically reduced larval olfactory system relieves the formidable molecular and cellular complexity found in other organisms. This thesis presents a study in four parts that investigates molecular and neuronal mechanisms of larval odor coding.

First, the larval odorant receptor (OR) repertoire was characterized. ORs define the olfactory receptive range of an animal. Each of the 21 larval olfactory sensory neurons (OSNs) expresses one or rarely two ORs, along with the highly conserved olfactory co-receptor *Or83b*. Second, odor response profiles of 11 larval OSNs were characterized by calcium imaging. A subset of larval neurons showed overlapping responses to the set of odorants tested, while other neurons showed either very narrow or very broad tuning. Third, the olfactory circuit for ethyl butyrate was investigated in detail. Three OSNs, expressing *Or35a*, *Or42a* and *Or42b*, responded with different sensitivity to ethyl butyrate. Second order projection neurons synapsing with each of these OSNs showed similar

concentration tuning, but inhibitory interneurons showed high response thresholds and were only activated at high odor concentrations. We correlated these concentration-dependent response properties with larval chemotaxis behavior. Fourth, the relevance of olfaction to animals was investigated in competitive rearing experiments. *Or83b* mutants experienced a selective disadvantage when they had to forage for limiting food sources, particularly when competing against larvae with normal olfactory function.

Thus, odor coding is achieved both by peripheral tuning and central circuit modulation.

Acknowledgements

No word of gratitude will suffice to express how much I appreciate the mentorship and support of Dr. Leslie Vosshall. Not only is she unafraid of taking risks, as eloquently demonstrated by accepting me as a rotating student on summer 2002 despite my little knowledge of fly genetics and imperfect English speech, but also does she encompass outstanding intelligence and dedication to science. She has taught me what science is: that is the greatest education I have ever had.

I thank no less to all the past and present Vosshall laboratory affiliates. In particular, I would appreciate technical and moral support from Dr. Silke Sachse and Dr. Mathias Ditzen. Without their expertise on calcium imaging and data processing, my project would not have existed. Matthieu Loius has been an invaluable collaborator throughout the exploration of larval olfaction. His contribution, scientific and otherwise, was much greater than providing behavioral data to bring our project to completion. I am unable to name and thank all the other individuals who provided stimulating discussion and camaraderie, but it does not diminish my gratefulness toward them by any means.

Outside of the Vosshall laboratory, Dr. C. Giovanni Galizia at the University of Konstanz, Germany, deserves my utmost recognition and respect. While at the University of California, Riverside, he provided me with crucial technical training in calcium imaging. His generous help truly opened up my scientific endeavor.

I am also grateful to have opportunities to mentor several young scientists – Ifije Ohiorhenuan (MD-PhD rotating student) Konstantin Fishilevich (summer

technician), Liza Tevelev (outreach student) and Emilie Russler (SURF student). Above all, however, I would like to especially thank Viktoryia Pavlenkovich (Bard BRSS student) for her sincere attitude toward science as well as her excellent technical help. She has been a true source of inspiration to me, and I am grateful to the Bard/Rockefeller joint outreach program.

My thesis committee member has always been encouraging and supportive of my sometimes difficult project. I deeply thank Drs. A. James Hudspeth (chair) and Shai Shaham for their insightful comments, penetrating criticism, and informative discussion during our annual meetings. I am equally to Dr. Larry Abbott, my external examiner, for kindly taking time out of his busy schedule to share his expertise to finalize this work.

It has been an honor for me to be in The David Rockefeller Graduate Program for as long as 5 years and a half. I am grateful to supports from our Dean, Dr. Sidney Strickland, and members of the Dean's Office, namely Ms. Kristen Cullen and Ms. Marta Delgado.

Lastly, I have been – and will be – always appreciating love and support of my family back in my home country. Ties with my parents and two brothers have been strengthened despite the distance of more than 10,000 km over the last 5 years while I have been away. I hope that the completion of this work will raise the spirits of my father, who is scheduled to undergo surgery at about the time I defend my thesis.

Table of Contents

List of Figures

Abbreviations

AEL – after egg-laying

AL – antennal lobe

AMPA – alpha-amino-3-hydroxy-5-methylisoxazole-4-propionic acid

AOB – accessory olfactory bulb

cVA – 11-*cis*-vaccenyl acetate

GABA – gamma-aminobutyric acid

GFP – green fluorescent protein

GR – gustatory receptor

LAL – larval antennal lobe

LN – local interneuron

MB – mushroom body

M/T – mitral/tufted

NMDA – *N*-methyl-D-asparate

OR – odorant receptor

OSN – olfactory sensory neuron

PCR – polymerase chain reaction

PN – projection neuron

RASSL - receptor activated solely by a synthetic ligand

S.E.M. – standard error of the mean

TAAR – trace amine-associated receptor

TRP – transient receptor potential

Introduction: Organization and function of the sensory systems

What we assume to be the chemical or physical properties of objects – smell, taste, texture, temperature, color, or motion – are actually our interpretation of the objects. “Blue” is not a physical existence. “Blue” is the sensation that our nervous system creates when the visual system processes the electromagnetic wave with the wavelength of around 450nm through the eyes. Things are not what they are. They appear what our nervous system tells us what they are. Thus, we shall regard an object as a filtered image of its chemical and physical entity.

Each organism on the earth has evolved under unique selective pressures. Their nervous systems, therefore, have been sculpted to extract the most relevant information about the object most efficiently. We humans rely highly on the visual aspect of an object. For dogs, the chemical aspect of an object may be more salient. The acoustic sensations of bats serve as their “eyes” for navigation and foraging. The parts of the nervous system dedicated to detect and process these external stimuli are collectively called sensory systems. Sensory systems are subdivided into several modalities based on with which aspect of chemical or physical properties they deal.

Among these modalities, olfaction, or the sense of smell, poses a special challenge to an animal. Smell is related to the long-range chemical property of an object, which is characterized by small, volatile compounds. This type of information provides many useful clues about an object of interest to animals

(Ache and Young, 2005). They can tell the presence of predators or undesirable conditions from the distance (Whittaker and Feeny, 1971). They can assess the presence and value of potential food without ingesting it. It is known that many animals use olfactory cues to find potential mates and to communicate among individuals (Brennan and Zufall, 2006). Such social interactions by olfaction often play a crucial role in animal behaviors. A challenge to the olfactory system, however, is the vast variety of odors (Ache and Young, 2005). There are numerous volatile chemicals on the earth and most odors can appear in wide range of intensities. Light or sound, for example, has only two parameters: amplitude and frequency (wavelength). Temperature has just one dimension. Parameters defining chemical structure are far more diverse, on the other hand, since there are many degrees of freedom as to how carbon, hydrogen, oxygen, and other atoms can bind to each other in forming an organic molecule. Moreover, there is a problem of mixture. In most cases, an odor is a blend of multiple kinds of molecules in different ratios. This means that the olfactory system must detect multiple qualitatively different types of stimuli at the same time, and process them simultaneously. Perhaps partly because of the elusive nature of odors, many key neural mechanisms underlying the olfactory system remain unknown.

In this Introduction, I will summarize common principles found across sensory systems and relate these common themes to those explored in my thesis experiments (Figure 1.1):

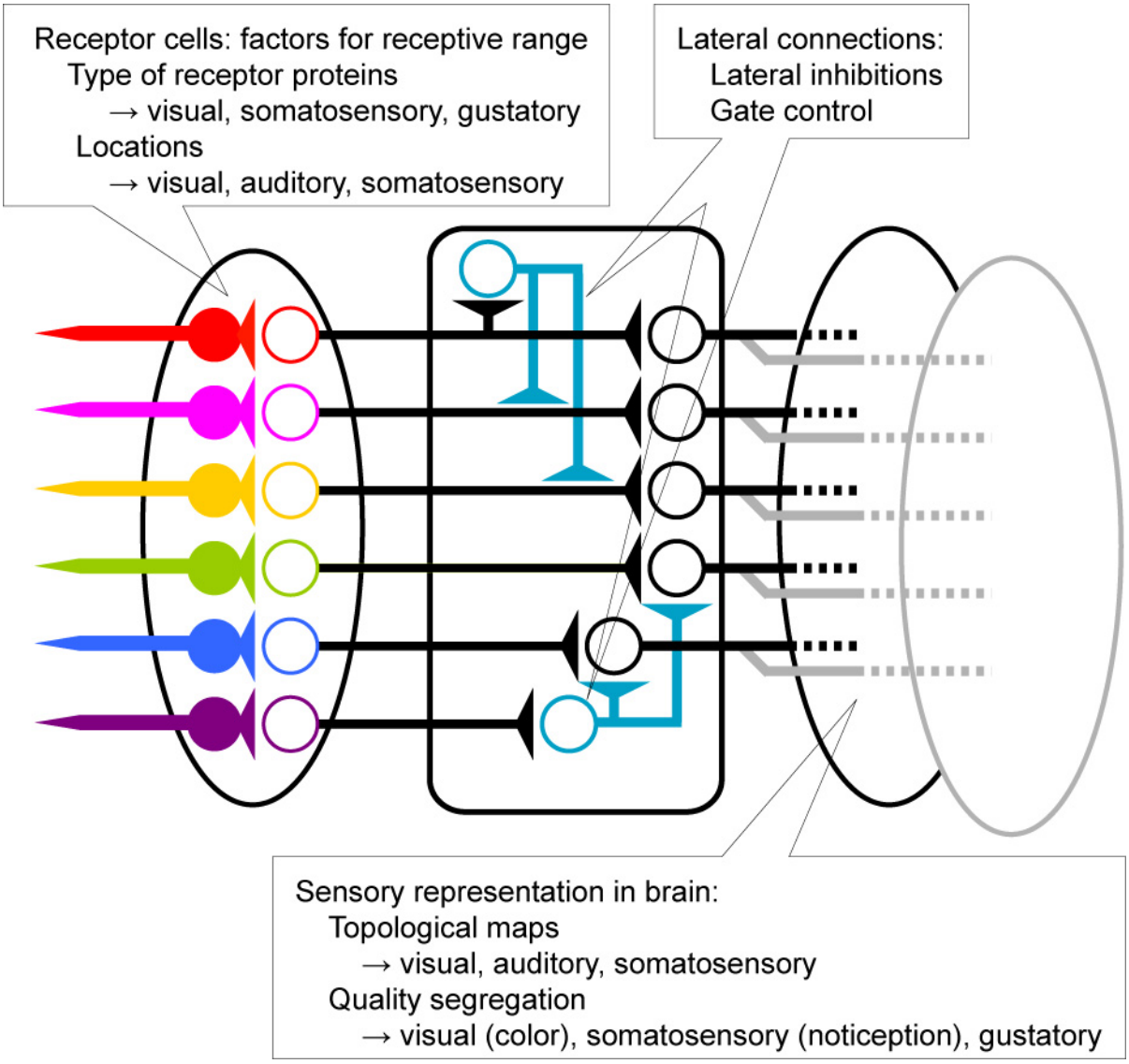

Figure 1.1: Organization of sensory systems

1) Within a given sensory modality, receptor cells are subdivided into several populations with a specific receptive range, which is largely determined by receptor proteins together with the location of receptor cells in a sensory organ.

2) Significant integration and processing of sensory information occur at the periphery.

3) Sensory information of the physical senses—vision, touch, hearing—is topographically mapped onto relay and higher processing centers. Central representation of the chemical senses—taste and smell—is less clear but there may be chemotopic mapping related to the stimulus type.

4) Lateral connections integrate inputs from multiple discrete ranges where necessary, although its neuronal mechanism is poorly understood.

I will first briefly review other sensory systems to illuminate both the common neural principles and the unique problems of the olfactory system.

1.1. Visual system

Among sensory systems, the visual system is predominant in human perception, perhaps explaining why it has been most intensively studied. Research on other sensory systems, including the olfactory system, has been influenced by existing knowledge of the visual system. Therefore, it will be informative to spend more space to browse the visual system here than for other sensory systems, even though the nature of stimulus for the visual system is distinct from that of the olfactory system.

The visual system perceives light through specialized cells called photoreceptors. In most animals, photoreceptors reside in the eye, which is a sophisticated device to collect light efficiently. Each photoreceptor detects light

from a specific and small area in the visual field of an animal. Like a pixel on digital camera, therefore, a photoreceptor encodes information about where the light originates in the visual field. The molecules that absorb light are the opsins, evolutionary conserved proteins (Terakita, 2005) classified into subtypes with different peak absorption wavelengths. Since a photoreceptor express only one of several opsins in the genome, each of the photoreceptors on the retina is optimized to a specific range of wavelengths defined by the type of opsin it expresses (Gegenfurtner and Kiper, 2003).

The information about the relative position of a photoreceptor on the retina, or the topography of photoreceptors, is preserved in the brain. Vertebrate photoreceptors transmit information to the retinal ganglion cells via bipolar cells. Since a ganglion cell receives input from a small number of photoreceptors, each ganglion cell is sensitive only to light on a limited area on the visual field. As axons of ganglion cells maintain their relative positions, they form an orderly retinotopic map in the brain (Sincich and Horton, 2005).

In vertebrates, segregation of color and motion starts early in the retina. Color-sensitive ganglion cells are connected by only one photoreceptor (Gegenfurtner and Kiper, 2003). These ganglion cells therefore have very limited spatial selectivity, but retain color selectivity imposed by the type of opsin that the cognate photoreceptor expresses. Motion-sensitive ganglion cells, on the other hand, are connected by multiple photoreceptors (Gegenfurtner and Kiper, 2003). As a result, these ganglion cells can integrate inputs from relatively wide range of the visual field. Pooling of photoreceptors results in loss of color information, but

it instead provides higher spatial resolution. Along with the retinotopic map, segregation of color and motion is also maintained in the brain, forming parallel pathways of visual information (Sincich and Horton, 2005).

Extensive lateral connections provided by local interneurons in the retina are thought to play major roles in shaping both color and motion sensitivity. A subpopulation of horizontal cells has lateral connections to a selective class of photoreceptors (Dacey et al., 1996). These horizontal cells are therefore color-sensitive, and can assist in segregation of color information. Likewise, another class of retinal local interneuron called amacrine cells are motion sensitive (Euler et al., 2002). This selectivity is thought to be achieved by a biased distribution of pre- and post-synaptic sites on the extensive dendrites of amacrine cells (Lee and Zhou, 2006). Therefore, motion-sensitive amacrine cells can transmit to the ganglion cells information regarding from which direction the light is approaching (Fried et al., 2002; Taylor et al., 2000), not only whether there is light or not on a given area. The detailed neuronal mechanism of such color and motion sensitivity is not yet fully understood, and is a focus of active research.

1.2. Auditory system

Sound is a series of vibrations of air, comprising waves of alternating air pressure, which is converted to mechanical vibration of cochlear fluid in the mammalian ear and is sensed by auditory hair cells. Since hair cells sense vibration, they may be categorized as mechanosensory cells. However, most animals, even fruit flies, have dedicated organs and neuronal circuits to process sound. Vocal

communication has been documented in various species such as birds, dolphins, bats, and humans.

Auditory hair cells are the vertebrate receptors of sound. They align in the organ of Corti in the cochlea situated in the inner ear (Hudspeth, 1989; Raphael and Altschuler, 2003). Unlike in the retina, where spectral tuning is a property of selective opsin expression, hair cell tuning selectivity in the cochlea does not seem to be the biochemical property of the sensory receptors expressed. Rather, it is a physical property of the sensory organ itself. The basilar membrane, on which the organ of Corti is attached, becomes thinner as it approaches the tip. A given part of the basilar membrane therefore has a unique frequency with which it can resonate. When entering the cochlea, various frequencies consisting of sound are resolved along the cochlea since only one frequency can vibrate a given part of the basilar membrane (Dallos, 1992; Hudspeth, 1989). This vibration is presumably amplified and sharpened by outer hair cells (Dallos, 1992; Nobili et al., 1998), and detected by inner hair cells. Amplification (Chan and Hudspeth, 2005) is a crucial step to assist frequency selectivity of inner hair cells (Dallos, 1992), and the relative length of stereocilia, which is the cellular sensor of vibration, further ensures that an inner hair cell is excited by a limited range of sound frequency (Hudspeth, 1989).

The molecular identity of the auditory mechanoreceptor remains elusive. It has been long proposed that it is an ion channel directly gated by mechanical force (Hudspeth, 1989). Although a type of transient receptor potential (TRP) channel is genetically required for auditory sensing in flies (Gong et al., 2004;

Kim et al., 2003) and zebrafish (Sidi et al., 2003), direct demonstration that this channel can be opened directly by mechanical force is lacking.

Cochlear ganglion cells receive receptor potential from hair cells (Keen and Hudspeth, 2006). Similar to the visual system, the auditory system maps sensory information in a topographic fashion, in this case a tonotopic map in the brain. The position of hair cells along the basilar membrane encodes frequency (Dallos, 1992). Cochlear ganglion cells preserve the relative location of the hair cells they innervate as they project to the brain, resulting in the representation of frequency range in a tonotopic map (Hudspeth, 2000; Sakai and Suga, 2001). Although sound itself has only two dimensions, frequency and amplitude, animals extract information about which direction it comes or how far the source is by intricate comparison of sound from two ears. Parallel processing mediates this neuronal calculation (Cant and Benson, 2003).

1.3. Somatosensation (mechanosensation, thermosensation and nociception)

Physical and thermal stimuli are sensed not by a distinct, specialized organ like visual or auditory stimuli, but by the entire body surface. In addition to sensors for “normal” mechanical stimuli or temperature, a special sensory neuron called a nociceptor detects an extreme range of both stimuli, such as acute pinching or excessive hot/cold temperature (Julius and Basbaum, 2001). Somatosensory receptor cells are surprisingly poorly characterized (Lumpkin and Caterina, 2007). Although dorsal root ganglion cells are known to transmit somatosensation, it is

not necessarily clear whether free nerve endings or associated epidermal structures are the receptor for mechanical or thermal stimuli (Lumpkin and Caterina, 2007).

The last decade has witnessed exhaustive molecular characterization of thermosensory receptors (Wang and Woolf, 2005). A general picture is that TRP channels mediate thermosensation. Vertebrates possess many temperature-sensitive TRP channels, each of which is activated by distinct range of temperature (Caterina et al., 1999; Caterina et al., 1997; McKemy et al., 2002; Peier et al., 2002; Story et al., 2003). Thus, like the visual system, the temperature spectrum is coded by distinct classes of receptors. Little is known about molecular identity of mammalian mechanosensory receptors, however (Christensen and Corey, 2007). In flies, TRP channels are thought to mediate mechanosensation (Walker et al., 2000) as well as thermosensation (Rosenzweig et al., 2005).

Which part of the body experiences touch or particular temperature is just as important information as the identity of the sensation. Although cutaneous mechanosensation and thermosensation/nociception ascend two different pathways in the vertebrate spinal cord, the relative position of their origin is preserved in the brain (Gardner, 2000). Hence, relay neurons of somatosensation form a representation of the body in the brain. Coding of positional information by topographic mapping therefore seems to be a common strategy of sensory systems. On the other hand, quality segregation of touch and

temperature reminds one of parallel pathways in both visual and auditory systems.

Interestingly, the receptor for extremely low temperature is co-expressed with the receptor for extremely high temperature in one nociceptor (Story et al., 2003). This finding explains why cold temperatures can cause the same painful sensation as hot temperature does. Nociceptors are unique in that they are sensitive to acute mechanical stimuli and pungent compounds (Bandell et al., 2004; Caterina et al., 1997; Jordt et al., 2004) as well as extreme temperature. Thus, nociceptors are polymodal. In contrast to finely tuned photoreceptors or hair cells, nociceptors discard distinctions between the qualities of stimuli. For animals, it must be beneficial to detect all noxious and potentially harmful stimuli by a single population of sensory cells, which results in alarming, acute sensation which we know as pain. Thus, nociception carries out important integration of sensory inputs at earliest stages in the sensory cells themselves.

Although pain appears such a universally commanding sensation, the percept of pain is highly subjective. A “painful” stimulus to one person may be totally ineffective in others, and the same stimulus can be sensed as painful or not by the same person under different conditions. To explain the varying threshold of pain perception, Melzack and Wall proposed a “gain control” mechanism (Melzack and Wall, 1965). According to their theory, nociceptors make synaptic connection to two kinds of neurons at the dorsal horn. One is the transmitter neuron, or the projection neurons sending the signal to the brain. The other is the local inhibitory interneuron that makes synapse to the transmitter

neuron. Under such a configuration, the increased input from the nociceptors excites both the transmitter and inhibitory local interneurons simultaneously. Qualitatively, therefore, increased activity of the nociceptor is “gated” by accordingly increased inhibition to the transmitter neurons via the local inhibition. This model provides a good explanation for a well documented property of the sensory system called Weber-Fechner’s Law (Johnson et al., 2002): the stimulus increment detectable to an individual increases in proportion to the baseline stimulus they are experiencing. Although the neurons involved in this proposed circuit are not completely identified, the model suggests that local modulation of sensory input plays an important role in perception. The theory has inspired research into the neuronal modulation of pain and other sensory modalities.

1.4. Gustatory system

The gustatory system is of particular interest for a student of the olfactory system, since both systems detect chemical stimuli. In most animals, however, the two are both functionally and anatomically segregated. The separation of the two chemical senses may reflect evolutionary need to make distinctions between long-range volatile chemical cues and short-range solid or liquid phase chemical cues which are evaluated prior to ingestion. In vertebrates, taste is sensed solely by taste receptor cells on tongue (Chandrashekar et al., 2006). Insects, on the other hand, are thought to use gustatory cues for additional purposes beyond food evaluation, such as to identify a potential mate and to evaluate an oviposition site. Thus, gustatory sensory neurons are scattered around the body

(Stocker, 1994; Vosshall and Stocker, 2007). Progress of research on the gustatory system has been fast since the discovery of taste receptors both in the vertebrates and flies. Although evolutionarily independent, both animals have adopted surprisingly similar strategies of taste coding in the nervous system (Scott, 2005).

Vertebrates possess five distinctive qualities of taste: sweet, bitter, umami, sour, and salty. These qualities are what the nervous system assigned to each group of compounds, and are ultimately derived from five distinct classes of taste receptor cells, characterized by five classes of taste receptor proteins. There are two major G-protein coupled taste receptor families: T1Rs and T2Rs. T1R1 and T1R3 heterodimers form the amino acid receptor (Nelson et al., 2002). The human T1R1/T1R3 receptor primarily detects monosodium glutamate, which evokes the “umami” taste quality (Chandrashekar et al., 2006). The T1R2/T1R3 heterodimer, on the other hand, forms a sweet taste receptor (Nelson et al., 2001). Various T2R receptors constitute “bitter” receptors (Chandrashekar et al., 2000). There are many compounds that taste “bitter”, but molecularly they are the collective ligands for different types of T2R bitter taste receptors. Sour taste is mediated by distinct populations of taste receptors that express PKD2L1 and PKD1L3 (Huang et al., 2006; Ishimaru et al., 2006), which belong to TRP channel family. The molecular identity of salt sensing cells and the salt receptor is currently unknown.

Insect gustatory receptors (GRs) are unrelated to any of the known mammalian taste receptor gene families. Instead, GRs are distantly related to the

fly olfactory receptors, which will be discussed later (Robertson et al., 2003; Scott et al., 2001). Genetic and behavioral analysis revealed several functional classes of fly gustatory sensory neurons. A group of gustatory sensory neurons expressing *Gr5a* mediates sugar (trehalose) detection (Chyb et al., 2003; Marella et al., 2006), and another, non-overlapping group expressing *Gr66a* mediates detection of “bitter” compounds (Marella et al., 2006). Interestingly, many compounds that humans sense as bitter, such as caffeine or quinine, seem to be “bitter” for flies as well. Recently, water-sensing (Inoshita and Tanimura, 2006) and carbonated water-sensing (Fischler et al., 2007) subpopulations of gustatory sensory neurons have been found in *Drosophila*. These findings suggest that categories of taste quality in flies are distinct from five mammalian taste qualities.

There is strong experimental evidence to suggest that taste quality is coded in a “labeled line” fashion. This means that each of taste qualities remains segregated in the brain, and in some cases elicits distinct behavioral responses. Segregation of taste qualities at the periphery seems the most important information processing by the gustatory system.

The first line of evidence for labeled line coding in the gustatory system comes from knock-out mice. Knock-outs of T1R1 and T1R2 abolish both electrophysiological and behavioral responses to amino acid and sugar, respectively (Zhao et al., 2003), but leave other taste qualities intact. Similarly, knock-out of one of the T2R receptor, T2R5, abolishes electrophysiological and behavioral responses to cycloheximide, a known ligand of mouse T2R5 that tastes bitter to humans (Mueller et al., 2005), but has no effect on sweet or amino

acid taste. Ablation of PKD2L1-expressing acid-sensing cells results in the loss of both the electrophysiological and behavioral responses for low-pH solutions (Huang et al., 2006). Importantly, all of these genetic manipulations leave the other four taste qualities intact, both in electrophysiological and behavioral terms. Therefore, the five taste qualities are segregated at the periphery and transmit behaviorally relevant information independent of each other (Chandrashekar et al., 2006).

A second line of evidence supporting labeled line taste coding is that activation of these classes of taste receptor cells is sufficient to encode perceptive quality of the corresponding tastes. A mouse expressing RASSL, an opioid receptor with a synthetic agonist named spiradoline, in sweet-sensing cells is attracted by otherwise tasteless spiradoline (Zhao et al., 2003). Conversely, a mouse expressing RASSL in bitter-sensing cells avoids spiradoline (Mueller et al., 2005). These results convincingly demonstrate that mammalian taste qualities are hard-wired. In a biological point of view, it is the class of taste receptor cells that determines the perception of taste, not the compounds themselves. Anything that activates “sweet”-sensing cells, for example, is interpreted as sweet by the brain, regardless of the identity of the compound. A similar coding logic applies to the mammalian nociceptor, in which both hot temperature and capsaicin evoke the same noxious sensation through activation of the TRP channel TRPV1 (Caterina et al., 1997).

Like mammals, flies discriminate sugar and bitter compounds at the periphery and process them separately. Ablation of *Gr5a*-expressing cells

selectively abolishes behavioral attraction to sugars (Thorne et al., 2004; Wang et al., 2004b), and expression of TRPV1 in these sugar sensing cells results in attraction of flies to capsaicin, which in normal flies induces no behavioral response (Marella et al., 2006). The same is true for *Gr66a*-expressing cells: ablation of *Gr66a* cells abolishes bitter tastant avoidance behavior (Thorne et al., 2004; Wang et al., 2004b), and expression of capsaicin receptor in these cells makes flies avoid capsaicin (Marella et al., 2006). Thus, taste qualities seem segregated and processed independently in the fly.

This “labeled line” coding hypothesis is further supported by the non-overlapping projection patterns of these two populations of gustatory sensory cells. Unlike non-neuronal taste receptor cells in mammals, insect gustatory receptor cells are neurons whose axons terminate at the subesophageal ganglion (Stocker, 1994). *Gr5a*- and *Gr66a*-neurons project to segregated areas with virtually no overlap (Wang et al., 2004b). Thus, a taste quality map exists in the fly brain, and this segregation may be the basis of taste recognition and distinct behavioral response to bitter and sweet compounds (Thorne et al., 2004; Wang et al., 2004b). Interestingly, flies treat carbonated water as taste quality distinct from bitter and sweet, as the carbonated water-sensing neurons project to yet another area in the subesophageal ganglion (Fischler et al., 2007). In addition to the taste quality map, the fly taste system has a topographic map. *Gr66a*-expressing sensory neurons are found in mouthparts and legs in addition to the proboscis (Wang et al., 2004b). Projections from these different parts are segregated in the subesophageal ganglion (Wang et al., 2004b). Whether inputs

from different part of the body encode different perceptive quality is an intriguing question.

How are these taste qualities represented in the vertebrate brain? By analogy with the three modalities discussed prior to the gustatory system, it is tempting to speculate that there is a “gustotopic” map in the cortex. Judging from behavioral evidence, this putative map would have only 5 distinct areas, a significant reduction of complexity compared to retiontopic or tonotopic maps. The result from flies strongly implies such a map also exists in vertebrates, but it has yet to be demonstrated.

Although both vertebrates and insects possess many “bitter” receptors, they are usually co-expressed in one taste receptor cell. Many of 30 T2Rs in mouse are randomly co-expressed in one taste cell (Adler et al., 2000). Likewise, at least four gustatory receptors in flies are co-expressed in *Gr66a*-expressing neurons (Thorne et al., 2004; Wang et al., 2004b). Assuming that each receptor has its own set of ligands, they generalize any molecule that activates a receptor as “bitter”, discarding any distinction between them. Bitter taste is often associated with potential toxins, and animals probably do not need to discriminate between these compounds. This is in sharp contrast to the expression patterns of the olfactory receptors, as I discuss in the following Section.

1.5. Olfactory system

I have visited four sensory systems to show that they are organized according to the common principles outlined at the beginning of this Chapter. Do these principles apply to the olfactory system? A short answer is yes, as is explicit in the question. In the following sections, I will discuss vertebrate and insect olfactory systems separately. Their striking similarity demonstrates the benefit of the fruit fly *Drosophila melanogaster* as a model organism to understand the olfactory system of higher animals.

1.5.1. The vertebrate odorant receptors

Like other sensory systems, the olfactory system makes its first contact with the stimuli through specialized sensory cells. Both vertebrates and insects sense odors with neurons, termed olfactory receptor neurons or olfactory sensory neurons (OSNs) (Ache and Young, 2005; Hildebrand and Shepherd, 1997). Even though both terms are commonly used in the literature, I will use the latter term OSN throughout this thesis to avoid confusion with odorant receptors.

Odorant receptors (ORs) are membrane proteins serving as the interface between odorants and the olfactory system. Two gene families are known to encode ORs in vertebrates. The first family comprises the “classic” ORs, which are seven transmembrane G-protein coupled receptors (Buck and Axel, 1991; Mombaerts, 1999). They form the largest gene family in mouse genome, which is likely to be the case for other vertebrates including the humans. Mice have about 1,000 functional OR genes (Zhang and Firestein, 2002); the humans have nearly

400 and about the same number of pseudogenes (Niimura and Nei, 2003). In all sequenced vertebrate genomes, the ORs show considerable sequence diversity. The second class of vertebrate ORs is the trace anime-associated receptors (TAARs) (Liberles and Buck, 2006). This recently discovered receptor class contains far fewer members, 15 in mouse genome, and merely 6 in the human genome. They may play an important role in social interactions since some TAARs have been shown to respond to volatile amines often found in urine (Liberles and Buck, 2006).

A striking finding is that an OSN expresses only one type of OR. Although not confirmed in every class of OSNs, negative feedback regulation presumably prevents co-expression of multiple ORs in one OSN (Lomvardas et al., 2006; Serizawa et al., 2003) (but see Fuss et al., 2007). Therefore, OSNs are highly heterogeneous, consisting of numerous classes which is defined by the OR it expresses. This is in sharp contrast to receptor expression patterns in bitter sensing taste cells or nociceptors in vertebrates, where multiple receptor genes with distinct receptive ranges are co-expressed in one sensory cell. As I introduce in the following section, the functional diversity of the OSNs seem to be key in detection and processing of olfactory information.

1.5.2. Insect odorant receptors

Only one class of insect ORs has been identified to date. The repertoire seems relatively small compared to the vertebrate ORs: the fruit fly *Drosophila melanogaster* has 62 ORs in its genome (Robertson et al., 2003; Vosshall et al.,

2000), the malaria mosquito *Anopheles gambiae* has 79 (Hill et al., 2002), and the honeybee *Apis mellifera* has about 170 (Robertson and Wanner, 2006). Their sequences imply that they have seven transmembrane domains (Clyne et al., 1999; Gao and Chess, 1999; Vosshall et al., 1999), but they are unlikely to be related to the vertebrate ORs (Bargmann, 2006). In fact, they may not be G-protein coupled receptors, as the topology of the protein is “inside-out” compared to conventional G-protein coupled receptors: their N-terminus faces the cytoplasmic side (Benton et al., 2006; Lundin et al., 2007; Wistrand et al., 2006). Although many publications maintain that a G-protein signaling cascade is involved in insect olfactory signal transduction (reviewed in Hildebrand and Shepherd, 1997), evidence to support these claims is weak. Insect ORs form a highly divergent superfamily with insect gustatory receptors, suggesting that transduction mechanisms will be conserved between ORs and GRs.

One or at most three odorant receptors are expressed in an insect OSN (Couto et al., 2005). The majority of OSNs express only one OR (Couto et al., 2005; Fishilevich and Vosshall, 2005; Vosshall et al., 2000), however, and it is unclear if all ORs present in one OSN contribute functional receptors to these neurons (Dobritsa et al., 2003). Therefore, the expression pattern of ORs in insect OSNs generally follows a principle similar to that in vertebrates. An OSN of the nematode *Caenorhabditis elegans*, on the other hand, is known to express multiple ORs (Bargmann, 2006). Animals in other phyla therefore may follow a distinct logic of OR expression.

Fruit fly OSNs co-express another ubiquitous OR called *Or83b* in addition to the "conventional" ORs mentioned above (Larsson et al., 2004). This protein is not considered to be directly involved in odor detection; instead, it traffics other ORs to the dendritic tip of an OSN (Benton et al., 2006), presumably by forming a heterodimer (Benton et al., 2006; Neuhaus et al., 2005). Without *Or83b*, OR proteins are retained in the endoplasmic reticulum and therefore cannot function as a receptor (Benton et al., 2006; Larsson et al., 2004). Importantly, *Or83b* homologues are widely found in other insect species and are functionally orthologous (Jones et al., 2005; Nakagawa et al., 2005). The requirement of this OR co-receptor further supports the notion that insect ORs are of distinct origin from vertebrate ORs, and that signaling cascade in an insect OSN may not use conventional G-protein transduction mechanisms.

1.5.3. "Combinatorial" coding of an odorant at periphery

The "combinatorial coding model" argues that the quality, or the identity, of an odor is "coded" as a specific combination of OSNs activated by it (Malnic et al., 1999) (Figure 1.2). Although ORs were only relatively recently shown to be both necessary (Dobritsa et al., 2003; Elmore et al., 2003) and sufficient (Bozza et al., 2002; Dobritsa et al., 2003) to evoke odor-dependent responses in OSNs, the diversity of ORs strongly implied that each of them was responsible for detecting relatively limited kinds of odorants. In fact, it has been long known that a given OSN can be excited by many kinds of odorants. Conversely, a given odorant can excite multiple classes of OSNs (de Bruyne et al., 1999; de Bruyne et al., 2001;

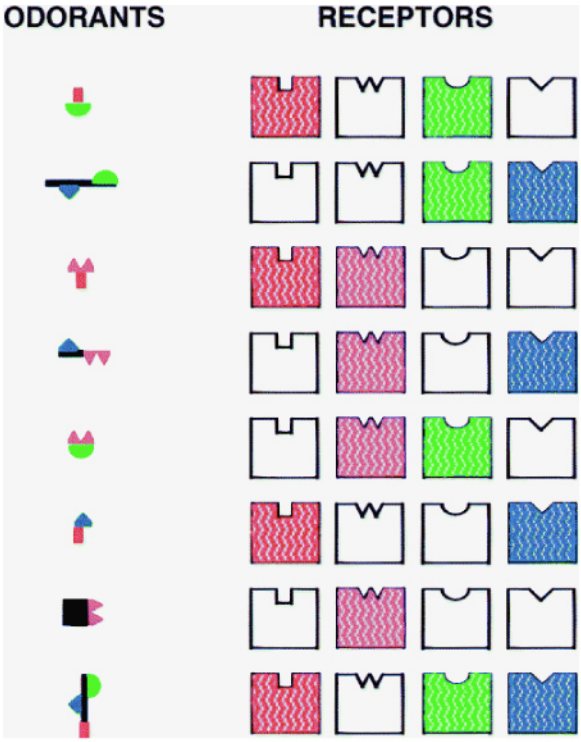

Figure 1.2: Combinatorial odor coding

An odorant can be recognized by multiple classes of OSNs since ORs have different affinities. Whether ligand affinity is based on the functional groups of the odorant, as this figure suggests, is not known. Adapted from Malnic et al., 1999.

Sato et al., 1994; Sicard and Holley, 1984). In other words, the “receptive ranges” of OSNs are distinct but overlapping.

The discovery of the ORs made it possible to link the physiological property of an OSN to the molecular identity of the OSN, which is defined by the expression of its OR (Hallem et al., 2004; Malnic et al., 1999; Touhara et al., 1999). In the past decade, numerous articles have sought to define the “receptive range” conferred by ORs both in vertebrates and insects (reviewed in Bargmann, 2006; Mombaerts, 2004). Overall, these findings are consistent with the

combinatorial coding hypothesis. Although some ORs seem to be highly tuned to specific odorants, most ORs are capable of activating OSNs in response to many odorants. Whether such combinatorial recruitment of OSNs by an odorant is necessary for olfactory perception has not been experimentally demonstrated. However, usage of combination appears mathematically reasonable solution to encode vast number of odorant molecules and their mixtures by limited number of coding units.

Such combinatorial coding logic at the olfactory periphery adds a twist to sensory reception scheme. An OSN does not have the kind of unique and narrow receptive range that is assigned to an individual photoreceptor or auditory hair cell. Neither does an OSN pool diverse stimuli into one category like taste receptor cells or nociceptors do. In a sense, the combinatorial code stands somewhere in between the selectivity of the visual and auditory system and the pooling of the gustatory system. Because of its efficacy and its consistency with physiological observations, combinatorial coding has been the dominant and popular theory in the field of olfaction.

1.5.4. Neuronal architecture of the vertebrate olfactory system

In vertebrates, the OSNs are situated in the olfactory epithelium in the nasal cavity. It is a reasonable place to sample odorants since a large volume of air or water can go through the nasal cavity as an animal sniffs (Ache and Young, 2005). OSNs have cilia embedded in nasal mucosa. Odorants in the air are thought to diffuse into the mucosa and reach the ORs on the surface of cilia.

Although ORs largely determine which odorant can activate OSNs, the mucosa itself can influence odor response profiles of OSNs (Oka et al., 2006). Nasal mucosa contains various degradation enzymes and odorant binding proteins, which can modify odorant molecules before they reach the ORs (Carr et al., 1990). However, to which degree such perireceptor processes influence odorant perception remains unclear.

OSNs send axons to the main olfactory bulb. This is the first olfactory relay of the vertebrate brain and it appears to be of ancient origin: it is found in all vertebrates including the lamprey, with the exception of exclusively aquatic mammals such as whales, dolphins, or manatees (Meisami and Bhatnagar, 1998). The olfactory bulb is located at the anterior end of most vertebrate brains, and consists of several layers including the glomerular layer, granule cell layer and mitral cell layer (Shepherd, 1972). Glomerular layers are formed from numerous spheroidal neuropils called glomeruli. Axons of the OSNs terminate in this structure, where they synapse with olfactory bulb neurons. Several distinct populations of olfactory bulb neurons are documented. They can be largely classified to two groups: one is the projection neurons, which extend dendrites in the olfactory bulb and send axons to other part of the brain, and the other is the local interneurons, whose dendrites and axons are confined to the main olfactory bulb (Shepherd, 1972). Olfactory bulb projection neurons are called mitral cells and tufted cells. They are both excitatory, and send axons to the olfactory cortex

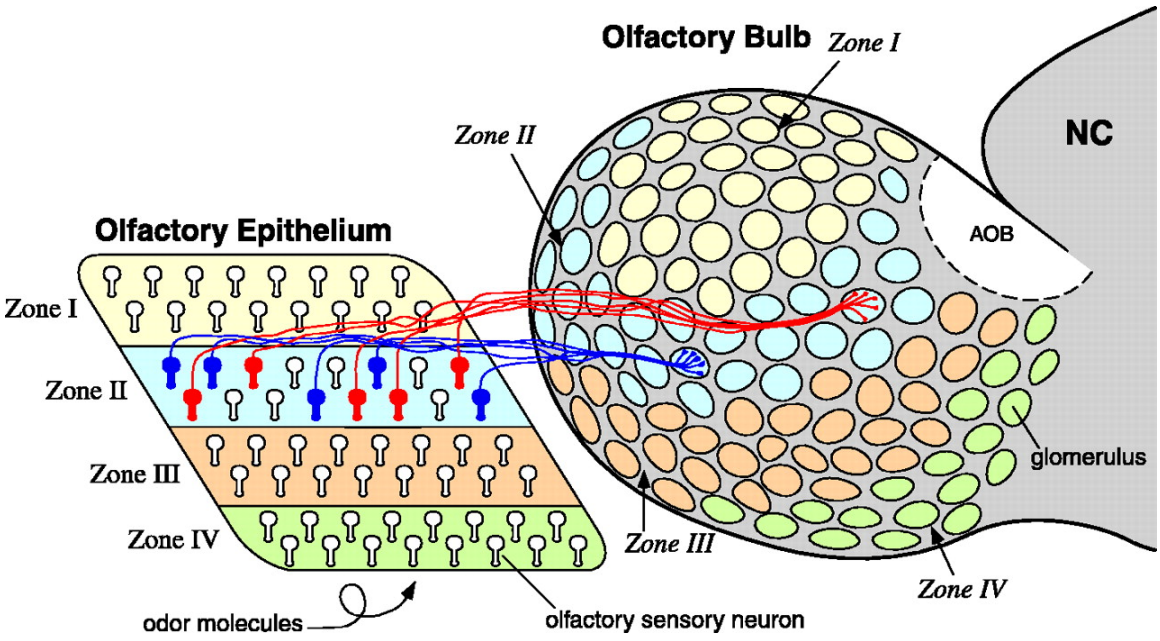

Figure 1.3: OSNs form a map on the olfactory bulb

OSNs expressing the same OR converge on a single glomerulus. The mirror image is formed on the medial side of the hemisphere. The accessory olfactory bulb (AOB) is located adjacent to the main olfactory bulb. The zonal organization described in this figure has been reported for some ORs, but it is not clear if the same rule applies to all ORs. Adapted from Mori et al., 1999.

of the cerebrum. Local interneurons include periglomerular cells, granule cells, and short-axon cells. These cells constitute a network localized within the olfactory bulb.

An important neuroanatomical finding in the olfactory system is that there is an “olfactory map” (Figure 1.3). A class of OSNs expressing the same OR converges on specific glomeruli (Mombaerts et al., 1996). This fact confirms previous speculation that glomeruli are functional units in the olfactory bulb (Hildebrand and Shepherd, 1997). As an OR determines to which odorants

OSNs are excited or inhibited, a glomerulus is a pooling site of a specific receptive range of the olfactory spectrum. A given class of OSNs converges to one glomerulus in each of the two halves of a main olfactory bulb, medial and lateral sides. The class of OSNs expressing the same OR therefore form four distinct glomeruli as functional units, two on left and right hemispheres of the olfactory bulb (Mombaerts, 2004). Cell bodies of mitral cells and tufted cells, often collectively called M/T cells despite their distinct morphologies, are located outside of the glomerular layer (Shepherd, 1972). Each M/T cell sends apical dendrites to one specific glomerulus, and is thus engaged in receiving exclusive input from one class of OSNs (Shepherd, 1972). M/T cells also possess laterally extended dendrites. Periglomerular cells are located around a glomerulus, and make dendrodendritic connections with M/T cells innervating the same glomerulus (Murphy et al., 2005). Granule cells, on the other hand, extend dendrites to the external plexiform layer, just below the glomerular layer, and connect multiple classes of M/T cells via lateral dendrites (Shepherd et al., 2007). There are relatively poorly documented short axon cells, a type of local interneuron in the glomerular layer (Aungst et al., 2003). These differ from periglomerular cells in having long dendrites that reaches multiple neighboring glomeruli.

The “olfactory map” formed by the specific connection of OSNs and M/T cells at glomeruli seems to offer a fundamental basis of odor recognition in vertebrates. Specific combinations of OSNs activated by a given odorants are translated into a specific combination of glomeruli in the olfactory bulb (Bozza et

al., 2004; Friedrich and Korsching, 1997; Meister and Bonhoeffer, 2001; Rubin and Katz, 1999; Uchida et al., 2000; Wachowiak and Cohen, 2001). There, the corresponding classes of M/T cells are presumably activated and transmit odor information to the olfactory cortex (Mori et al., 1992). Although no spatial topology is involved in the olfactory information itself, this manner of sensory representation resembles, at least in principle, that of the visual system or auditory system. The relative location of an object in the visual field in the visual system or an array of frequency in the auditory system is maintained in respective sensory centers. Likewise, a map defined by the repertoire of ORs is projected on the glomerular layer of the olfactory bulb. Compared to other sensory systems, however, the olfactory map beyond the olfactory bulb has not been well characterized. Further studies are required to elucidate how olfactory information is represented at the cortex.

1.5.5. Insect olfactory system – properties and resemblance to the vertebrates

The olfactory system plays a crucial role in insect behavior. It is speculated that the expansion of insects coincided with diversification of angiosperms (Bronstein et al., 2006; Crane, 1995), which are characterized by fragrant and colorful flowers. Plants also synthesize various chemical substances in their bodies to protect themselves (Whittaker and Feeny, 1971). The long range chemical senses must therefore have been under strong evolutionary selection for insects to detect proper host plants and avoid toxic species.

Insect OSNs are situated on chemosensory appendages on the head. In flies, the antennae and maxillary palps are the two olfactory organs (Stocker, 1994). This can be different from species to species, since in the malaria mosquito *Anopheles gambiae*, OSNs are also found on the proboscis (Kwon et al., 2006), which is a gustatory organ for flies (Stocker, 1994). Insect olfactory organs are covered with very large numbers of small sensory hairs called olfactory sensilla, which house between one and four OSNs (Couto et al., 2005; Stocker, 1994). In flies, three major types of olfactory sensilla are known: trichoid, basiconic, and coeloconic (Stocker, 1994). Recent advances in documenting fly OR expression has made it possible to related the expression of specific OR genes to identified trichoid and basiconic sensilla (Couto et al., 2005; Fishilevich and Vosshall, 2005). Coeloconic sensilla, except the one expressing *Or35a* (Yao et al., 2005), remain to be molecularly characterized (Vosshall and Stocker, 2007). This class of OSNs does not express *Or83b*, which suggests that odor detection in these cells is mediated by another family of receptor proteins. This is a similar situation to the vertebrate olfactory epithelium, in which a small number of TAAR-expressing OSNs exist alongside larger numbers of conventional OR-expressing neurons.

OSNs innervate the antennal lobe, which like the vertebrate olfactory bulb is divided into morphologically identifiable glomeruli (Galizia et al., 1999a; Laissue et al., 1999). There, the olfactory projection neurons extend dendrites and make synaptic contact with the OSNs. Projection neurons send their axons to two major olfactory centers in the insect brain, the mushroom body calyx and

lateral horn of the protocerebrum (Stocker et al., 1990). As seen for the vertebrate olfactory bulb, insect inhibitory local interneurons form lateral connections in the antennal lobe (Stocker et al., 1990).

The idea that vertebrate and insect glomeruli are functionally equivalent is strongly supported by the finding that insect OSNs expressing the same OR converge to a specific glomerulus (Couto et al., 2005; Fishilevich and Vosshall, 2005; Gao et al., 2000; Vosshall et al., 2000). Moreover, projection neurons are also characterized by uniglomerular dendritic innervations in which most of them send dendrites to only one glomerulus (Marin et al., 2002; Wong et al., 2002). Therefore, the “olfactory map” based on the repertoire of ORs exists on the antennal lobe (Figure 1.4). Local interneurons, meanwhile, connect projection neurons across the antennal lobe and also possibly modulate OSNs (Christensen et al., 1993; Fonta, 1993; Stocker et al., 1990; Wilson and Laurent, 2005). Most local interneurons are GABAergic (Wilson and Laurent, 2005) and therefore appear analogous to the inhibitory granule cells in the vertebrate olfactory bulb.

How is the olfactory map at the antennal lobe represented in the higher centers of the insect brain? Evidence from the fruit fly seems to suggest that it is preserved, at least to some extent. Clonal analysis of projection neurons first demonstrated that the neurons whose dendrites innervate the same glomerulus terminate their axons at stereotypical positions in the lateral protocerebrum of the fly (Jefferis et al., 2007; Lin et al., 2007; Marin et al., 2002; Tanaka et al., 2004; Wong et al., 2002). As in the mouse, these projections are both distinct from and

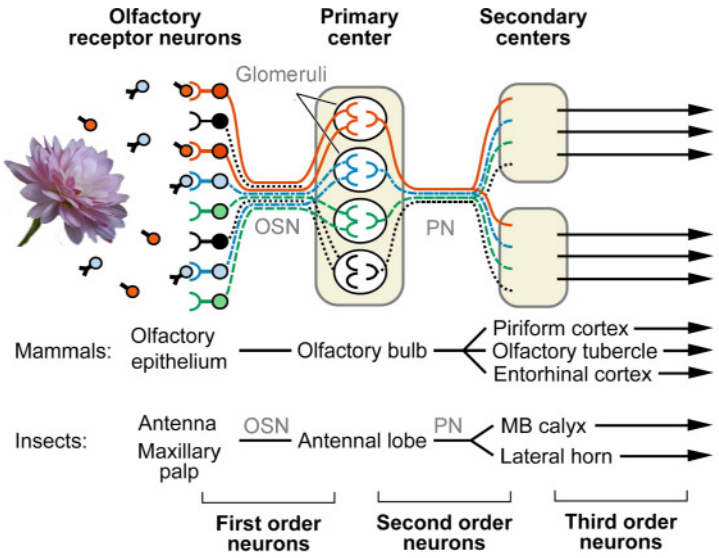

Figure 1.4: The insect olfactory system is analogous to the vertebrate olfactory system

The olfactory map is formed in the antennal lobe, where most projection neurons (PNs) innervate a single glomerulus similar to mitral or tufted cells in the vertebrate olfactory system. Adapted from Vosshall and Stocker, 2007.

intermingled with projections from functionally unrelated second order neurons. Notably, projection neurons receiving input from glomeruli tuned to pheromones (Ha and Smith, 2006; Kurtovic et al., 2007; Stockinger et al., 2005) are clearly segregated from the rest of the projection neurons (Jefferis et al., 2007). This suggests that pheromonal input is segregated from “general” olfactory input.

The presence of the olfactory map in higher order brain centers is in accord with organizational principles in other sensory systems. How animals use such a map for olfactory perception is an important and highly contested question.

One important factor that could modify the olfactory map is the lateral connection at the olfactory bulb or the antennal lobe.

1.5.6. The local interneurons: lateral connections in the olfactory bulb and antennal lobe

Lateral connections in the sensory systems are proposed to influence the coding of stimuli in a highly significant manner. As was mentioned in Section 1.1, retinal local interneurons such as horizontal cells and amacrine cells are thought to be an integral part of color and motion detection. Although poorly characterized, putative “gating” inhibitory neurons involved in nociception have been long suspected to mediate pain perception (Melzack and Wall, 1965). Likewise, growing attention is being paid to the local interneurons in the olfactory system as an indispensable player of odor coding. Most local interneurons in vertebrate olfactory bulb or insect antennal lobe are GABAergic inhibitory neurons, and I will first discuss the known physiological impact of this population of neurons.

Granule cells are thought to cause lateral inhibition in the olfactory bulb (Shepherd et al., 2007) (Figure 1.5A). They connect several mitral cells by extensive dendritic branches. Upon excitation by the lateral dendrite of a mitral cell, granule cells release GABA onto dendrites of synapsing mitral cells and hyperpolarize them (Schoppa and Urban, 2003). In one of the most convincing experiments to address the inhibitory effect, Kensaku Mori and his colleagues demonstrated that lateral inhibition exists between rabbit mitral cells (Yokoi et al., 1995). They found several mitral cells excited preferentially by aldehydes with

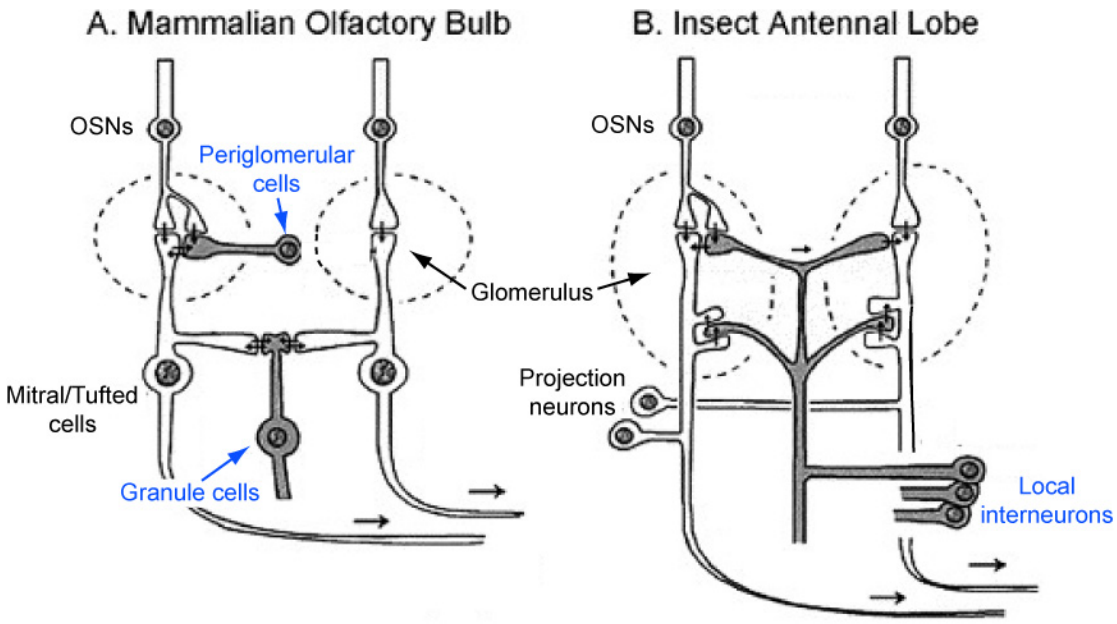

Figure 1.5: Lateral inhibitory connections in mammalian olfactory bulb and insect antennal lobe

Neurons indicated in blue are known inhibitory local interneurons. **A)** The mammalian olfactory bulb has two local interneuron populations. Among these, periglomerular cells are thought to mediate mainly intraglomerular inhibition while granule cells are thought to mediate lateral inhibition. **B)** Insect local interneurons laterally connect projection neurons. Diagram is adapted from Ache and Young, 2005.

specific carbon chain length. Aldehydes with carbon chains slightly longer or shorter than the preferred length, on the contrary, inhibited the mitral cell. After blocking granule cell activity with AMPA and NMDA antagonists, mitral cells showed no such inhibition. Based on the result, they proposed that granule cells that were excited by dominant input from a mitral cell inhibited surrounding mitral cells through lateral connections. This dendro-dendritic inhibitory circuit was later functionally demonstrated in rat olfactory bulb (Isaacson and Strowbridge, 1998). Lateral inhibition is thought to enhance contrast between two close points in

visual or mechanosensory stimulus space. For lateral inhibition to enhance contrast of two closely related odorants, OSNs with similar olfactory receptive range have to converge on nearby glomeruli. In mouse and rat olfactory bulb, similar odorants tend to activate neighboring and partially overlapping glomeruli (Meister and Bonhoeffer, 2001; Rubin and Katz, 1999; Uchida et al., 2000), implying that such “odor-topic” convergence might take place. This provides a simple neuronal circuit for effective lateral inhibition.

Similar contrast-enhancement is suggested to play in the insect olfactory system, again requiring the activity of local interneurons (Figure 1.5B). Insect projection neurons can be inhibited by GABA (Christensen et al., 1993; Sachse and Galizia, 2002; Wilson and Laurent, 2005). Application of the GABA antagonist picrotoxin results in increased excitation of projection neurons to an odorant compared to untreated preparations (Sachse and Galizia, 2002; Wilson et al., 2004). Unlike granule cells in vertebrates, insect local interneurons often extend dendrites throughout the entire antennal lobe (Christensen et al., 1993; Fonta, 1993; Ng et al., 2002; Wilson et al., 2004). Consistent with their morphology, these local interneurons are often excited by many odorants (Ng et al., 2002; Wilson et al., 2004). Therefore, this type of local interneurons would impose global inhibition on the entire population of projection neurons in response to virtually all odorants detected by OSNs. Precisely speaking, this type of inhibition is not “lateral inhibition” since it does not serve to enhance the “edge” of molecular images of similar odorants. Rather, this process can be regarded as “gating control” by the local interneurons.

A minority of local interneurons in both vertebrate and insect is excitatory. They are not as well characterized as the inhibitory local interneurons, but recent evidence indicates that they may play an important role in reshaping OSN input. In mouse olfactory bulb, non-GABAergic short axon cells extend both axons and dendrites in the glomerular layer (Aungst et al., 2003). They can sometimes reach 10-12 glomeruli far from the cell body location. Upon excitation from one glomerulus, a short axon cell excites periglomerular cells located at a distance (Aungst et al., 2003). A periglomerular cell is another population of inhibitory local interneuron in the olfactory bulb, and extends dendrites only to one glomerulus (Murphy et al., 2005; Schoppa and Urban, 2003). Periglomerular cells therefore inhibit only one class of M/T cells projecting to the same glomerulus. Short axon cells can establish longer-range inhibition, which can reach far across the olfactory bulb, thus forming “center-surround” domains (Aungst et al., 2003; Luo and Katz, 2001).

Candidate excitatory local interneurons have been recently found in the *Drosophila* antennal lobe (Shang et al., 2007). Like inhibitory homogeneous local interneurons, they extend axon throughout the antennal lobe. They are cholinergic, and can be excited by many odorants. The cholinergic local interneurons are therefore proposed to modify the activities of projection neurons. Thus, a complex neuronal network exists in both the olfactory bulb and the antennal lobe. This network can influence the “odor code” provided by the OSNs, and the resultant neuronal activity of M/T cells or projection neurons go through a

layer of modifications before they transmit odor information to higher brain centers.

How is the combinatorial code at the periphery transmitted to the brain? To what extent is it preserved from, or intermingled with, other codes? Which part of a code is relevant for the animal's perception and behavioral response to an odorant? These are questions not only applicable the olfactory system, but to other sensory systems in general. Answers to these questions may be obtained through genetic and physiological dissection of the olfactory circuit, accompanied by behavioral studies. A large number of ORs and OSNs, however, pose a serious challenge to such an approach. A model organism with small set of ORs and OSNs is highly desirable to relieve the difficulty. Which organism is most suitable? I propose the larva of the fruit fly which has an anatomically simple olfactory system that nevertheless includes all the main components of the vertebrate olfactory system.

1.5.7. Neuroanatomy of the larval olfactory system

The fruit fly is a holometabolous insect that goes through larval and pupal stages before completing its developmental program. The larval stage is devoted to accumulating nutrition and energy, while the adult stage is specialized for reproduction. The pupal stage bridges these two stages by transforming the insect's body from a crawling maggot to a flying adult in a process is known as metamorphosis.

Although larvae take only 4-5 days to become pupae in laboratory conditions, they possess specialized olfactory and gustatory organs (Stocker, 1994). The larval olfactory organ is called the dorsal organ (Cobb, 1999). It consists of a porous dome and surrounding pits, and 21 olfactory sensory neurons, bundled as seven triplets, which insert their dendrites to the dome (Python and Stocker, 2002; Singh, 1984). Their function as OSNs is supported by electrophysiological recordings (Oppliger et al., 2000) and genetic ablation of dorsal organ neurons (Heimbeck et al., 1999; Larsson et al., 2004). The surrounding pits are innervated by putative gustatory sensory neurons (Stocker, 1994).

The cell bodies of larval OSNs are situated at the dorsal organ ganglion. From there, they send axon to the larval antennal lobe, the functional homologue of the adult antennal lobe (Tissot et al., 1997). Although all the larval OSNs are assumed to degenerate during metamorphosis (Tissot and Stocker, 2000), the larval antennal lobe anatomically resembles the adult antennal lobe. Immunostaining reveals subdivisions in the larval antennal lobe, reminiscent of the glomerular structure of the adult antennal lobe (Python and Stocker, 2002). Clonal analysis of OSNs confirms the functional subdivisions of the larval antennal lobe (Ramaekers et al., 2005). By randomly labeling one of 21 OSNs, Reinhard Stocker and colleagues demonstrated that one OSN extends its axon terminal only to a small, confined area in the larval antennal lobe (Ramaekers et al., 2005). Therefore, although anatomical characterization of glomeruli is

challenging, the OSNs project to the larval antennal lobe in the same manner as adult OSNs.

Both local interneurons and projection neurons are found in larvae. Again, their innervation in the larval antennal lobe resembles the adult counterparts. At least 20 local interneurons extend dendrites exclusively to the antennal lobe with no apparent projection elsewhere (Ramaekers et al., 2005). Projection neurons innervate mainly the larval mushroom body and, less clearly, the lateral protocerebrum (Marin et al., 2005; Ramaekers et al., 2005). Interestingly, a larval projection neuron extends dendrites only to a small part of the antennal lobe, which seems to correspond to a “glomerulus” definied by the projection neuron communicating with a single OSN (Ramaekers et al., 2005). Since only one larval projection neuron occupies this presumptive glomerulus, the total number of projection neuron should be close to 21, the number of larval OSNs (Vosshall and Stocker, 2007).

Overall, at an anatomical level the larval olfactory system closely resembles the adult olfactory system (Figure 1.6). Stereotypical innervation of the OSNs and projection neurons at the antennal lobe, and similarly orderly map formed by dendritic arbors of the projection neurons all appear to be miniature version of the adult counterpart.

1.5.8. Benefits of larvae as a model system

Although the larval olfactory system appears to be very similar to the adult olfactory system, its numerical simplicity makes larvae an attractive alternative as

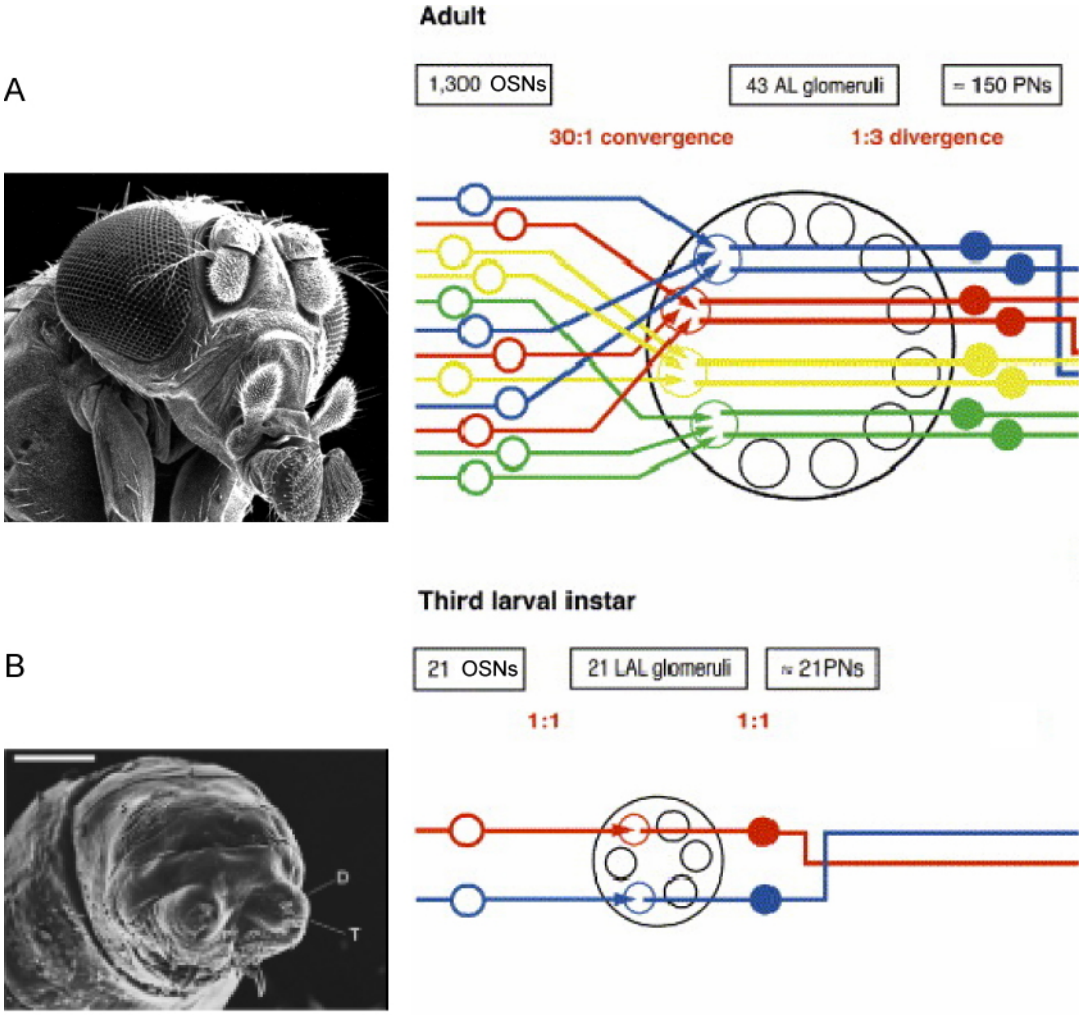

Figure 1.6: Comparison of adult and larval olfactory system

A) In the adult, about 1,300 OSNs converge upon 43 glomeruli in the antennal lobe (AL) (electron micrograph courtesy of Jürgen Berger, MPI-Tübingen, Germany). **B)** Larvae have only 21 OSNs, each of which forms an individual glomerulus in the larval antennal lobe (LAL) (electron micrograph adapted from Cobb, 1999). Schematics adapted from Ramaekers et al., 2005.

a model of olfaction. The numbers of neurons involved in the olfactory circuit is highly reduced at all levels (Figure 1.6). The number of the larval OSNs is compressed to about 1/60th of the adult (Vosshall and Stocker, 2007), greatly

limiting the initial neuronal input to the system. This is a significant advantage for research, since highly reduced redundancy likely illuminates a role of individual neuronal components more clearly than in the adult. The other major benefit of the larvae is in the fact that all the larval OSNs express and require *Or83b* for function (Larsson et al., 2004). In contrast, the adult olfactory system contains *Or83b*-independent components, mainly in coeloconic olfactory sensilla. The larval dependency on *Or83b* affords greater genetic control of the olfactory system.

Robust chemotaxis behavior of larvae has been documented in various studies (Aceves-Pina and Quinn, 1979; Boyle and Cobb, 2005; Cobb, 1999; Cobb and Domain, 2000; Scherer et al., 2003; Schroll et al., 2006). In spite of such a small number of OSNs, larvae are attracted by a surprisingly large number of odorants (Cobb, 1999; Larsson et al., 2004), suggesting that their simple olfactory system does not seem to compromise their odorant detection capacity.

In the following sections, I present the identification of the larval OR repertoire (Chapter 2), followed by the functional characterization of larval OSNs to a panel of odorants (Chapter 3). Armed with these basic findings, functional dissection of the larval olfactory circuit was carried out to illuminate the neuronal process by which larvae encode behaviorally relevant information of an odorant by the “olfactory map” and lateral connections (Chapter 4). The thesis closes with a discussion of the relevance of olfaction for larval survival under conditions of limiting food (Chapter 5).

2. The odorant receptor repertoire of the *Drosophila* larvae

2.1. Introduction: identification of larval odorant receptors

Which ORs do larvae use to smell, and how are they expressed in larval OSNs? This is a fundamental question preceding all the exciting investigations possible in this system. If the simple “one receptor – one OSN” rule applies to the larval olfactory system, it may truly open up the possibility to use larvae as a powerful model organism. If one OSN expresses multiple ORs to compensate for the small number of OSNs, as is the case for the nematode *Caenorhabditis elegans*, we must conclude that larvae use a different odorant coding strategy from adult flies or most vertebrates.

In this Chapter I will characterize the larval odorant receptor repertoire and its expression profile. With only 21 OSNs, it will be possible to characterize all the ORs expressed in all the larval OSNs. This information will be an invaluable foundation toward molecular and cellular dissection of the larval olfactory system.

2.2. Materials and methods

2.2.1. DNA templates

The coding region of the following ORs was used as the template to transcribe RNA probes (size is indicated in the parenthesis): *Or1a* (3.5kb); *Or2a* (1.3kb); *Or7a* (1.4kb); *Or10a* (1.2kb); *Or13a* (1.8kb); *Or22a* (0.8kb); *Or22c* (0.7kb); *Or24a* (0.8kb); *Or30a* (1.5kb); *Or33a* (0.9kb); *Or33b* (0.8kb); *Or35a* (1.0kb); *Or42a*

(1.2kb); *Or42b* (1.1kb); *Or43b* (1.0kb); *Or45a* (1.1kb); *Or45b* (1.2kb); *Or47a* (1.4kb); *Or49a* (1.4kb); *Or59a* (0.9kb); *Or63a* (1.6kb); *Or67b* (1.3kb); *Or74a* (1.0kb); *Or82a* (1.2kb); *Or83a* (1.5kb); *Or83b* (1.4kb); *Or85c* (1.2kb); *Or92a* (1.1kb); *Or94a* (1.1kb); *Or94b* (1.1kb); *Or98b* (1.0kb). They were derived from the fly genome DNA except *Or2a*, *Or22a*, *Or43b*, *Or67b* and *Or83b*, which were derived from *Drosophila* antennal cDNA. Previously described plasmids were used (Vosshall et al., 2000) as templates except for *Or30a*, which was newly amplified from genomic DNA and subcloned into pGEM-T Easy (Promega).

2.2.2. RNA probes

Digoxigenin-conjugated RNA probes were transcribed from the following template DNAs as described previously (Vosshall et al., 2000) (also see http://vosshall.rockefeller.edu/protocols/WebInSituProtocol.pdf): *Or13a*, *Or22c*, *Or30a*, *Or33b*, *Or42a*, *Or42b*, *Or45b*, *Or47a*, *Or59a*, *Or63a*, *Or74a*, *Or83a*, *Or83b*, *Or85c*, *Or92a*, *Or94a*, *Or94b*, *Or98b*. The probes of the rest of tested ORs were taken from the batch previously made (Vosshall et al., 2000) and stored at -20 ^{o}C in formamide.

2.2.3. *in situ* hybridization

Oregon-R (A) third instar larvae were decapitated in 1 × PBS and dissected to remove the digestive tube posterior to esophagus, the salivary gland and fat bodies. The heads were then transferred to plastic embedding molds containing Tissue-Tek OCT (Sakura Finetek), and they were aligned so that the dorsal side

faced the bottom surface. The samples were frozen, and 12 μm frozen sections were processed for *in situ* hybridization with alkaline phosphatase staining as described previously (Vosshall et al., 1999) (also see http://vosshall.rockefeller.edu/protocols/WebInSituProtocol.pdf). Sections were examined under differential interference contrast (Nomarski) microscopy (Eclipse E800, Nikon Instruments), which permitted identification of the dorsal organ ganglion by its characteristic position and morphology.

2.3. Results

2.3.1. Direct detection of the odorant receptor mRNAs expressed in the larval olfactory sensory neurons

I tested mRNA probes for 30 *Drosophila* ORs. Among them, expression of 24 ORs plus *Or83b* was detected by *in situ* hybridization (Figure 2.1C). Each OR was detected in the cell body of only one of the 21 *Or83b*-expressing OSNs per side. Comparison of OR expression among multiple animals implied that a given OR is expressed in an OSN at a stereotypical location (data not shown). This is reminiscent of the topological OR expression on the antenna of adult flies. I did not detect expression of *Or10a*, *Or43b*, *Or49a*, *Or92a* and *Or98b* (data not shown).

In parallel to the *in situ* hybridization screening, Dr. Elane Fishilevich, a former graduate student, generated Gal4 driver lines with promoters of most *Drosophila* ORs (see Fishilevich et al., 2005 for experimental procedures and

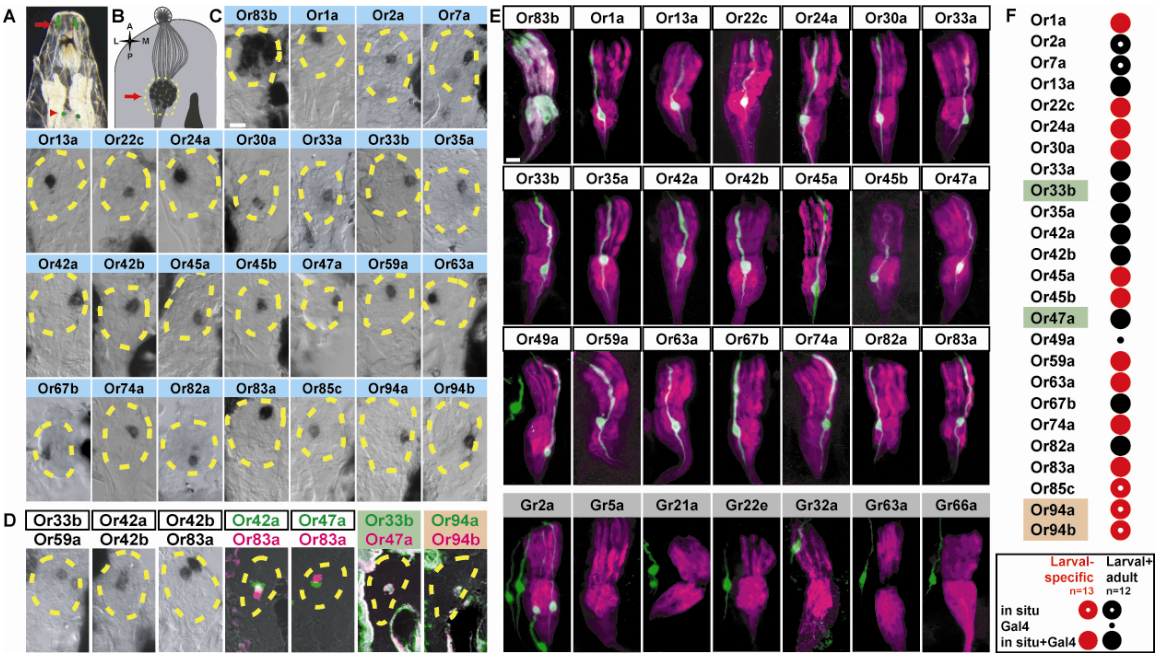

Figure 2.1: Molecular neuroanatomy of the dorsal organ of *Drosophila* larvae

A) Live imaging of GFP in a third instar *Or83b*-Gal4/UAS-GFP larva. Dorsal organ OSNs (red arrow) extend axons that innervate the larval antennal lobe (red arrowhead). **B)** Schematic diagram of the left dorsal organ with the OSN cell bodies indicated with the yellow dotted line. Red arrow is at the same relative position as in A. Orientation of samples in **B-E** is indicated at the left. **C)** RNA *in situ* hybridization shows that *Or83b* mRNA is broadly distributed in the larval dorsal organi and that expression of each larval OR is restricted to a single OSN. The border of the dorsal organ ganglion is indicated by the yellow dotted line in each sample. The scale bar = 10 µm. **D)** RNA in situ hybridization with mixtures of two OR probes reveal five cases of non-overlapping OR expression (left) and two cases of OR co-expression (right). The border of the dorsal organ ganglion is indicated by the yellow dotted line in each sample. **E)** Whole-mount immunofluorescence staining of left larval dorsal organ of 21 different *OrX*-GAL4 driver lines crossed to UAS-GFP with *OrX*-Gal4/UAS-GFP transgenes in green and *Or83b*::Myc in magenta. *Or49a*-GAL4/UAS-GFP labels a single terminal organ gustatory neuron in addition to a single dorsal organ OSN. *GrX*-Gal4/UAS-GFP-positive neurons (green) are distinct from OSNs labeled with *Or83b*::Myc (magenta). The scale bar = 10 µm. **F)** Summary of larval OR gene expression with symbols at bottom of panel. Adapted from Fishilevich et al., 2005.

descriptions of Gal4 lines). To visualize gene expression in the dorsal organ, she crossed these Gal4 lines with a UAS-GFP transgenic line and screened the offspring for GFP expression in larval OSNs. She found expression that 21 out of

42 OR-Gal4 lines (Figure 2.1E) labeled only one larval OSN, with the exception *Or83b*-Gal4, which labeled all 21 larval OSNs. Some gustatory receptors (GRs) are expressed in adult antennae and thus are thought to be involved in olfaction (Jones et al., 2007; Scott et al., 2001). In larvae, however, seven GR-Gal4 lines only labeled the terminal organ neurons or non-olfactory dorsal organ neurons (Figure 2.1E). Observation of OR expression by *in situ* hybridization and Gal4 lines were consistent except for *Or49a*, which was not detected by *in situ* hybridization. The *Or49a*-Gal4 line labeled one OSN in the dorsal organ and another neuron in the terminal organ (Figure 2.1E). Also, five ORs (*Or2a*, *Or7a*, *Or85c*, *Or94a* and *Or94b*) were only verified with *in situ* hybridization, since Gal4 lines for these genes were not available. Overall, we detected expression of 25 ORs and *Or83b* (Figure 2.1F).

As in the adult, co-expression of ORs seems rare (Figure 2.1D). The expression of 25 ORs in 21 OSNs, is achieved by at least two cases of co-expression of multiple ORs per OSN: *Or33b* with *Or47a*, and *Or94a* with *Or94b* (Figure 2.1D). We predict that there are two more cases of OR co-expression in the larva, but they remain unknown thus far.

2.3.2. Organizational principle of larval olfactory sensory neurons

As was previously reported (Tissot et al., 1997), larval OSNs project to the larval antennal lobe (Figure 2.2A,B), the functional homologue of the adult antennal lobe. Dr. Fishilevich visualized the projection of OSNs in the larval antennal lobe using Gal4 lines (Figure 2.2C). Each OSN terminated its axon at a part of the

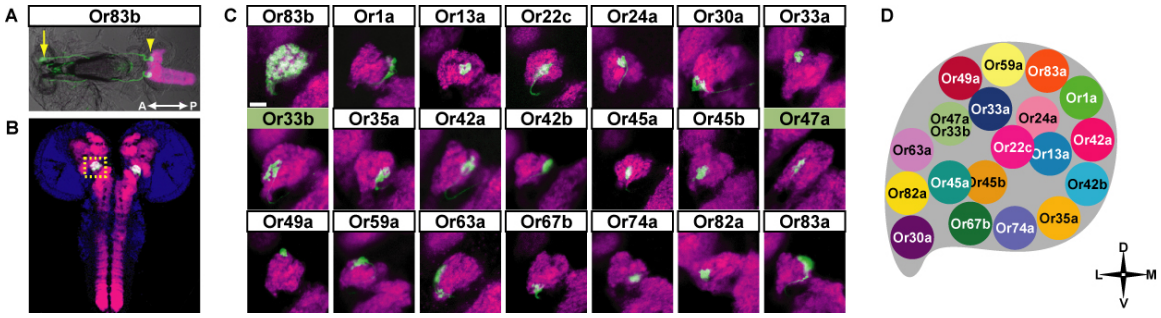

Figure 2.2: Olfactory map in the larval antennal lobe

A) Lateral view of the anterior tip of an *Or83b*-Gal4/UAS-GFP larval with dorsal organ OSNs (geen: yellow arrow) extending axons to the brain (yellow, arrowhead), counterstained with the neuropil antibody nc82 (magenta). The animal is oriented anterior left, posterior right. **B)** Whole mount immunofluorescence staining of an *Or83b*-Gal4/UAS-GFP larval brain which terminals of OSNs (green) in the larval antennal lobe (indicated by yellow dashed square, magnified in **C**. Counterstaining is nc82 (magenta) and a nuclear stain (TOTO-3; blue). **C)** Left antennal lobes of *OrX*-Gal4/UAS-GFP or UAS-CD8::GFP larvae stained with GFP (green) and nc82 (magenta). The left larval antennal lobe is centered in the box. The scale bar = 10 µm. **D)** Flattened representation of the larval antennal lobe glomerular map showing relative positions of glomeruli receiving input from an OR-expressing sensory neuron. Partially overlapping circles represent glomeruli whose position cannot be unambiguously resolved. Orientation of samples **C-D** is indicated at bottom right. Adapted from Fishilevich et al., 2005.

antennal lobe that anatomically resembled a glomerulus-like structure (Python and Stocker, 2002; Ramaekers et al., 2005). The relative position of the "glomerulus" formed by each *OrX*-Gal4 line is consistent across animals. Thus, like in adult antennal lobe, larval OSNs form a map in the antennal lobe identified by the ORs expressed in each of the 21 OSNs (Figure 2.2D). These findings are consistent with the description by another group (Kreher et al., 2005).

2.4. Discussion

2.4.1. Conservation and simplicity of the odorant receptor repertoire in larvae

The results presented above, together with a report from another group (Kreher et al., 2005), established that the larval OSNs follow the same rule of OR expression as adult OSNs. An OSN expresses only one, or in a few cases, two ORs. Moreover, the projection pattern of OSNs in the larval antennal lobe appears analogous to the adult antennal lobe (Couto et al., 2005; Fishilevich and Vosshall, 2005; Vosshall et al., 2000). A big difference between the two developmental stages is that a larval "glomerulus" is formed by only one OSN, contrary to the convergence of many OSNs to a glomerulus in the adult antennal lobe (Vosshall and Stocker, 2007).

Consolidating the screening results from *in situ* hybridization and Gal4 lines, we tested 50 out of 62 *Drosophila* ORs, and concluded that 25 ORs as well as *Or83b* were expressed in the larval olfactory system. There is a possibility that some of the untested ORs are expressed in larval OSNs, resulting in slightly more ORs in the complete larval OR repertoire. However, our results are overall consistent with reports from other groups published at similar time (Kreher et al., 2005). Notably, we are the only group that directly demonstrated OR expression with *in situ* hybridization. The *Drosophila* larva is the first organism in which the complete expression profile of all ORs is characterized for all OSNs.

Out of 25 larval ORs (excluding *Or83b*), 13 are expressed only in the larval OSNs while the remaining 12 ORs are also expressed in adult antennae

and maxillary palps (Couto et al., 2005) (also see Figure 3.4). With the exception of a small cluster of phylogenetically related larval ORs (Hill et al., 2002; Robertson et al., 2003), most larval ORs are not clearly segregated from adult ORs. Interestingly, *Or33b* and *Or47a* are co-expressed in the same OSN(s) both in larvae and adults.

An interesting question is whether ORs specific to the larval stage are common among holometabolous insects. We have to wait for studies in other species since virtually nothing is known about larval ORs in other species apart from yellow fever mosquito *Aedes aegypti*. Larvae of this mosquito species express 23 out of 131 putative ORs, 15 of which are larval specific (Bohbot et al., 2007). Larvae of holometabolous insects usually have very different niche from adults, possibly to avoid direct conflict with adults as well as to focus on accumulating nutrients. It is likely that larvae experience a different olfactory environment than adults, which may necessitate a different set of ORs.

Transcriptional control of larval ORs is another intriguing issue. In *Drosophila*, larval OSNs degenerate during metamorphosis. Unlike in rodents, insect ORs seem to play no role in OSN axon guidance (Dobritsa et al., 2003) and thus are likely to be downstream of OSN fate determination. It is possible that larval OR genes have a *cis*-regulatory element specifically recognized by larval transcriptional factor, as is reported in adults (Ray et al., 2007). Similarly ORs shared with both larvae and adults might possess at least two sets of regulatory elements, one for adult expression and the other for larval expression. In an evolutionary perspective, I would like to speculate that these “shared” ORs

might actually have come first. By this reasoning, ORs of hemimetabolous insects might not show stage-specific expression. During the speciation of holometabolous insects, some ORs could have lost responsiveness to the adult gene regulatory machinery and become larval-specific. Alternatively, new ORs might have been created by gene duplication and have come under the control of adult gene expression regulatory elements. No experimental support is currently available for any of these hypotheses, but studies of OR expression in hemimetabolous insects, such as locusts or cockroaches, could shed light on the evolution of adult and larval ORs.

Lastly, the absence of OSN convergence is an interesting phenomenon. It has been suggested that the OSN convergence reduces influx of noise into the system (Bhandawat et al., 2007). If that is the case, the larval olfactory system has to tolerate a relatively low signal to noise ratio. Whether this affects larval olfactory capacity awaits further investigation.

3. Peripheral odor coding in the larval olfactory system

3.1. Introduction: Odor response profiles of OSNs

3.1.1. Quest for OR ligands

How can we define a natural ligand for ORs? This is not as straightforward question as it is for pharmacologically well characterized receptors. A receptor ligand is a molecule that binds to the receptor of interest and induces a physiological response in cells that express the receptor. The $GABA_A$ receptor, for example, is a chloride channel that opens when GABA (gamma-aminobutyric acid) binds to it (Stephenson, 1988). GABA is known to be present in the nervous system of various species, and is established as a natural ligand of the $GABA_A$ receptor. The AMPA receptor, on the other hand, opens upon binding of glutamate in the brain (Nakanishi, 1992) but is also activated by the pharmacologically identified agonist AMPA. Since AMPA is not present in the vertebrate nervous system, it is not a natural ligand.

The huge number of potential “ligands” and the rather promiscuous nature of ORs (discussed in Chapter 1) is the main obstacle in the quest for OR ligands. Although there are attempts to locate potential odor-binding sites in ORs (Katada et al., 2005; Man et al., 2004), virtually no prediction is available about the affinity of a given OR or the molecular properties of potential odorant ligands. The best approach for matching potential ligands to a specific OR is to catalogue which odorants activate a given OR. I call such a panel of odorants and the response dynamics of an OR-expressing cell the “odor response profile” of the OR. A body

of work has shown that the odor response profile of the OSN expressing a given OR is largely determined by the odor response profile of the OR itself (Bozza et al., 2002; Dobritsa et al., 2003). It should be noted, however, it is not necessarily true for several reasons which I will discuss in the following section.

The odor response profile is a useful initial step toward understanding the neuronal odor code. For example, the specificity of the *Or67d*-expressing OSN in *Drosophila* trichoid sensilla is illuminated by the odor response profile. Out of 86 chemical compounds tested, *Or67d*-expressing OSNs respond only to the pheromone 11-*cis*-vaccenyl acetate (cVA) (van der Goes van Naters and Carlson, 2007; Xu et al., 2005). Similarly, *Gr21a*-expressing OSNs responds exclusively to carbon dioxide (de Bruyne et al., 2001; Jones et al., 2007; Kwon et al., 2007; Suh et al., 2004). As I will revisit in Section 4.1.4, cVA and CO_2 are examples of highly selective ligands that elicit stereotypical behavioral responses. Apart from these exceptions, most conventional ORs show a varied degree of responses to a much wider range of chemicals. It has been suggested that some ORs are “specialists”, responsive to only a small number of odorants, while other ORs are “generalists”, which can be excited by various odorants (Bargmann, 2006; Hildebrand and Shepherd, 1997). This classification may be misleading since the classification is often based on only dozens of odorants. Additional dozens of new odorants in the panel may entirely change conclusions reached with a small odor panel. However, an odorant that elicits response can have behavioral consequence. In the process of narrowing down candidate ligands that can be behaviorally relevant (which will be the main topic in Chapter 4), an odor

response profile from relatively a few odorants can be a useful experimental guide.

3.1.2. Conventional approaches

In vivo recording from OSNs is preferable to reconstruction of ORs in heterologous cells in capturing the odor response profile. Although widely used, heterologous expression of ORs has a major drawback in missing accessory proteins that assist proper OR function (Carr et al., 1990). Without these perireceptor molecules, ORs may fail to respond properly to odorants. Examples include vertebrate membrane proteins required for proper OR translocation to the cell membrane (Saito et al., 2004; Zhuang and Matsunami, 2007), insect odorant binding proteins (Xu et al., 2005) and an accessory membrane protein (Benton et al., 2007) necessary for pheromone-evoked activity in fly OSNs, and even unknown components in vertebrate nasal mucosa (Oka et al., 2006). As was mentioned in Section 1.5.2., insect *Or83b* orthologues can be considered one such an accessory molecule.

Extracellular recording of odor-evoked spikes of native OSNs present in a given sensillum is the most direct readout of odor-evoked activities. In cases where multiple OSNs are present in a given sensillum, spike sorting can be carried out to distinguish different single cell responses. In larvae, all 21 OSNs are present in the same dorsal organ dome, precluding meaningful analysis of electrophysiological recording in this preparation (Kreher et al., 2005; Oppliger et al., 2000). To circumvent this problem, John Carlson and his colleagues

expressed larval ORs in an adult OSN genetically depleted of its endogenous ligand binding ORs. In this so-called “empty neuron” approach (Dobritsa et al., 2003), mutant flies lacking *Or22a* and *Or22b* show no odor-evoked responses in the ab3A class of neuron (Dobritsa et al., 2003). By using the Gal4-UAS system, insect ORs lacking known ligands can be expressed in this otherwise “empty” OSN (Hallem et al., 2004). His group expressed a subset of larval OSNs and compiled odor response profiles (Kreher et al., 2005). One potential disadvantage of profiling larval ORs in the adult “empty” OSN system is the potential to miss larval specific perireceptor molecules or OR co-expression in the response profile.

3.1.3. *in vivo* calcium imaging

Calcium imaging is a powerful alternative to link odor ligands with individual larval OSNs. This technique is extensively used for mammalian OSNs, since calcium is a crucial second messenger in G-protein mediated signal transduction cascade (Zufall et al., 1994). Application of calcium imaging in *Drosophila* has been also successful. A recent study suggests that insect ORs themselves form non-selective cation channel, so calcium may flux into an OSN when odorants bind to the ORs (Sato, 2008). In fact, insect OSNs show robust increases in intracellular calcium in response to odorants, which can be measured both in the OSN cell bodies and at axonal terminals in the antennal lobe (Pelz et al., 2006; Silbering and Galizia, 2007; Wang et al., 2003). Since insect glomeruli are anatomically identifiable, recording across the antennal lobe with calcium imaging makes it

possible to visualize the functional odor “map”. This can be an enormously efficient approach to generate odor response profiles in multiple classes of OSNs. Moreover, the same technique can be applied to other populations of neurons in the olfactory system (Fiala et al., 2002; Wang et al., 2003; Wang et al., 2004a; Yu et al., 2003; Yu et al., 2005). Versatility of *Drosophila* genetics allows expression of genetically encoded calcium indicator in specific population of neurons. This approach eliminates ambiguity of the origin of signal in bath application of synthesized calcium indicator, which is commonly used for heterologous systems or animal preparations where genetic tools are not yet available (Galizia et al., 2000; Galizia et al., 1999b; Jorerges, 1997).

Calcium release is an indirect readout of the electrical response of neurons. Intracellular calcium is usually maintained at low concentration in a cell, and calcium ions are likely to flow into cytoplasm through non-selective cation channels or voltage-gated calcium channels in an activated neuron (Augustine et al., 2003; Reid et al., 2003). At presynaptic sites, in particular, calcium plays an integral part of the synaptic vesicle fusion process (Rizo et al., 2006; Sudhof, 1995). A precise correlation of spike frequency and calcium ion increase in a neuron may not be achievable and most certainly differs with neuronal types. Thus, caution should be taken to interpret the calcium signal, especially as it has been shown that low frequency neuronal firing goes undetected by calcium indicators (Pologruto et al., 2004). It is desirable to calibrate calcium imaging responses with electrical responses to verify and aid in the meaningful interpretation of calcium imaging data.

I chose to use the calcium imaging approach to obtain insight into peripheral olfactory coding of larvae. Functional larval OSNs are equipped with all the molecular machinery necessary for signal transduction. Since the calcium indicator can be monitored in the larval OSNs, the response is likely to reflect "true" odorant-evoked activity.

3.2. Materials and methods

3.2.1. Fly stocks

yw: GC56; CyO/Sp; GC25 is a gift from Dr. Allan Wong (Columbia University, New York). This fly carries two *UAS- G-CaMP1.3* (Nakai et al., 2001) on the X chromosome (*GC56*: (Wang et al., 2003)) and another two *UAS- G-CaMP1.3* on the third chromosome (*GC25*: Allan Wong, personal communication). Higher copy number of *UAS- G-CaMP1.3* was necessary to elevate fluorescence in larval OSNs. This fly was crossed with the following flies carrying *OrX-GAL4* on the second chromosome to generate *yw: GC56; OrX-GAL4/(CyO); GC24*:(Fishilevich et al., 2005) *Or1a-GAL4, Or13a-GAL4, Or22c-GAL4, Or33a-GAL4, Or35a-GAL4, Or42a-GAL4 #1, Or42a-GAL4 #2, Or42b-GAL4, Or47a-GAL4, Or49a-GAL4, Or82a-GAL4, Or83a-GAL4*. Among them, fluorescence from the axon terminal of *Or49a*-expressing OSN was too weak to image, and thus was not used for the calcium imaging experiment described in Section 3.2.2.

To generate *yw: GC56; Or42a-GAL4 #2; Or83b^2: UAS-Or83b: GC25*, a recombinant of *GC25* and *Or83b^2* was first made. Then, *UAS-Or83b: Or83b^2* and *UAS-Or83b^2: Or83b^2* were crossed to obtain *w1118; +; UAS-Or83b: Or83b^2:*

GC25. Genotypes were confirmed with diagnostic PCR. *Or83b*^{2} (Larsson et al., 2004) and *UAS-Or83b* (Benton et al., 2006) were previously described.

3.2.2. Sample preparation

yw: GC56; OrX-GAL4; GC25 virgin female flies and *yw: GC56; OrY-GAL4; GC25* males (OrX and OrY were one of the fly strains listed on Section 3.2.1.) were crossed to generate F1 *yw: GC56; OrX-GAL4/OrY-GAL4; GC25* larvae, which were used for imaging experiments. The only exception was *yw: GC56; Or83a-GAL4/CyO; GC25*, from which larvae were directly used since *Or83a-GAL4* caused homozygous lethality.

Feeding third instar larvae were collected and rinsed in 1 × PBS briefly to remove food particles. Larvae were then transferred to the imaging Ringer's solution (Wang et al., 2003) without calcium, and were dissected to remove the digestive tube posterior to esophagus, the salivary gland and fat bodies. This reduced head preparation was then transferred to the imaging plastic frame. This frame, cut in 20mm × 20mm from HybriSlip (Grace Biolabs), have four round holes (2mm diameter) covered with a small square piece of western blot plastic bag. A small rhomboid-shaped window was cut inside each hole on the membrane, and the frame was fixed on the hole (18mm diameter) punched in the middle of the Petri dish top with dental wax (Modern Materials). One larval head was introduced in the droplet of the imaging Ringer's solution with 2mM calcium on each hole. Thus, there were four samples on one frame. The Ringer's solution was temporarily drained, and the head was inserted through the window so that

the anterior end of the head, including the dorsal organ, faced down below the membrane while the brain remained above the membrane. The 10μl of the Ringer's solution containing 2mM calcium and 0.5% low melt agarose (type IX, Sigma) was then applied to the each hole, and the samples were briefly chilled at 4 degree for 3 minutes to solidify the agarose. The samples were then immediately used for the imaging experiment.

3.2.3. The odor stimulation device

All the odors were obtained from Sigma-Aldrich or Fluka (except for 4-methyl phenol, which was from Spelco) at high purity, and their common names together with CAS numbers are as follows: geranyl acetate (CAS 105-87-3), ethyl acetate (CAS 141-78-6), ethyl butyrate (CAS 105-54-4), isoamyl acetate (CAS 123-92-2), pentyl acetate (CAS 628-63-7), hexyl acetate (CAS 142-92-7), octyl acetate (CAS 112-14-1), 1-hexanol (CAS 111-27-3), 1-octen-3-ol (CAS 3391-86-4), isoamyl alcohol (CAS 123-51-3), cyclohexanol (CAS 108-93-0), 2-phenyl ethanol (CAS 60-12-8), 2-heptanone (CAS 110-43-0), cyclohexanone (CAS 108-94-1), E2-hexenal (CAS 6728-26-3), octanal (CAS 124-13-0), acetophenone (CAS 98-86-2), anisole (CAS 100-66-3), methyl salicylate (CAS 119-36-8), 4-methyl phenol (CAS 106-44-5), acetyl furan (CAS 1192-62-7), propyl sulfide (CAS 111-47-7).

Five microliters of pure odorant were diluted into 495μl of paraffin oil to make 10^{-2} dilution odorant stock. This stock was prepared fresh every month. Ten microliters of the diluted odorant was applied to a piece of 1/4" filter paper

(Whatman), which was subsequently pushed into a 1ml plastic syringe (BD Life Science), called an odorant syringe. The same odorant syringe was used no more than 3 times.

A constant air stream (1000 ml/sec) from an aquarium pump was humidified and filtered with an active charcoal filter (Whatman). The air was guided with Teflon tubing (1/8” diameter, Fisher Scientific) to a solenoid valve (The Lee Co.) connected to BPS-4 valve control box (ALA Scientific Instruments). The “Normally Closed” side was connected with an odorant syringe, which was merged with the “Normally Open” side at the downstream. The tubing exit was located about 1cm away from the dorsal organ of the larvae under the microscopy. To avoid contamination, the tubing directly connecting an odor syringe was exchanged after each use. During the experiment, air from the odor delivery system was constantly removed with vacuum.

3.2.4. Calcium imaging setup and data acquisition

Calcium imaging was performed with Eclipse E600FN microscopy (Nikon Instruments) with x60 water immersion lens. The samples on the Petri dish (described in Section 3.2.2.) were placed under the objective lens with aluminum ring. The excitation light was provided by a metal halide lamp (X-Cite 120, EXFO Photonics Solutions, Inc.) and an image was acquired from a charge-coupled device (CCD) camera (SensiCamQE, pco. imaging) through narrow-band GFP filter (excitation wavelength: 480 nm, emission wavelength: 510nm, 41020,

Chroma). The intensity of the excitation light was reduced with either ND4 or ND8 filter to avoid bleaching of G-CaMP during the imaging.

One session of a sample consists of applications of 22 odors and paraffin oil. We call the individual application of an odor a trial: thus, one session consists of 23 trials. Each odor was applied only once unless the sample moved out of the region of interest during a trial. The order of the odors was randomly determined for each session. The interval of each trial was about 100 seconds, and the saline was replaced every 15 minutes.

In a trial, images were acquired at five frames per second at a resolution of 72 x 72 pixels (binned 8 x 8). The exposure time was 50 milliseconds. The electrically controlled shutter allowed the excitation light to reach the sample only during the image acquisition in order to reduce bleaching of G-CaMP. Three seconds after the initiation of imaging, the valve was flipped to the “Normally Closed” side for 1 second. Thus, 1 second of an odor pulse was applied to the sample. Images were taken 8 seconds thereafter. Thus, the total time for one trial was 12 seconds (3 seconds for pre-stimulus, 1 second for odor stimulus and 8 seconds for post-stimulus). An acquisition of images by CCD camera, the shutter, and the opening of valve were all controlled by a custom-made protocol program on TILL visION software (TILL Photonics, Inc.).

Trials of “reference odors” were inserted several times during and at the end of a session. This was intended to check that the condition of samples remained stable over the entire session. A session was excluded from data analysis if the amplitude and time course of responses to reference odors

underwent a gross change (loss of response, belated onset of response etc.). Some samples showed decreased amplitude of response to reference odors during the session (up to 20%), but it was not considered as a gross change.

3.2.5. Data analysis

The data was analyzed using a custom program in IDL6.2 (ITT), which was written and kindly provided by Dr. Mathias Ditzen for our use. Trials that suffered from excessive movement were discarded, and the rest of the trials underwent movement correction if necessary. This was carried out by shifting each frame relative to the reference frame (frame #14) so that axon terminals of OSNs were situated on the same coordinate throughout the trial. The fluorescent value was then calculated by averaging the fluorescence intensity within the region of interest for each OSN in each frame (designated as F_n for n-th frame). The relative change of the fluorescence, or ΔF/F, was then calculated as follows:

$$\left(\frac{\Delta F}{F}\right)_n = \left(F_n - \frac{\sum_{i=10}^{14} F_i}{5}\right) \Bigg/ \frac{\sum_{i=10}^{14} F_i}{5}$$

$(\Delta F/F)_n$ is thus defined as fluorescence intensity relative to the average fluorescence intensity during one second right before the onset of odor stimulation.

The first one second was excluded from the false color-coded plots since the bleaching of fluorescence was significant. Nonetheless, the fluorescence of OSNs usually decreased by about 10% by the end of each trial. No correction was made for the bleaching, since odor-evoked responses, if existed, were strong and robust enough. The time courses of ΔF/F were then converted to the false color-coded plots by using Matlab (The Mathworks).

3.3. Results

3.3.1. Odor-evoked increase of the intracellular calcium concentration

G-CaMP is a genetically encoded calcium indicator derived from GFP. It increases its intensity when calcium ion binds and restores GFP conformation (Nakai et al., 2001). Thus, excitation of OSNs by an odorant can be visualized by positive change of relative fluorescence intensity (ΔF/F). When G-CaMP was expressed in a pair of OSNs by using a larval OR-Gal4 driver, the fluorescence could be unambiguously monitored for each of these genetically labeled OSNs (Figure 3.1B).

I invented a sample preparation to allow semi *in vivo* recording from the axon termini of OSNs (Figure 3.1A). Odor stimulation was applied in the air phase for one second. An example of the time course of ΔF/F is shown in Figure 3.1C. G-CaMP becomes brighter immediately after the onset of odor stimulation, and gradually returned to the basal level of fluorescence. The duration of elevated fluorescence depended on the combination of OSN and odorant. For example, both hexyl acetate

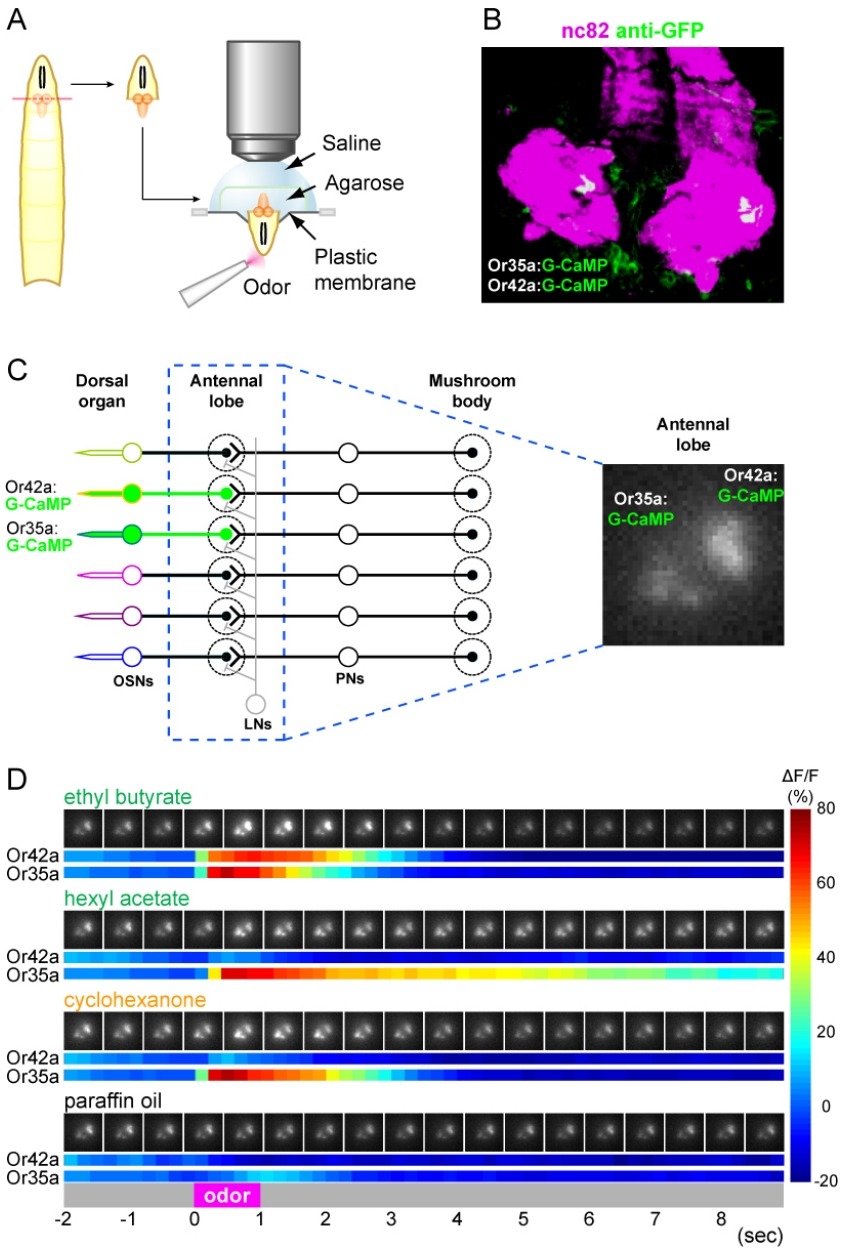

Figure 3.1: Odor-evoked activity of OSNs is visualized in the larval brain

A) Schematic representation of the imaging setup. Reduced semi *in vivo* preparation of a larva is placed under the microscope. **B)** Whole mount immunofluorescence staining of an *Or35a*-Gal4/*Or42a*-Gal4; *UAS- G-CaMP* larva with terminals of the two OSNs in the larval antennal lobe. G-CaMP was stained with anti-GFP antibody (green), and neuropil was stained with nc82 (magenta). **C)** Schematic for measuring functional activation of the larval OSNs using G-CaMP (left) and intrinsic G-CaMP fluorescence of the two OSNs viewed through the imaging microscopy (right). **D)** Calcium dynamics in response to three odorants and paraffin oil (solvent) are visualized with G-CaMP. The interval between the raw fluorescent images is 600 milliseconds. Below are false color-coded time traces represented by ΔF/F (see Materials and Methods 3.2.5. for definition). Scale of ΔF/F(%) is on right. Time axis is at the bottom, with the time point zero set at the odor stimulus onset.

and cyclohexanone evoke robust fluorescence increase at the axon terminal of the *Or35a*-expressing OSN, but not in the *Or42a*-expressing OSN. The duration of signal, however, is significantly longer in the response to hexyl acetate than in the response to cyclohexanone.

3.3.2. The odor response profile of selected larval olfactory sensory neurons

I prepared a panel of 22 odorants to construct odor response profile of 11 OSNs. The odor panel consists of various types of chemicals such as esters, alcohols, aromatics and so on. For each OSN, 7 to 9 recordings from different animals were made. Figure 3.2 represents such odor response profiles. The responses are fairly consistent across samples: odorants evoke responses in only a subset of OSNs, and their durations vary among them. I did not observe consistent decrease of ΔF/F, which could represent inhibitory response. Basal activity is largely absent in all the OSNs except the *Or82a*-expressing OSN, which often showed spontaneous fluctuation of fluorescence intensity.

Among the tested OSNs, the OSNs expressing *Or35a*, *Or47a* and *Or82a* have been studied in adult antennae with single sensillum recording (Hallem and Carlson, 2006). The response profiles of these ORs, represented as spike frequency, qualitatively matched my data (Figure 3.3), supporting the idea that calcium signal well reports excitatory response of OSNs. The result suggests that the OR predominantly determines odor response profile of OSNs in both adult and larva.

Figure 3.2: Odor-evoked responses in the subpopulation of larval OSNs

Odor response profiles of 11 OSNs against the panel of 22 odorants and paraffin oil (solvent) are shown. Chemical structures and categories of 22 odorants are shown at top left corner. Each trace represent ΔF/F (%) scaled according to the scale bar at bottom right. Responses of an OSN to one odorant are stacks of traces from 7-9 independent animals.

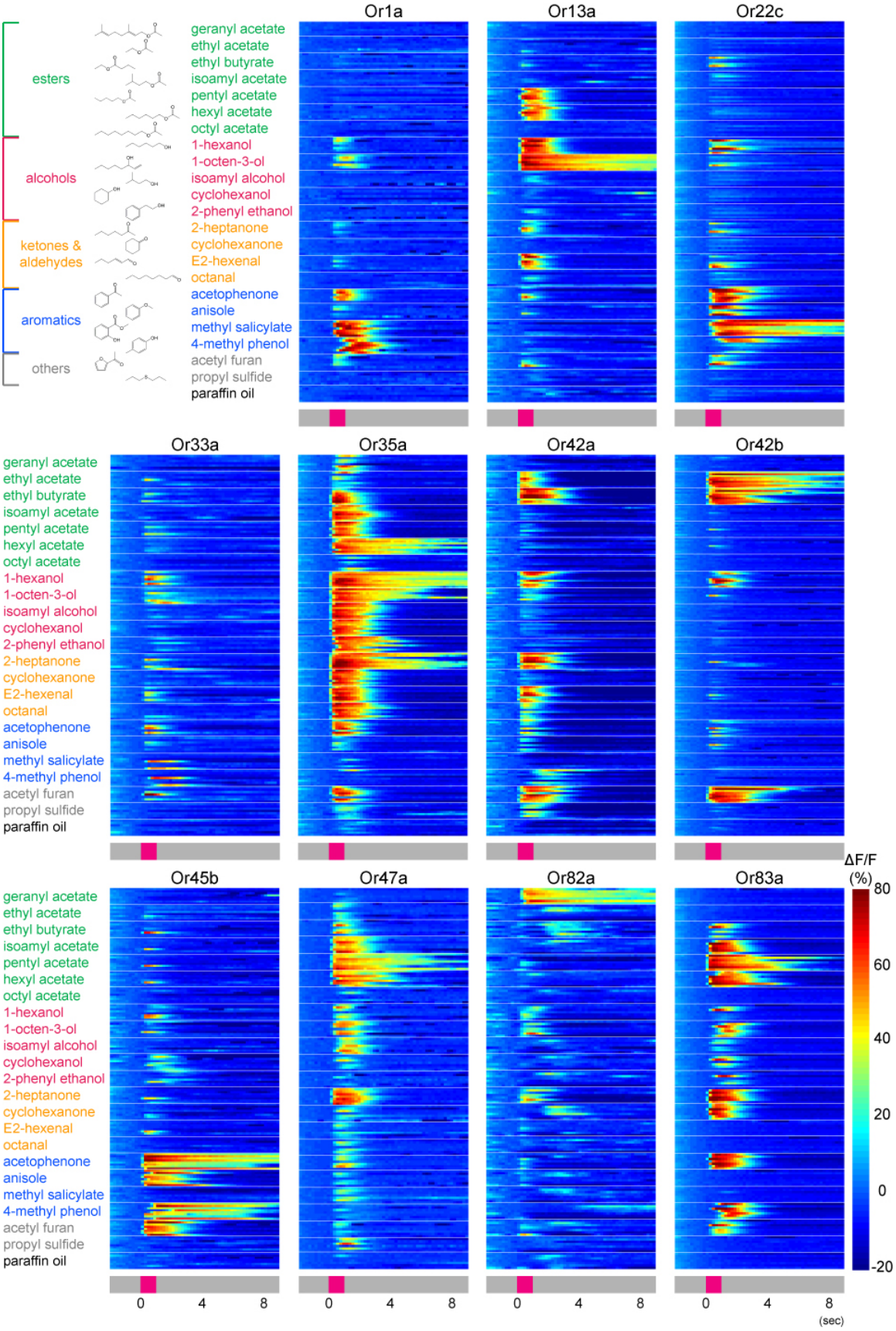
esters
alcohols
ketones & aldehydes
aromatics
others
geranyl acetate
ethyl acetate
ethyl butyrate
isoamyl acetate
pentyl acetate
hexyl acetate
octyl acetate
1-hexanol
1-octen-3-ol
isoamyl alcohol
cyclohexanol
2-phenyl ethanol
2-heptanone
cyclohexanone
E2-hexenal
octanal
acetophenone
anisole
methyl salicylate
4-methyl phenol
acetyl furan
propyl sulfide
paraffin oil
Or1a
Or13a
Or22c
Or33a
Or35a
Or42a
Or42b
Or45b
Or47a
Or82a
Or83a
ΔF/F (%)
80
60
40
20
0
-20
0
4
8
(sec)

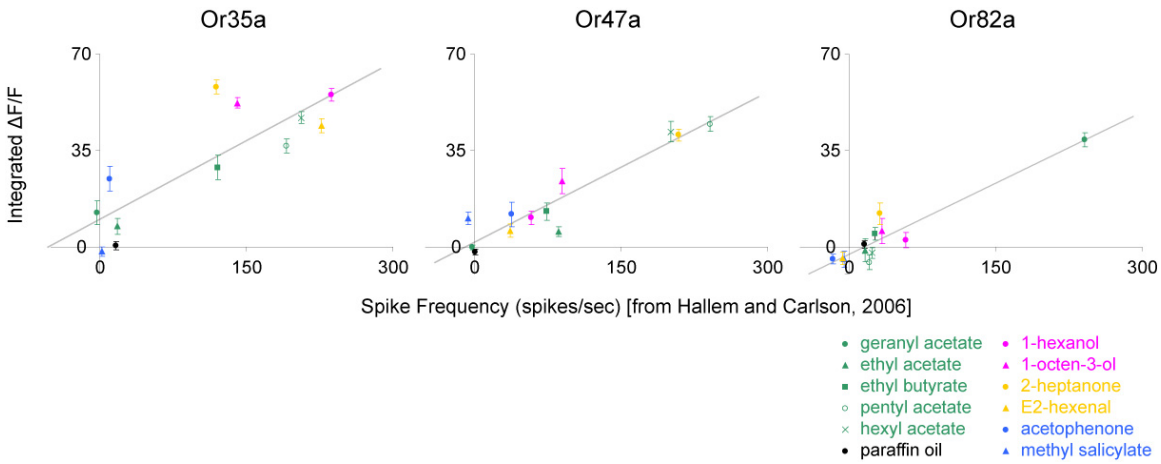

Figure 3.3: Calcium signal correlates with spike frequency

Integrated ΔF/F was calculated as the average ΔF/F during 0-3 seconds after the onset of odor stimulus. Error bars represent S.E.M. (n = 7 for *Or47a* and *Or82a*, n = 8 for *Or35a*). Spike frequencies are adapted from Hallem and Carlson, 2006. Odorant legends are listed at bottom right. Regression equation (grey line) for each OR is: y = 0.190x + 10.0 for *Or35a* (R^2 = 0.689), y = 0.182x + 1.61 (R^2 = 0.830) for *Or47a,* y = 0.172x – 2.79 for *Or82a* (R^2 = 0.890)

While this study was conducted, another group characterized a subset of larval ORs by expressing them in adult "empty" ab3A OSNs (Kreher et al., 2005). They tested 11 larval ORs; among them, *Or42a* (also expressed in adult maxillary palp) and *Or45b* were examined in my study. Although exact figures of spike frequency were not published, their qualitative odor response profiles of these two ORs match well with my calcium imaging data. By consolidating these two data and additional publications, odor response profile of 19 out of 25 larval ORs (19 larval OSNs) are now available.

Previous findings suggested that the larval ORs could be categorized into Class 1 (sensitive to aliphatic compounds) and Class 2 (sensitive to aromatic

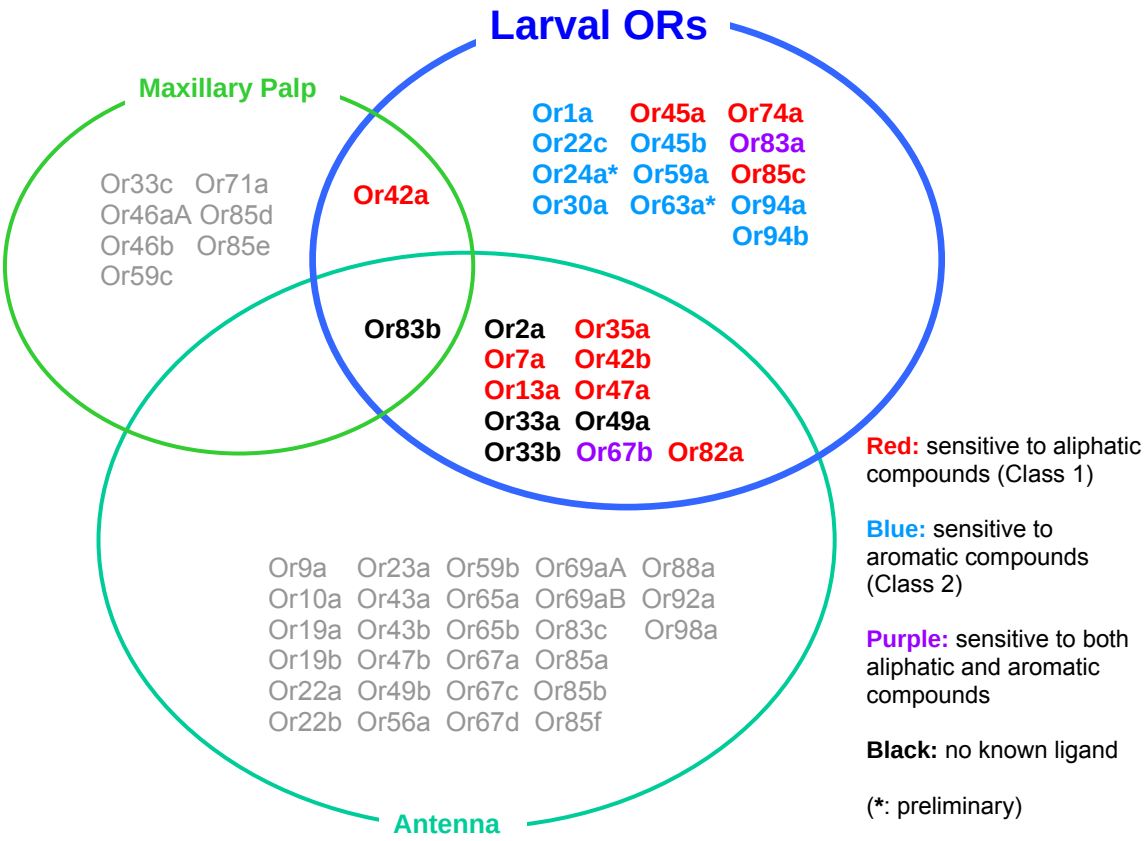

Figure 3.4: Expression pattern of *Drosophila* ORs in adult and larval olfactory organs

OR expression in adult antenna and maxillary palp is based on Fishilevich and Vosshall, 2005 and Couto et al., 2005. Classification of larval ORs (listed lower right) is based on the current study, Kreher et al., 2005 and Hallem and Carlson, 2006. *Or24a* and *Or63a* appear to be Class 2 receptors based on my preliminary data.

compounds) (Kreher et al., 2005). Among the OSNs I tested here, *Or1a, Or22c*, and *Or45b* are members of Class 2 receptors while the rest except *Or33a* are Class 2 receptors. I did not find an odorant which consistently activated *Or33a*-expressing OSNs. Preliminary data implies that *Or24a* and *Or63a* belong to Class 2 (data not shown), although more studies are needed to confirm this.

Interestingly, ORs expressed only in larval OSNs are almost all Class 2 receptors, while ORs shared with adult and larva tend to be Class 1 receptors (Figure 3.4).

3.4. Discussion

3.4.1. Calcium imaging: application to larval neurons

Calcium imaging is useful in monitoring neuronal activities in larval OSNs, which are not easily accessible either by extracellular recording or the electro-dorsogram, which records spikes from all 21 OSNs by inserting an electrode in the dome of the dorsal organ. At axon termini, calcium is required for synaptic vesicle fusion because the function of SNAREs requires calcium ions, which means that the calcium increase there likely represents synaptic transmission of neurons. Indeed, the odor response profile obtained in this research agrees well with electrophysiological data about the ORs presented elsewhere.

In this study, only two OSNs were imaged simultaneously. Thus, the major advantage of imaging technique that many neurons can be recorded was not fully exploited in this work. It was mainly because fluorescent signals from all OSNs by using *Or83b-Gal4* could not be spatially resolved (data not shown). As was stated in Chapter 2, glomeruli in the larval antennal lobe cannot be identified unless individual OSN termini are labeled.

This is the first recording of an odor-evoked response from molecularly defined larval OSNs. Their odor response profiles are in good agreement with those characterized as OR odor response profiles (*Or35a*, *Or42a*, *Or45b*, *Or47a* and *Or82a*) in adult “empty OSN” preparation (Hallem and Carlson, 2006; Kreher

et al., 2005). Among them, *Or45b* is a larval-specific OR. *Or45b* therefore seems to require no additional molecule to function even when ectopically expressed in an adult OSN.

3.4.2. Classification of the olfactory sensory neurons by odor tuning: implications

Apart from *Or24a* and *Or63a*, all the larval ORs are now functionally characterized by this study and the previous study by (Kreher et al., 2005). This means that *Drosophila* larva provides the most extensive information about peripheral representation of odorants among the model organisms.

It is curious that larval-specific ORs tend to respond to aromatic odorants preferentially. Aromatic odorants seem to be rather rare in fruits where larvae usually forage for food. Nonetheless, there should be undiscovered odorants in larval niche, possibly emitted from fruits or yeast, the larval food source. It is possible that, as was stated in Chapter 2, unknown aromatic odorants could play an important role specifically for larvae. Such odorants can be of low abundance. Combining calcium imaging with gas chromatography-mass spectrometry (GC-MS) analysis could help to identify natural ligands for these OSNs (Stensmyr et al., 2003b).

ORs shared with adult and larval stages are mostly sensitive to aliphatic compounds. Esters, alcohols and ketones are widely found in fruits. Thus, Class 1 receptors may be tuned to odorants important for both adults and larvae. It is interesting to note that only one of the ORs expressed in adult trichoid sensilla

(Couto et al., 2005), *Or2a*, is expressed in larvae. Trichoid sensilla are not sensitive to food odors, but a subset of trichoid OSNs recognizes odors emitted from adult flies, including the pheromone cVA (van der Goes van Naters and Carlson, 2007). Such odorants possibly mediate social behaviors specific to adults. If it is indeed the case, the trichoid ORs are unnecessary for larval stage. Indeed, all the four ORs sensitive to fly odors are specific to adults (van der Goes van Naters and Carlson, 2007). This includes *Or67d*, the cVA receptor (Ha and Smith, 2006), which has been already mentioned several times. These ORs might be added to *Drosophila* OR repertoire after they differentiated from hemimetabolous insects.

4. From perception to behavior: how ethyl butyrate is encoded in the olfactory network

4.1. Introduction: models of the odor coding by higher order neurons

The odor response profile of larval OSNs provides a glimpse into the initial mechanism by which an odorant is encoded by the ensemble of OSNs. But how is this peripheral odor information transformed into the percept of the odorant in the brain of the larva? Theories on the neural basis of odor coding have been repeatedly proposed. The primary focus has been on the vertebrate olfactory bulb and insect antennal lobe, since the orderly neuronal connections and numerous intrinsic local interneurons offers substrates for computation and processing, like the retina in the visual system. Because of technical limitations, these theories largely rely on physiological observation and computational modeling. There are two main theories of odor coding: *faithful transmission* and *dispersed coding*. Although often presented as mutually exclusive theories, I believe they merely represent two sides of the same theory, with only a difference of emphasis. I also must point out the validity of either theory still awaits behavioral and cognitive validation.

4.1.1. Faithful transmission of odor response

The *faithful transmission* theory maintains that OSN input to the olfactory bulb or antennal lobe is “faithfully” transmitted to second order neurons with essentially no modification. In this way, the combinatorial “odor code” encoded by

populations of OSNs is translated to the activity of corresponding combination of M/T cells or projection neurons. Such faithful transmission has been proposed in studies of how mitral cells in vertebrates respond to odorants (Mori et al., 1992). It has further been confirmed in optical imaging experiments in the *Drosophila* antennal lobe, in which excitatory activities of the OSN axon termini are faithfully relayed to the activities of PN dendrites in the fly antennal lobe (Ng et al., 2002; Wang et al., 2003). The same set of glomeruli was recruited no matter whether they were imaged from OSNs or projection neurons. Thus, the combinatorial code at the antennal lobe is shared between the two populations of the olfactory neurons, and the antennal lobe seems to play minimal, if any, role in processing the olfactory information. The identity of an odorant is determined by the specific combination of OSNs, and remains unaltered thereafter.

There are several weaknesses in this simple theory. A part of the weakness arises from the technical limitations of optical imaging. In calcium imaging, it is unclear if calcium increases at OSN axon termini and projection neuron dendrites (Wang et al., 2003) are functionally comparable. Also, presynaptic sites in projection neuron dendrites are not documented by electron microscopy or molecular markers, so it remains a mystery from where the signal of synaptic vesicle release derives (Ng et al., 2002). It is difficult to reconcile faithful transmission with the richly documented inhibitory and excitatory networks in the antennal lobe. If there is no change before and after “processing” in the antennal lobe, what is the meaning of having the antennal lobe anyway? Indeed, if the projection neurons only passively receive OSN inputs, neuronal

activity remains localized to selected projection neurons, contradicting the hypothesized optimal distribution of firing across population of projection neurons (Abbott and Luo, 2007).

A compromise is that the antennal lobe “sharpens” the odor code presented by the OSNs. As was mentioned in the first Chapter, vertebrate lateral inhibition is proposed to enhance contrast among closely related odorants. Likewise, the GABA-mediated inhibitory network in honeybee is considered to optimize the glomerular code in the projection neurons (Sachse and Galizia, 2002). This hypothesis states that weak activity of OSNs is quenched by global inhibition in the antennal lobe. As a result, projection neurons can be excited by OSNs with the most robust activity. The overall glomerular odor code is therefore maintained, but unreliable activity is filtered out. Even though this is not mechanistically the same as lateral inhibition in other sensory centers, global inhibition can nonetheless increases signal-to-noise ratio of the olfactory information. Interestingly, a minimum threshold of activity is necessary to evoke lateral inhibition in mouse olfactory bulb (Arevian et al., 2008). This finding implies that only a strongly excited glomerulus can impose inhibition to the surround, thus sharpening its activity against the background.

4.1.2. Dispersed activity as the substrate of odor code

Electrophysiological examination of projection neurons in *Drosophila* has revealed more complicated odor-evoked firing pattern than the faithful transmission theory anticipates. Instead of “sharpening”, the projection neurons

seem to disperse the odor code. They show high spontaneous activity (Wilson et al., 2004), and can be excited to differing degrees by many more odorants than expected based on the odor response profile of the OSNs innervating the same glomerulus (Bhandawat et al., 2007; Schlief and Wilson, 2007; Wilson et al., 2004). For example, projection neurons innervating the DM2 glomerulus in the *Drosophila* antennal lobe can respond to many more odorants than the *Or22a*-expressing OSNs that project to the DM2 glomerulus (Wilson et al., 2004). These data are a strong rebuke to faithful transmission of the combinatorial odor code from OSNs to the projection neurons.

What could be the mechanism of the dispersed projection neuron activities? As was mentioned, the *Drosophila* antennal lobe has excitatory local interneurons (Shang et al., 2007). It is possible that the excitatory interneurons can activate projection neurons innervating different glomeruli in response to excitation from limited number of glomeruli (Olsen et al., 2007). Alternatively, convergence of OSNs can improve signal-to-noise ratio, which can result in a more reliable and sensitive response of the projection neurons (Bhandawat et al., 2007). The discrepancy between the response of OSNs and projection neurons on the same glomerulus may not be as large as is argued (Bargmann, 2006). Thus, what is thought to be the promiscuous activation of projection neurons may be simply due to the pooling of OSN inputs. If even one OSN fires at a low rate, summation of 30 such OSNs can reliably excite cognate projection neurons. Furthermore, if a spike from an OSN can increase excitability of the synapsing projection neurons to spikes that follow afterwards, relatively few OSN spikes can

induce vigorous spiking in the projection neurons. Such positive feedback effect by “facilitating synapses” (Abbott and Regehr, 2004) can even enhance the convergence effect on a glomerulus.

Dispersed coding, as seen in the unexpectedly broad activity of projection neurons, has important implications for how the brain sees odors. It may appear difficult to encode a large number of odorants if the same spreading phenomenon is applied to every odorant, since there will be a huge overlap between any two codes at the level of the projection neurons. Supporters of dispersed coding therefore argue that temporal information is important for the complete coding of an odorant by the projection neurons (Wilson et al., 2004). In principle, the temporal aspect of neuronal activity will increase dimension and thus afford more “space” to encode more odorants (Wilson et al., 2004). Distributing odor-evoked activity dispersed to a wide population of projection neurons can theoretically optimize discriminatory power (Abbott and Luo, 2007). At least in mammals, the time window for the integration of temporal dynamics should be rather short. Rats or mice can discriminate odorants within 300 ms after odor stimulation (Abraham et al., 2004; Rinberg et al., 2006; Uchida and Mainen, 2003). Based on behavioral evidence, the slow evolution of odor identity from neuronal activities noted in the fish olfactory system (Friedrich and Laurent, 2001) is therefore most likely behaviorally irrelevant.

4.1.3. Olfactory “labeled line” coding: odor perception without combinatorials

Lastly, I would like to introduce the simplest scheme for odor coding. In this scheme, if the OSN specialized for the detection of the odorant is sufficient to evoke the behavior, all the downstream neurons must be hard-wired all the way down to the set of motorneurons. Thus, the excitation of the OSN can trigger all the necessary activities of the neuron to induce the specific behavior. This dedicated circuit is called a labeled line. A key factor is that there is only one input channel: no neuronal integration is necessary.

Anatomical and physiological studies of fly pheromones support the labeled line model. In *Drosophila*, *Or67d*-expressing OSNs are the entrance of one labeled line to suppress courtship behavior toward males and mated females. It is because the only known ligand of *Or67d*, cVA, is sufficient to suppress courtship behavior of males, and deletion of *Or67d* causes abnormally high rate of courtship behavior toward males and mated females (Kurtovic et al., 2007). Moreover, artificial activation of this OSN is sufficient to evoke the same courtship suppression (Kurtovic et al., 2007). Likewise, *Gr21a*-expressing OSNs form another labeled line. *Gr21a*-expressing OSNs sense carbon dioxide (de Bruyne et al., 2001; Suh et al., 2004), which is a strong repellent to flies. Again, artificial activation of this population of neurons is sufficient to cause avoidance behavior (Suh et al., 2007). These are similar to taste coding in both vertebrates and insect, where activity of a certain population of gustatory sensory neurons causes attraction or avoidance to animals.

Why not use labeled line coding for other OSNs? In this scheme, one species of odorant molecule is “coded” by only one glomerulus, which is responsible for the entire perception of that particular odorant. This idea was proposed based on the finding that natural scents, such as coffee or clove smell, presented at low concentrations activated relatively few glomeruli in mouse olfactory bulb (Lin et al., 2006). By fractioning these smells, it was revealed that the activity of individual glomeruli was accounted for by single compounds in the scent. Thus, the complex representation of natural scent could be reconstructed by addition of individual odorant molecule, each of which activates only one or a few glomeruli (Lin et al., 2006).

This rather radical proposal, discarding both combinatorial coding of an odorant and complicated interactions among the projection neurons or M/T cells, is worth considering. Namely, it addresses a fundamental problem of research on olfaction. In almost all the research, pure odorants are used as olfactory stimulus, but the “natural” concentration of odorants is virtually unknown. Thus, the concentration is often set arbitrarily, which raises a concern that the tested intensity may not reflect stimulus that the olfactory system is usually designed to handle. Also widely observed is that higher concentration of an odorant activates more OSNs than the lower concentration of the same odorant does (Bozza et al., 2004; Hallem and Carlson, 2006; Wachowiak and Cohen, 2001). In the other terms, the peripheral “code” for an odorant in low concentration is different from that in high concentration. However, it is hard to imagine that the same odorants have different perceptive values in concentration-dependent manner. This begs

the question of what the perceptive and behavioral relevance of the OSN inputs recruited only at relatively high concentration is. Is combinatorial activation of OSNs and corresponding glomeruli by a single odorant functionally relevant? Does the complex electrophysiological response of the projection neurons matter for animals to discriminate odorants? Without showing the behavioral impact of these phenomena, we are unable to answer these difficult questions.

The labeled line model is, in fact, not mutually exclusive to either of combinatorial coding or dispersed coding. One glomerulus can be considered the simplest “combinatorial” code of a given odorant, and that one class of OSNs can generate complicated spike patterns in the higher olfactory centers. The labeled line model nonetheless contrasts with other coding model in suggesting that the decisive olfactory processing may happen at the sensory neuron level. The vertebrate retina contains color and motion sensitive ganglion cells, meaning that the peripheral sensory tissue can process what was once considered to be features extracted by an intricate neuronal network. Categorization of taste qualities largely happens at the periphery. These facts do not mean that interaction among distinct sensory channels, such as color or taste, never happens. It instead mean that sensory system tends to filter the most relevant information at the sensory neurons and immediate downstream. This initial filtering can therefore account for the most important factors of sensory perceptions. It is worth examining if the same principle applies to the olfactory system.

4.1.4. Larval chemotaxis modulated by a single OSN

Drosophila larvae offer a novel approach to address where and how behaviorally relevant information is encoded in the olfactory system. *Or83b* null larvae are anosmic (Larsson et al., 2004). In this genetic background, *Or83b* can be expressed in only one OSN by using Gal4/UAS system. This is a functional rescue of *Or83b* gene in specific larval OSN, and I will call this genetic manipulation "*OrX* functional" thereafter. The odor response profile of *Or42a*-expressing OSN in *Or42a* functional larvae remains largely unchanged from that in wild type larvae (Figure 4.1).

Rather surprisingly, *Or42a* functional larvae can chemotax to wide range of odorants (Fishilevich et al., 2005). *Or1a* functional and *Or49a* functional, in contrast, failed to chemotax to any of the 53 odorants tested (Fishilevich et al., 2005). These results suggest that only one OSN can support chemotaxis behavior in both an odorant and OSN-dependent manner. While the larval chemotaxis assay by itself does not discriminate detection and perception, the *OrX* functional manipulation opened up a new possibility to dissect the olfactory circuit. The olfactory system can function in the absence of combinatorial activation of OSNs. Investigation of larvae with such reduced olfactory inputs allows us to assess the impact of a limited number of functional OSNs on larval behavior and the physiology of its olfactory system.

We became particularly interested in one odorant, ethyl butyrate. This odorant smells like pineapple to humans and activates only three larval OSNs – *Or35a*, *Or42a* and *Or42b*. Therefore, it seems to be a good model to address the

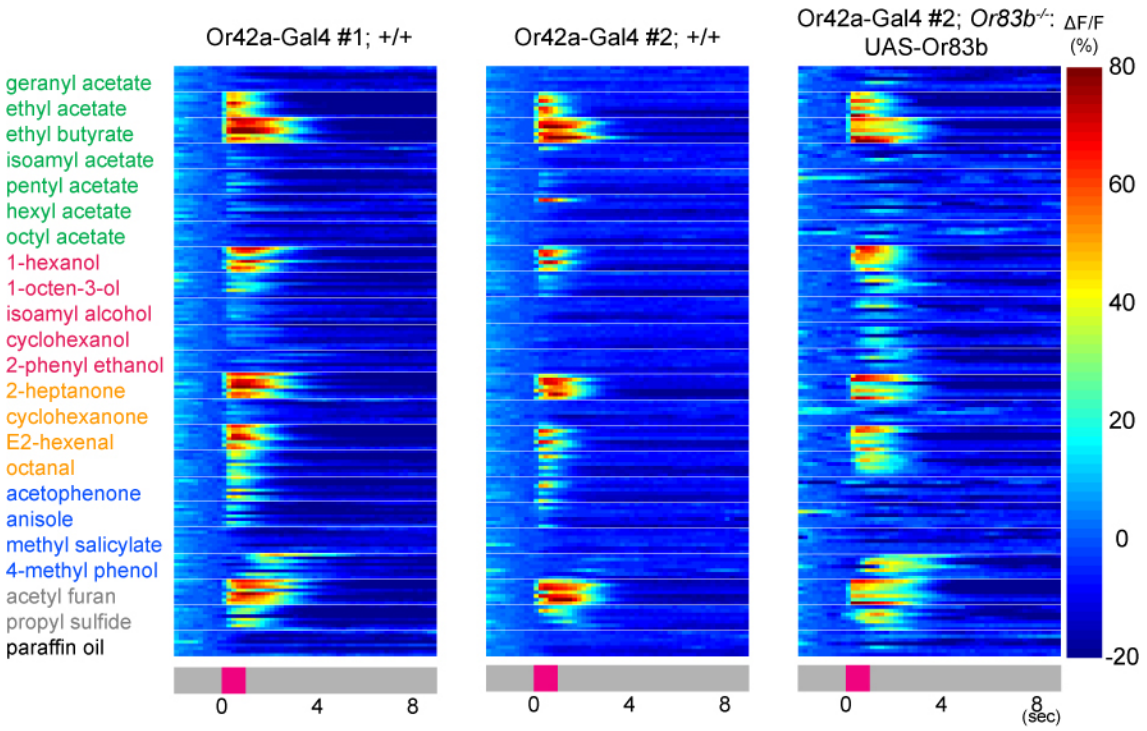

Figure 4.1: *Or42a* functional manipulation does not alter odor response profile of *Or42a*-expressing OSN

Odor response profiles of *Or42a*-expressing OSN obtained from wild type animals with two independent *Or42a*-Gal4 lines are shown in left and middle panel (left one is reproduced from Figure 3.2). Odor response profile of *Or42a*-expressing OSN obtained from *Or42a* functional animals (genotype is shown in Materials and Methods 3.2.1.) is shown in right. Traces represent ΔF/F(%) according to the scale at the right. Odorants used are listed at the left.

significance of combination of OSNs on larval behavior. Dr. Matthieu Louis, a former postdoctoral fellow in the laboratory, expanded the larval behavioral paradigm with controlled gradients and more quantitative measures of larval chemotaxis behavior (Louis et al., 2008). The new method can illuminate fine differences of chemotaxis behavior that may be missed with the conventional larval chemotaxis assay. Indeed, he observed that *Or42a* functional larvae could

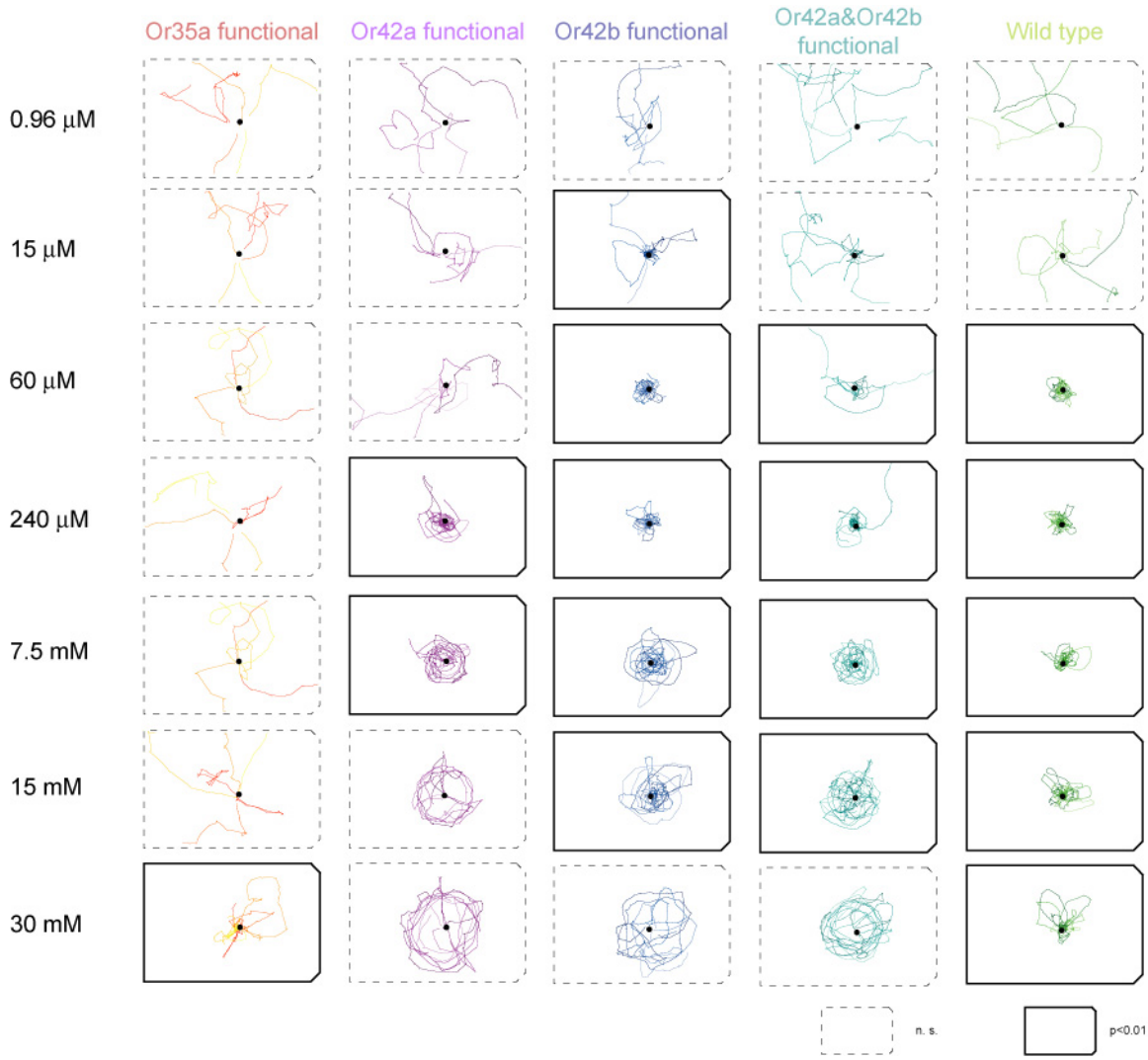

Figure 4.2: Chemotaxis behavior by *OrX* functional larvae reveals differential contribution of OSNs to larval behavior

Various concentration (shown at the left) of ethyl butyrate dilute was placed at the center of the arena (black solid or dotted lines), and third instar larvae introduced right under the odor source were tracked for 3 minutes or until a larva reached at the border of the arena as described in Louis et al., 2008. Five representative tracks were superimposed in one arena. Tested genotypes are shown at the top. Wild type is a *w1118; +;* + larva. Percentage of time spent in the "odor zone" (diameter 1.4cm) is compared with that of $Or83b^{1}/Or83b^{2}$ larvae with 60mM of ethyl butyrate at the odor source, and statistically significant ($P < 0.01$) accumulation of larvae in the odor zone is indicated with solid border of the arena (Wilcoxon test).

chemotax to ethyl butyrate (Figure 4.2, second left column) in a highly concentration-dependent fashion. At higher concentration, *Or42a* functional larvae maintain a stable and stereotyped distance from the odor source, resulting in “circling” behavior of larvae. The radius of the circle gets larger as the source concentration gets higher.

Under the same conditions, *Or35a* and *Or42b* functional larvae could also chemotax to ethyl butyrate, but each animal showed a limited range of concentration in which it would chemotax. *Or35a* functional larvae chemotax to only high concentrations of ethyl butyrate (Figure 4.2, leftmost column). *Or42b* functional larvae chemotax to the low concentration of ethyl butyrate to which neither of *Or35a* nor *Or42a* functional larvae response (Figure 4.2, middle column) and also show circling behavior at high ethyl butyrate concentrations.

These results suggest that there is a behavioral threshold of ethyl butyrate concentration for each of the three *OrX* functional animals. *Or42b* has the lowest threshold, followed by *Or42a* and then *Or35a*. Interestingly, wild type larvae have higher behavioral threshold than *Or42b* functional larvae. Wild type larvae chemotax at a concentration of 60μM (Figure 4.2, rightmost column), while *Or42b* functional larvae can chemotax at a concentration of 15 μM. *Or42b* functional larvae are therefore “super-smellers” of ethyl butyrate.

How does the olfactory input from two or three OSNs influence larval behavior? Dr. Louis created *Or42a* and *Or42b* “dual” functional larvae, and tested their chemotaxis ability to ethyl butyrate. Interestingly, the minimum concentration to which they chemotax (60μM) is intermediate between the

behavioral threshold of *Or42b* functional (15μM) and *Or42a* functional (240μM) (Figure 4.2, second right column). This result implies that the information about ethyl butyrate from these two OSNs is somehow consolidated, and causes the intermediate behavioral response.

An important message here is that ethyl butyrate can evoke behavioral response from three different OSNs. This means that ethyl butyrate is not coded in a labeled line. Instead, behaviorally relevant olfactory information can be coded by multiple OSN input. Moreover, these OSNs are not functionally redundant. While the behavior of *OrX* rescue discussed above does not prove that the odor identity or odor quality is coded in a combinatorial fashion, it nonetheless supports the idea that OSN combinatorials contribute to odor coding. These behavioral results may help to resolve the two theories of odor coding – faithful transmission or dispersed activity – which are based solely on physiological observations of the fully functional, “wild type” system. I believe that the genetic approach laid out here will help us isolate the influence of each of the coding components on the whole system. This Chapter concerns the concentration-dependent physiology of neurons in the olfactory circuit and its correlations with larval chemotaxis behavior. The results are used to propose a neuronal mechanism for the encoding of behaviorally relevant olfactory information by the antennal lobe.

4.2. Materials and methods

4.2.1. Fly stocks

Flies were maintained with standard food at room temperature. The enhancer trap line GH146 was previously described (Marin et al., 2005; Ramaekers et al., 2005; Stocker et al., 1997). The enhancer trap lines LN1 and LN2 were reported (Sachse et al., 2007).

4.2.2. Whole-mount and section immunostaining of the larval brain

Whole mount brain immunostaining of the third instar larvae was performed as described (Fishilevich et al., 2005) with primary antibodies of 1:2000-1:5000 rabbit anti-*Or83b* ((Larsson et al., 2004)), 1:10 mouse anti-elav (9F8A9, Developmental Studies Hybridoma Bank), 1:100 rabbit anti-GFP (Molecular Probes) and 1:10 mouse nc82 (gift from Dr. Reinhard Stocker), and with secondary antibodies of 1:1000 goat anti-rabbit Alexa 488 (Molecular Probes) and goat anti-mouse Cy3 (Jackson ImmunoResearch). Twelve micron sections of larval heads were made as described in Section 2.2.3., and immunostained as previously described. Samples were mounted in Vectashield medium (Vector Laboratories Inc.), and images were collected with an LSM 510 laser scanning confocal microscope (Zeiss).

4.2.3. Characterization of *UAS- G-CaMP1.6* transgenic flies

pUAST- G-CaMP1.6 (Ohkura et al., 2005) was a gift from Dr. Andre Fiala (The University of Wuerzburg, Germany). Transgenic flies were produced (Genetic

Services Inc. Cambridge, MA, USA) and balanced using standard methods. Among them, two had the insertion on the X chromosome. These strains were named *UAS- G-CaMP1.6 #1* and *UAS- G-CaMP1.6 #2*, respectively. *UAS- G-CaMP1.6 #1* was used for all the imaging experiments except the imaging from local interneurons using LN2, in which *UAS- G-CaMP1.6 #2* was used. Please see Section 4.2.8. for details.

4.2.4. Expression vector of nsyb::tdTomato under the promoter of *Or42a*

pRSETB-tdTomato (Shaner et al., 2004) was a gift from Dr. Roger Tsien. pBS-nsyb::GFP was described previously (Estes et al., 2000).

The amplification of nsyb::tdTomato fused DNA was performed in two steps. First, the n-synaptobrevin (nsyb) coding sequence with the first 18 base pairs of tdTomato fused to the 3' end in frame was amplified from pBS-nsyb::GFP plasmid using primers 5'-GGC TCT AGA CAA AAT GGC GGA CGC TGC ACA A-3' and 5'-CTC GCC CTT GCT CAC CAT CAC GCC GCC GTG ATC GCC-3'. This construct also contained XbaI site and CAAA fly Kozak sequence (Dr. Barry Dickson, personal communication) immediately upstream of the start codon. Simultaneously, the whole tdTomato coding sequence with the last 18 base pairs of n-synaptobrevin fused to the 5' end in frame was amplified from pRSETB-tdTomato plasmid using primers 5'-GGC GAT CAC GGC GGC GTG ATG GTG AGC AAG GGC GAG-3' and 5'- GGC ACT AGT TTA CTT GTA CAG CTC GTC-3'. This construct also contained SpeI site immediately downstream of the stop codon. The PCR products produced using the Platinum *Pfx* DNA

polymerase (Invitrogen) were gel-purified, which were mixed and used as templates of the second round PCR. Primers 5'-GGC TCT AGA CAA AAT GGC GGA CGC TGC ACA A-3' and 5'- GGC ACT AGT TTA CTT GTA CAG CTC GTC-3' were used to amplify the DNA construct of nsyb::tdTomato fusion protein with XbaI site and Kozak sequence at the 5' end and SpeI site at the 3' end. The PCR product produced using Expand Hight Fidelity PCR System (Roche) was gel-purified and cloned into pGEMT-Easy (Promega). The inserts were wholly sequenced to verify coding regions and restriction sites. The resultant pGEMT-Easy-nsyb::tdTomato was digested with XbaI and SpeI, gel-purified and subcloned into XbaI-digested pCasPeR-AUG-GAL4-X (Vosshall et al., 2000) using DNA Ligation Kit Ver.2.1 (TaKaRa).

The promoters of *Or42a* was previously described (Fishilevich et al., 2005). It was amplified from the genomic DNA of isogenic line *y[1]; cn*^{1} *bw*^{1} *sp*^{1} (Bloomington stock number 2057) using primers 5'-TTC TTC CCT AAA ACG AGA CCC-3' and 5'-AGT GAA TGC ACT CTA ATT TCA ACA ATT G-3'. The PCR product produced using Expand Hight Fidelity PCR System (Roche) was gel-purified and cloned into pGEMT-Easy (Promega). pGMET-Easy-*Or42a* promoter was digested with NotI, gel-purified and subcloned into NotI-digested pCasPeR-AUG-nsyb::tdTomato.

4.2.5. Characterization of *Or42a->nsyb::tdTomato* transgenic flies

Transgenic flies were produced (Genetic Services Inc. Cambridge, MA, USA) and balanced using standard methods. Among 5 independent insertions, two

were on the second chromosome. Larval brains of the two strains were examined under Eclipse E600FN epifluorescent microscopy (Nikon) with DsRed2 filter (excitation wavelength: 540nm, emission wavelength: 600nm, 42005 Chroma). Both showed clear fluorescence at axon termini of a pair of OSNs. One of them was subsequently chosen for imaging experiments.

4.2.6. Expression *Or83b* under control of odorant receptor promoters

The *Or83b* coding sequence was initially cloned from Oregon-R antennal cDNA (a gift from Dr. Richard Benton) using primers 5'-GCC TCT AGA GTT CCG GAA AGC CTC ATA TC-3' and 5'-GCC TCT AGA CAC TAC ACA TTT ATT TAG TTT GC-3'. The PCR product produced using Expand Hight Fidelity PCR System (Roche) was cloned into pGEMT-Easy (Promega). The insert had the entire coding region of *Or83b* and putative Kozak and poly-A site, franked by XbaI sites on both 5' and 3' ends. In order to replace 3' XbaI site with SpeI and to remove poly-A site, PCR from the plasmid mentioned above was carried out using primers 5'-GCC TCT AGA GTT CCG GAA AGC CTC ATA TC-3' and 5'-GGC ACT AGT TCG CAG CAA CTT ACT TG-3' The PCR product produced using Expand High Fidelity PCR System (Roche) was gel-purified and cloned into pGEMT-Easy (Promega). The insert was wholly sequenced to verify the coding region.

The resultant pGEMT-Easy-*Or83b* was digested with XbaI and SpeI, gel-purified and subcloned into XbaI-digested pCasPeR-AUG-IRES-nsyb::tdTomato. This plasmid contained putative *Drosophila* internal ribosomal entry site (IRES)

sequence (Halfon et al., 2002; Hart and Bienz, 1996) derived from *Ubx* gene immediately upstream of nsyb::tdTomato coding sequence in pCasPeR-AUG-nsyb::tdTomato. I will not detail the construction process of this part here, since the IRES sequence seemed to work very poorly. No fluorescence of tdTomato was observed in any of "*OrX->Or83b*" transgenic flies I generated from the construct (explained in Section 4.2.5.)(data not shown). Precisely speaking, this plasmid should be called pCasPeR-AUG-Or83b-IRES-nsyb::tdTomato. Because of inefficient nsyb::tdTomato expression, however, I will simply refer to it as pCasPeR-AUB-*Or83b* thereafter.

The promoters of *Or35a* and *Or42b* were previously described, and had been cloned into pGEMT-Easy (gifts from Elane Fishilevich). pGEMT-Easy-*Or35a* promoter was digested with Asp718, gel-purified and subcloned into Asp718-digested pCasPeR-AUG-*Or83b*. pGEMT-Easy-*Or42a* promoter and pGEMT-Easy-*Or42b* promoter were digested with NotI, gel-purified and subcloned into NotI-digested pCasPeR-AUG-*Or83b*.

4.2.7. Characterization of transgenic *Drosophila* larvae

Transgenic flies were produced (Genetic Services Inc. Cambridge, MA, USA) and balanced using standard method. Seven out of 11 independent *Or35a->Or83b* strains, 4 out of 7 independent *Or42a->Or83b* strains, and 5 out of 9 independent *Or42b->Or83b* strains had the insertions on the third chromosome. Their males were crossed with *w1118; CyO/Bl; Or83b*^{2} virgin females, and the F1

females were crossed with *w1118; CyO/Bl; TM2/TM6B*. The F2 males were screened for the recombinants of *OrX->Or83b* and $Or83b^2$ by PCR.

Six *Or35a->Or83b* insertions recombined with $Or83b^2$: five of them were tested for immunostaining. Among them, one recombinant showed staining of *Or83b* in one of the OSNs and was subsequently chosen for imaging experiments. It should be noted that only about 20% of them showed *Or83b* staining and physiological response in the PNs. Thus, the *Or35a->Or83b* transgene may function rather inconsistently. Three *Or42a->Or83b* insertions recombined with $Or83b^2$: two of them were tested with immunostaining. Both of them showed staining of *Or83b* in one of the OSNs, and one of them was subsequently chosen for imaging experiments. Four *Or42b->Or83b* recombined with $Or83b^2$: two of them were tested with immunostaining. Among them, one recombinant showed staining of *Or83b* in one of the OSNs, and was subsequently chosen for imaging experiments. Both *Or42a->Or83b* and *Or42b-Or83b* transgenes seemed to express *Or83b* consistently (data not shown).

4.2.8. Characterization of LN2 enhancer trap line

Enhancer trap lines LN1 and LN2 were previously described (Sachse et al., 2007). Larval brains from *LN2; UAS-GFP* showed selective immunostaining at the antennal lobe. *LN1; UAS-GFP*, on the other hand, mainly labeled the mushroom bodies. *w1118: LN2; +; +* males were crossed with *w1118: UAS- G-CaMP1.6 #1* and *w1118: UAS- G-CaMP1.6 #2* virgin females, and the F1 females were crossed with *FM7c; +; +* males. The F2 females were again

crossed with *FM7c; +;* + males, and each potential recombinant was expanded prior to PCR screening. LN2 and *UAS- G-CaMP1.6 #1* did not recombine efficiently, but three independent recombinants of LN2 and *UAS- G-CaMP1.6 #2* were obtained. One of them was subsequently chosen for imaging experiments.

4.2.9. Fly strains for calcium imaging

Fly strains described in 3.2.1 were used for calcium imaging from *Or35a*-, *Or42a*- and *Or42b*-expressing OSNs.

For calcium imaging from projection neurons, the following genotypes were used for imaging experiments: F1 progeny of *w1118: UAS- G-CaMP1.6 #1; GH146/CyO; Or35a->Or83b: Or83b^2/TM6B* and *w1118: UAS- G-CaMP1.6 #1; GH146/CyO; Or83b^2/Or83b^2* (for PN imaging in "*Or35a* functional"), F1 progeny of *w1118: UAS- G-CaMP1.6 #1; GH146/CyO; Or42a->Or83b: Or83b^2* and *w1118: UAS- G-CaMP1.6 #1; GH146/CyO; Or83b^2/Or83b^2* (for PN imaging in "*Or42a* functional"), F1 progeny of *w1118: UAS- G-CaMP1.6 #1; GH146/CyO; Or42b->Or83b: Or83b^2/TM6B* and *w1118: UAS- G-CaMP1.6 #1; GH146/CyO; Or83b^2/Or83b^2* (for PN imaging in "*Or42b* functional"). For the calcium imaging from the local interneurons, the F1 progeny of *w1118: LN2: UAS- G-CaMP1.6 #2; +;* + and *w1118: LN2: UAS- G-CaMP1.6 #2; Or42a->nsyb::tdTomato;* + were used.

4.2.10. Acquisition and analysis of calcium imaging data

For imaging from projection neurons and local interneurons, only 8 out of 22 odorants listed in Section 3.2.3. (ethyl acetate, ethyl butyrate, 1-hexanol, 2-heptanone, pentyl acetate, cyclohexanol, acetophenone, methyl salicylate) were used to characterize the odor response profile. 10^{-4} dilution of ethyl acetate was prepared by mixing 5 µl of 10^{-2} ethyl acetate dilution and 495 µl of paraffin oil. 10^{-1} dilution of ethyl butyrate was prepared by mixing 50 µl of pure ethyl butyrate and 450 µl of paraffin oil. This was sequentially diluted 1:10 by paraffin oil to prepare dilution series of ethyl butyrate up to 10^{-7} dilution.

Imaging from OSNs with a dilution series of ethyl butyrate was carried out as described in sections 3.2.2, 3.2.3 and 3.2.4, and the data was analyzed as described in Section 3.2.5. Some modifications were applied to the imaging from projection neurons and local interneurons. One session of a sample consists of application of 8 odors, paraffin oil and 7 dilution series of ethyl butyrate. Trials of reference odors were inserted every 5-7 trials to monitor the condition of the sample. In a trial, images were acquired with the resolution of 96 x 96 pixels (binned 8 x 8). Six seconds after the initiation of imaging, an odor was applied for 1 second, and images were taken 9 seconds thereafter. Thus, the total time for one trial for the projection neurons and local interneurons was 16 seconds (6 seconds for pre-stimulus, 1 second for odor stimulus and 9 seconds for post-stimulus). Otherwise, experiments were carried out as described in sections 3.2.2., 3.2.3 and 3.2.4. $\Delta F/F$ of data from projection neurons and local interneurons was calculated as follows:

$$\left(\frac{\Delta F}{F}\right)_n = \left(F_n - \frac{\sum_{i=25}^{29} F_i}{5}\right) \Bigg/ \frac{\sum_{i=25}^{29} F_i}{5}$$

$(\Delta F/F)_n$ is thus defined as fluorescence intensity relative to the average fluorescence intensity during one second right before the onset of odor stimulation. This is the same as what $(\Delta F/F)_n$ from OSN imaging data means. Otherwise data analysis was carried out as described in Section 3.2.5. False color-coded images of PN responses at the mushroom body were pixel representation of ΔF/F at 600ms after the onset of odor stimulation, and false color-coded images of local interneuron responses at the antennal lobe were pixel representation of ΔF/F at 400ms after the onset of odor stimulation. These images were created with an IDL6.2 (ITT) custom program written by Dr. Mathias Ditzen.

4.3. Results

4.3.1. Peripheral representation of ethyl butyrate by three OSNs

To find neuronal correlates with the behavior of *Or35a* rescue, *Or42a* rescue and *Or42b* rescue larvae, I made various dilution of ethyl butyrate and measured calcium responses from the three OSNs. They showed markedly different concentration thresholds of activation (Figure 4.4A). *Or35a*-expressing OSNs require a concentration of 10^{-2} dilution to respond, while *Or42a*-expressing OSNs can reliably respond to the 10^{-3} concentration, and *Or42b*-expressing OSNs

seem most sensitive to ethyl butyrate and can respond to as low as the 10^{-5} dilution. Therefore, although all three OSNs respond to ethyl butyrate, their threshold sensitivity is distinct. Furthermore, these physiological concentration thresholds qualitatively matched with the behavioral threshold demonstrated by *Or35a*, *Or42a* and *Or42b* functional larvae (Figure 4.2). Physiologically and behaviorally, therefore, these OSNs are not redundant in detection of ethyl butyrate.

4.3.2. Odor-evoked responses of the projection neurons

Intrigued by both the imaging and behavioral results, I next wanted to ask how ethyl butyrate was represented by the projection neurons. As was reported previously, an enhancer trap line called GH146 labels 16-18 larval projection neurons (Marin et al., 2005; Ramaekers et al., 2005), representing a majority of all the larval projection neurons. G-CaMP1.6 is an improved version of G-CaMP1.3: it is about 30 times brighter than the old version (Ohkura et al., 2005). Two copies of *UAS- G-CaMP1.6* provided the larval projection neurons with sufficient intensity under the control of Gal4 derived from GH146 (Figure 4.3A).

Imaging from the projection neurons was hampered by several problems. First, I was not able to image reliably from the dendrites, which innervate the antennal lobe, because the proximity of strongly fluorescent cell bodies interfered with the image of dendrites. Also, odor evoked signal from the dendrites was small and difficult to detect (data not shown). In contrast, axon termini of the projection neurons at the mushroom body showed robust fluorescence increases

Figure 4.3: Odor representation by the larval olfactory circuit

A) Schematic for measuring functional activation of the larval projection neurons of *OrX* functional using G-CaMP at the mushroom body (top) and intrinsic G-CaMP fluorescence of the projection neurons at the mushroom body viewed through the imaging microscopy (bottom). Orientation of the sample is at the bottom right corner. **B)** Imaging projection neurons in the *Or83b* wild type larval mushroom body reveals modular yet widespread activity. **C-E)** Imaging projection neurons in the mushroom bodies of *Or35a* functional **(C)**, *Or42a* functional **(D)** and *Or42b* functional **(E)** larvae. In all cases, left column is a representative sample with activity of only 1 (*Or35a* functional and *Or42a* functional) or 2 (*Or42b* functional) major subdomain(s). Right column is a representative sample with activities of minor subdomain in addition to major subdomain(s). Observed number of samples is indicated at the bottom. In **B-E**, calcium responses to three odorants (listed left) and paraffin oil are taken 400 milliseconds after the onset of odor stimulus, and represented as ΔF/F (%) values according to the scale at the right. **F)** Odor response profiles of an *Or35a* major subdomain from *Or35a* functional larvae (left panel), an *Or42a* major subdomain from Or42a functional larvae (second left panel) and two *Or42b* major subdomains from *Or42b* functional larvae (second right and right panels). Nine tested odorants and paraffin oil are listed at the left, and time courses from 11-14 samples are represented according to the scale at the right. **G)** Schematic for measuring functional activation of the larval local interneurons using G-CaMP at the antennal lobe (left) and intrinsic G-CaMP fluorescence of the local interneurons at the antennal lobe viewed through the imaging microscopy (right). **H)** Imaging LN2 neurons assisted by a *Or42a-nsyb::tdTomato* marker line which labels one glomerulus at the larval antennal lobe. Left: immunofluorescence staining of a *LN2-GAL4; UAS- G-CaMP* larva at the larval antennal lobe. G-CaMP was stained with anti-GFP antibody (green), and neuropil was stained with nc82 (magenta). Second left: intrinsic fluorescence of G-CaMP (green) and nsyb::tdTomato (magenta) viewed through the imaging microscopy are superimposed. Right four images are calcium responses to three odorants and paraffin oil (listed top) taken 600 milliseconds after the onset of odor stimulus, and are represented as ΔF/F (%) values according to the scale at the right. **I)** Odor response profile of LN2 local interneurons at *Or42a* glomerulus. Nine tested odorants and paraffin oil are listed at the left, and time course from 6 samples are represented according to the scale at the left.

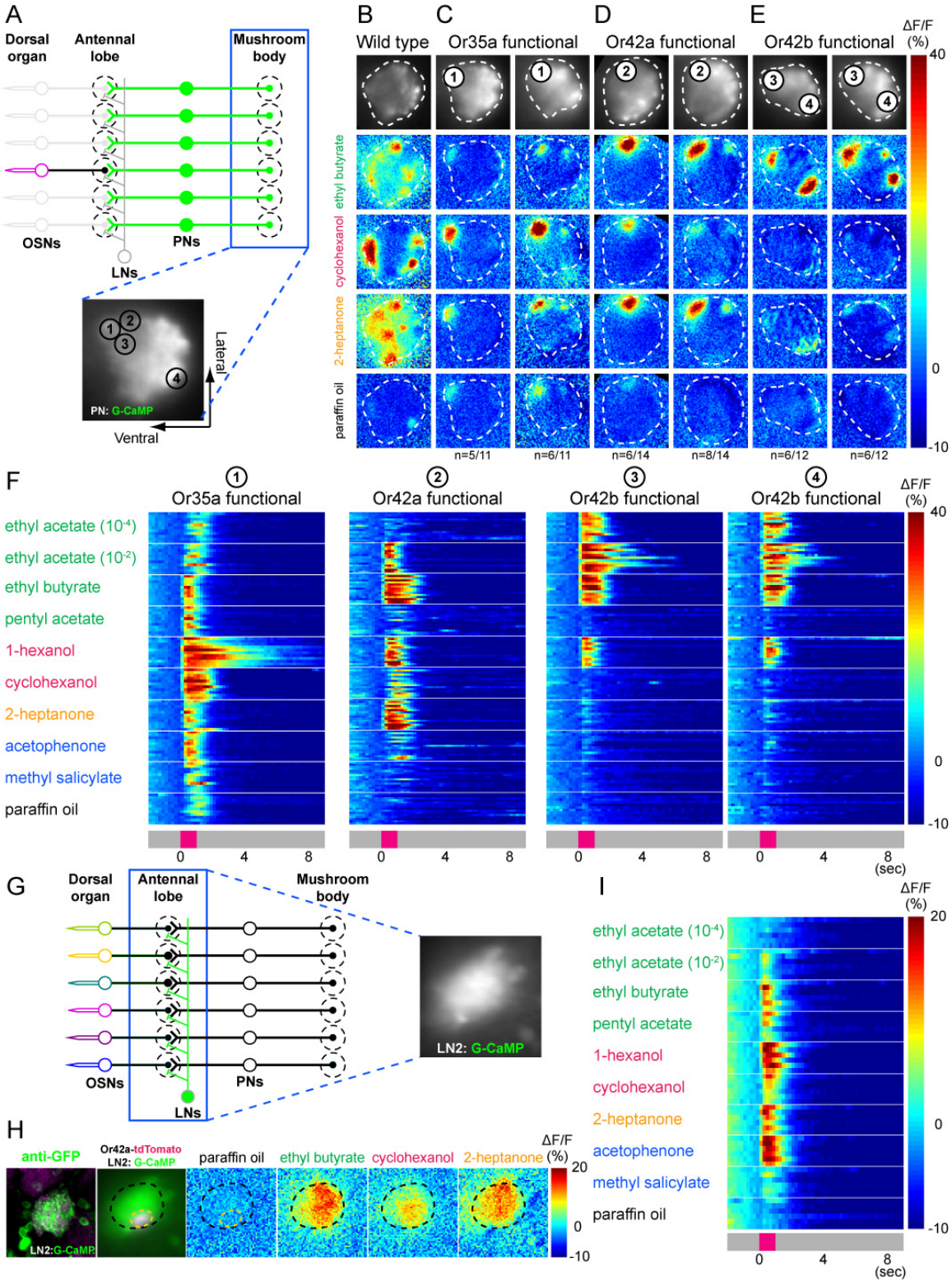
A
Dorsal organ
Antennal lobe
Mushroom body
OSNs
PNs
LNs
PN: G-CaMP
Lateral
Ventral
B
Wild type
C
Or35a functional
D
Or42a functional
E
Or42b functional
ΔF/F (%)
40
0
-10
ethyl butyrate
cyclohexanol
2-heptanone
paraffin oil
n=5/11
n=6/11
n=6/14
n=8/14
n=6/12
n=6/12
F
① Or35a functional
② Or42a functional
③ Or42b functional
④ Or42b functional
ethyl acetate (10-4)
ethyl acetate (10-2)
ethyl butyrate
pentyl acetate
1-hexanol
cyclohexanol
2-heptanone
acetophenone
methyl salicylate
paraffin oil
0
4
8
(sec)
G
Dorsal organ
Antennal lobe
Mushroom body
OSNs
PNs
LNs
LN2: G-CaMP
H
anti-GFP
Or42a-tdTomato
LN2: G-CaMP
LN2:G-CaMP
paraffin oil
ethyl butyrate
cyclohexanol
2-heptanone
ΔF/F (%)
20
0
-10
I
ethyl acetate (10-4)
ethyl acetate (10-2)
ethyl butyrate
pentyl acetate
1-hexanol
cyclohexanol
2-heptanone
acetophenone
methyl salicylate
paraffin oil
ΔF/F (%)
20
0
-10
0
4
8
(sec)

when odorant was applied. Odor-evoked responses were seen in a combination of active subdomains (Figure 4.3B). Because of the orderly glomerular innervation of the mushroom body by projection neurons, these subdomains likely represent by “glomeruli” from individual projection neurons. Moreover, presynaptic calcium increase may represent the more functional relevant activity of neurons. Therefore, to visualize the outcome of olfactory processing at the antennal lobe and to better dissect odorant perception in the higher centers, I focused on imaging projection neurons at axon termini in the mushroom body calyx.

However, another technical challenge was that the activity of projection neurons in wild type larvae was complex. The calyx is three dimensional, and signals from overlapping glomeruli interfere with each other. Moreover, calyx glomeruli can be reliably identified only after immunostaining. Thus, it was not possible to compare across multiple samples to draw odor response profile of individual glomerulus in a wild type larva with 21 functional OSNs.

To simplify olfactory input to the mushroom bodies, I created *Or35a*, *Or42a* and *Or42b* functional larvae by expressing *Or83b* under the direct control of OR promoters, instead of the Gal4/UAS system (see experimental procedure 4.2.4. and 4.2.5.). Flies were constructed in which the *Or83b* coding region was placed under the control of the promoter of a single larval OR gene to express *Or83b* in only one larval OSN (Figure 4.3A). Thus, by combining GH146 and *UAS- G-CaMP*, I could image the activity of projection neurons in *Or35a*, *Or42a* and *Or42b* functional larvae. Since each projection neuron forms synapses with a

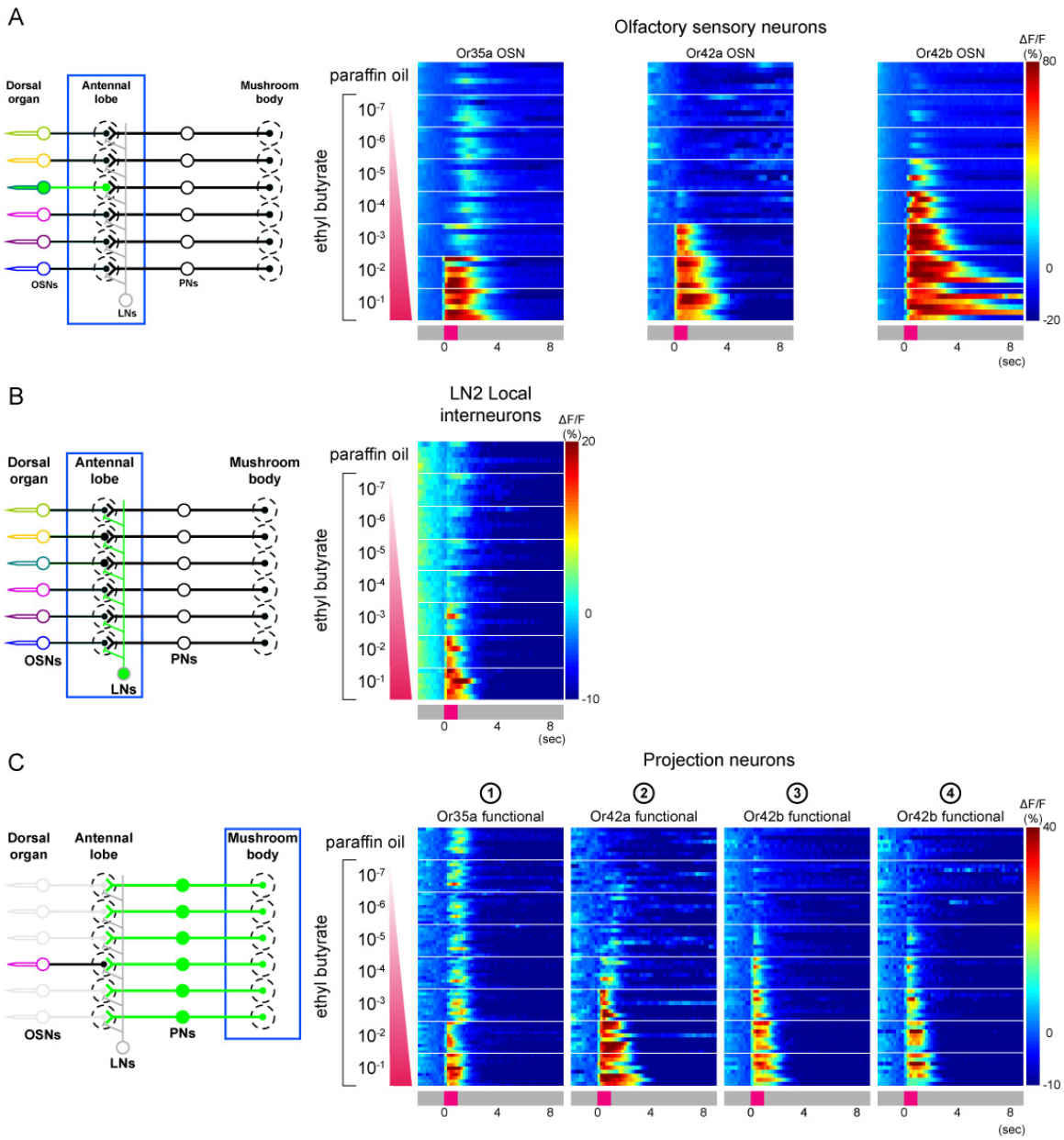

Figure 4.4: Encoding ethyl butyrate by the larval olfactory circuit

A) Left is schematic for measuring functional activation of the larval OSNs using G-CaMP at the antennal lobe. Dose-response time courses of *Or35a*-, *Or42a*- and *Or42b*-expressing OSNs at different ethyl butyrate concentrations are shown on right. Dilution factor is listed on the left, and time courses are represented according to the scale on the right. n = 6. **B)** Schematic for measuring functional activity of LN2 local interneurons using G-CaMP at the larval antennal lobe is on the left. Dose-response time courses of LN2 local interneurons are represented according to the scale on the right. Dilution factor of ethyl butyrate is listed on the left. n = 6. **C)** Schematic for measuring functional activation of the larval projection neurons of *OrX* functional using G-CaMP at the mushroom body is shown on the left. Dose-response time courses of *Or35a* major subdomain in *Or35a* functional larvae, of *Or42a* major subdomain in *Or42a* functional larvae and two *Or42b* major subdomains in *Or42b* functional larvae are shown on the right, respectively. Dilution factor is listed on the left, and time courses are represented according to the scale on the right. n = 8.

single OSN at the antennal lobe and forms one glomerulus at the mushroom body calyx, activities of the projection neurons at the mushroom body calyx in these *OrX* rescue larvae are likely to be limited to one glomerulus. If the lateral excitation is predominant at the antennal lobe, on the other hand, odor evoked response would be more widely distributed across the mushroom body calyx.

In *Or35a* and *Or42a* functional larvae, I consistently observed one active subdomain of the projection neurons in the calyx (Figure 4.3C,D), which I call the major subdomain. Each domain is excited by a subset of odorants which has been shown to excite *Or35a* or *Or42a* OSNs, respectively (Figure 4.3F, compare with Figure 3.2). The *Or35a* subdomain often responded to paraffin oil. This is presumably a mechanical response because the non-ligands for *Or35a*, ethyl acetate and methyl salicylate, evoked similar responses in *Or35a* subdomain. Locations of the major subdomains were consistent across samples (data not shown). About half the tested samples had no other active subdomains. The remaining half, on the other hand, had one or two more additional active subdomains in the calyx (Figure 4.3C,D, on the right column). Their signals were often weaker than the signals from major subdomains, but overall odor selectivity was otherwise similar to the odor response profile of the major subdomains. I call these inconsistent active subdomains minor subdomains.

Or42b functional larvae have two major subdomains, one at the ventrolateral side of the calyx and the other at medial side (Figure 4.3E). The subdomains respond to odorants in identical manner, in terms of odor selectivity, amplitude, and response duration, all of which are comparable to the response

profiles of the *Or42b* OSN (Figure 4.3F, compare with Figure 3.2). Again, about half the samples have mostly one minor subdomain (Figure 4.3E, on the right column).

4.3.3. Neuronal "code" of ethyl butyrate in the projection neurons

I next examined the response of major subdomains to various concentrations of ethyl butyrate. The *Or35a* subdomain responds to paraffin oil as well as 10^{-3} concentration of ethyl butyrate in similar manner (Figure 4.4C). The onset of response is usually about 600ms after the odor stimulation, and the peak $\Delta F/F$ value is around 15%. At concentration of 10^{-2}, however, the fluorescence increases right after the odor stimulation, and the peak value is markedly increased. I interpret that responses from ethyl butyrate with concentrations lower than 10^{-2} are mechanical responses observed in the odor response profile of *Or35a* major subdomain. Responses from 10^{-2} and 10^{-1}, on the other hand, appear to be odor responses. At these concentrations, fluorescence increased immediately after the odor stimulus, which was the case for all other responses in both OSNs and projection neurons. This interpretation results in a consistent concentration threshold for both the *Or35a* major subdomain and *Or35a* OSN.

Similarly, the *Or42a* subdomain consistently responds to ethyl butyrate with a concentration of 10^{-3} (Figure 4.4C). Two *Or42b* subdomains can respond to as low as 10^{-5} dilution (Figure 4,4C). Overall, the projection neuron concentration threshold values agree well with the threshold of corresponding OSNs. The difference of behavioral concentration thresholds for chemotaxis

toward ethyl butyrate among *Or35a*, *Or42a* and *Or42b* functional larvae, therefore, could be traced up to the activities of the projection neurons in the mushroom body calyx.

4.3.4. Inhibitory local interneurons as potential modulator of the olfactory network

Next, I examined the functional properties of local interneurons in the antennal lobe. Lateral connections make the antennal lobe the first site where interactions of neuronal inputs from different OSNs can occur (Figure 4.3G). An enhancer trap line named LN2 labels about 15 local interneurons of the larval antennal lobe (data not shown). Their dendrites innervate the entire larval antennal lobe uniformly with no apparent spatial bias (Figure 4.3H, left). In adults, LN2 labels GABAergic inhibitory local interneurons (Sachse et al., 2007). The neurotransmitter of larval local interneurons labeled by this LN2 line is currently unknown.

Odor stimulation evokes robust calcium increase at the dendrites of the local interneurons (Figure 4.3H). Consistent with the anatomy, the signal spread around the antennal lobe, but no obvious signal from the cell bodies were observed. Also consistent with the previous finding is that the local interneurons were activated by virtually all the odorants tested (Figure 4.3I). The amplitude seemed to vary, as some odorants (1-hexanol, 2-heptanone, acetophenone) activate the neurons more strongly than other odorants (ethyl acetate, methyl

salicylate). The duration of elevated fluorescence was also generally short, and returned to the basal level soon after the offset of odor stimulation.

Local interneurons were reliably activated by ethyl butyrate only at high concentrations at or exceeding the 10^{-3} dilution (Figure 4.4B) and the amplitude and duration of the local interneuron calcium response seemed to increase as the concentration was raised. It is worth noting that concentrations of 10^{-4} and 10^{-5}, which are sufficient to excite *Or42b*-expressing OSN but not *Or42a*-expressing OSN (Figure 4.4A), are ineffective to activate the local interneurons. Similarly, ethyl acetate with a concentration of 10^{-2} evoked weak activity in the local interneurons while the concentration 10^{-4} was ineffective. This failure to activate the local interneurons at these concentrations is surprising in light of my finding that ethyl acetate of 10^{-2} activates both *Or42a*- and *Or42b*-expressing OSNs and that 10^{-4} ethyl acetate activates the *Or42b*-expressing OSN. Therefore the local interneurons in the larva appear to have a very high threshold for activation.

4.4. Discussion and perspective

While this study is still ongoing, I would like to propose an interpretation of my current results and possible neuronal mechanism by which the larval olfactory system encodes the quality of ethyl butyrate.

4.4.1. Integration of the odor-response from the ensemble of the olfactory sensory neurons

If we suppose that ethyl butyrate is coded by a population of three OSNs, how is the "code" read in the projection neurons and above? If the dispersion of olfactory input from the OSNs is predominant, an activity from even a single OSN should result in broad activation of the projection neurons. Notably, Rachel Wilson and colleagues (Olsen et al., 2007) reported that activation of adult *Or42a*-expressing OSNs in the absence of other OSN inputs could laterally excite the projection neurons that did not innervate to the *Or42a* glomerulus. This was not the case in the larval mushroom body, in which activity from a single OSN induced only one (*Or35a* and *Or42a*) or two (*Or42b*) domains in the mushroom body. This is consistent with the anatomical observation that one projection neuron receive synaptic input from one OSN, and forms one glomerulus in the mushroom body calyx. The two *Or42b* subdomains may be due to the terminal branching of one projection neuron, which has previously been reported (Marin et al., 2005; Ramaekers et al., 2005). Currently, the contribution of this lateral excitation at the antennal lobe on behavior is unknown. As far as the major subdomain activities in the mushroom body can be correlated with chemotaxis behavior, I conclude that they are the most likely candidate of neuronal substrate for the perception of ethyl butyrate.

My data does not exclude that dispersion of activity does not take place in the "wild type" olfactory network. My *OrX* functional larvae allow me to examine the neural contribution of one OSN to the entire olfactory system, but an

ensemble of OSNs can certainly induce more widespread activity. Although I was unable to resolve glomerular activities of projection neurons at the mushroom body calyx in wild type larvae, their activity seemed widespread (Figure 4.3B and data not shown). Thus, activities that go undetected in *OrX* functional larvae can add up to distribute inputs from limited number of OSNs to whole population of projection neurons (Bhandawat et al., 2007; Wilson et al., 2004), which can optimize network capacity to code olfactory information (Abbott and Luo, 2007). In this regard, the lack of OSN convergence in the larval antennal lobe can accompany synaptic efficacy (Abbott and Regehr, 2004) between an OSN and a projection neuron that is different from that in adults. Thus, a larval projection neuron can be built to pick up input from the OSN that synapse it more faithfully than the adult projection neurons.

With three OSNs as behaviorally relevant coding units for ethyl butyrate, an interesting question is whether they are sufficient to reconstruct ethyl butyrate-evoked behavior seen in larvae with 21 functional OSNs. This experiment has not been done, but the intermediate chemotaxis behavior of *Or42a* and *Or42b* dual functional animals is suggestive. On the behavioral level, these two inputs are somehow integrated such that the *Or42b* OSN does not permit behavior when ethyl butyrate is presented at a low concentration. Therefore, multiple OSNs can synthesize a new behavioral response instead of simply sum them up and do not function as several independent labeled lines.

4.4.2. Neuronal mechanism of odor coding: comparison of the olfactory system with other sensory systems

Local interneurons can mediate communication among olfactory inputs from multiple OSNs. The high threshold for activation that I found in the larval local interneurons prompts me to speculate that these neurons can modulate ethyl butyrate perception in the larval antennal lobe. The physiological characteristics of the imaged local interneurons suggest that they can serve as a gate controller by pooling all the OSN inputs, and increase global inhibition to modulate output to the projection neurons. This function has been proposed for some time in pain perception (Melzack and Wall, 1965), and there is recent evidence that granule cells in the mouse olfactory bulb may perform such a role (Arevian et al., 2008). Gating modulation could explain the intermediate chemotaxis ability of *Or42a* and *Or42b* dual functional larvae. It is known that the OSNs fire spontaneously and I would speculate that local interneurons may be able to sense the spontaneous activities from OSNs and implement a baseline of inhibition, such that only input strong enough to overcome the baseline inhibition can synaptically transmit signal to the projection neurons. When only one OSN is active, there is virtually no inhibition at the antennal lobe, and any activation from the OSN is faithfully transmitted to the projection neuron. This is because in the absence of *Or83b* function, spontaneous activity is almost entirely absent (Larsson et al., 2004). Two functional OSNs, such as *Or42a* and *Or42b*, can increase the baseline inhibition and suppress activities of the projection neuron even when *Or42b* OSN is excited by low concentration of ethyl butyrate. As a result, larvae may not be

able to chemotax at the concentration which is effective for *Or42b* single functional larvae.

The same mechanism can also explain the circling behavior of *Or42a* rescue functional. The OSNs can signal progressively stronger signals to the antennal lobe. With the gate-controlling local interneurons, however, such excitation can be buffered and transmitted to the projection neurons in more graded manner. The antennal lobe of *Or42a* functional larvae may have no such inhibition, and the signal from *Or42a*-expressing OSN can impose over-saturated excitation on the cognate projection neuron. The nervous system may interpret this as a repulsive signal, and the larvae end up staying at a moderate concentration that excites *Or42a*-expressing OSNs mildly. In this context, it should be pointed out that the circling distance of *Or42a* and *Or42b* dual functional larvae appeared smaller than that of *Or42a* single functional larvae at high concentrations (Figure 4.2, second right column).

Several further experiments will be able to test these ideas. First, the activity of projection neurons when the two OSNs are rescued should be monitored. If the hypothesis is correct, at least one of *Or42b* major subdomains in *Or42a* and *Or42b* dual rescue larvae should show decreased sensitivity to ethyl butyrate. Second, local interneurons in the single rescue larvae should be examined. Although G-CaMP is not sensitive enough to monitor baseline inhibitory activities, the local interneurons in both *Or42a* and *Or42b* single functional larvae should have higher concentration thresholds to ethyl butyrate. This would imply that the overall excitability of the local interneurons is

decreased when there is only one functional OSN. To show that the local interneurons labeled in the LN2 enhancer trap line is inhibitory, immunostaining with GABA must be carried out.

I would also argue that the term “lateral inhibition” should be used with caution in the olfactory system, especially in insects. As was discussed in Section 1.1 and 1.5.6, lateral inhibition is the inhibition from neighboring sensory input that results in contrast enhancement. This means that inputs connected by the lateral inhibition network should have close receptive range – either physically or qualitatively – with each other. Apart from the moth macroglomerular complex, which often consists of a few glomeruli receiving inputs from OSNs tuned to chemically similar pheromone components (Berg et al., 2005; Christensen and Hildebrand, 1987), it is unclear whether such chemotopic juxtaposition of OSNs exists in insect antennal lobe. Even so, homogeneously innervating local interneurons would, in principle, erase such subdivisions. Besides, it is difficult to elucidate which feature of odorants the olfactory system regards as “similar”. Carbon chain length is often varied by experimenters, but how about the position of a functional group on the same length of a carbon chain? What if two or more functional groups are simultaneously present on it? How about esters or other species of chemicals which consists of two or more basic compounds bound by dehydration or reduction? Since we do not know the entire parameters defining the “olfactory space”, even in a way that appears to the olfactory system, we must be careful in

concluding that inhibition in the antennal lobe or in the olfactory bulb is homologous to that in other sensory systems.

In spite of the massive documentation of the physiological properties of the local interneurons in the olfactory system, their contribution to odorant perception has remained a mystery. This is partially because testing behavioral relevance of these neural events has been an immense challenge. As a result, the two theories of odor coding seem to have failed in finding a common ground. The deconstructive approach detailed here can settle the deadlock. The integration of genetic manipulation, calcium imaging, and behavioral analysis appears to give us a tremendous power to illuminate the logic of odor coding. Neuronal dissection of this tiny olfactory circuit can elucidate a part of the coding mechanism that may be common to the adult flies and, by analogy, to vertebrates as well.

5. The relevance of the olfactory system for larval survival

5.1. Introduction: why do larvae need to smell?

The visual system is important for animal survival. For instance, we humans rely so much on the visual system that a sighted person pondering the loss of vision feels an immediate sense of despair and helplessness. However, animals that are devoid of a visual system such as the cave fish and the blind mole rat exist and appear to thrive. Therefore, a sensory system can be dispensable under certain condition. This raises the question of how sensory systems are actually crucial for animal survival and under which conditions.

The olfactory system is no exception. While many fly behaviors are show to be dependent on the part of the olfactory system, most of these olfactory mutants are viable and healthy under laboratory conditions. The most dramatic example is the *Or83b* mutants. While the larvae are completely anosmic and adults have a severe olfactory deficit (Larsson et al., 2004), they are healthy, develop normally, and reproduce well. This may simply mean that the laboratory condition is overly protective or that the fly is equipped with various “backup” systems to make up the loss. Nonetheless, the question of whether the olfactory system is important for fly survival remains unanswered.

In this last Chapter, I present a series of experiments to address the direct impact of the olfactory system on fly development. The focus of this study is to know if there is a condition that illuminates selective advantage that the olfactory

system offers. Particularly, I would like to focus on the environment in which larvae develop, since the olfactory system could play a major role in the foraging capacity at the larval stage, during which accumulating nutrition is the main purpose.

5.1.1. *Drosophila* larvae in natural and laboratory environment

As mentioned in the first Chapter, the ecology of *Drosophila melanogaster* larvae is not well understood. Field studies of other *Drosophila* species imply that they feed on yeast growing on spoiled fruits or plant parts (Fogleman et al., 1981; Phaff, 1956). Some species are “generalist” feeders, and eat a wide variety of yeast species. Others are “specialists”, feeding on only one or very few species of yeast (Fogleman et al., 1981). Therefore, the common name “fruit flies” may be slightly misleading as far as larval feeding behavior is concerned. Since yeast grows in patches, the surface of spoiled fruits or plant parts can create microenvironments characterized by distinct species of yeast. It is possible that larvae have to move around these patches for ideal feeding sites, which can be more important for specialist eaters. In fact, some *Drosophila* species have preference for certain yeast species (Cooper, 1960; Lindsay, 1958). Unfortunately, few *Drosophila melanogaster* have been captured by the field researchers above, possibly because they are closely associated with human habitats (Keller, 2007).

In the laboratory, larvae usually feed on standard corn meal fly food, which also contains yeast. This is experimentally and empirically shown to be sufficient

for fly development. A major difference between fly food and the presumptive natural habitat of *Drosophila melanogaster* is that the food is always available for larvae. Adult female flies deposit embryos on the food, and larvae feed and grow without crawling around. This is obviously a highly protective environment, and can explain why *Or83b* null mutants and many other mutant flies with sensory or other deficits have no overall developmental problems.

5.1.2. The olfactory behaviors of *Drosophila* larvae

Drosophila larvae chemotax robustly to various odorants (Cobb, 1999). Interestingly, few odorants may be repellents for larvae and they are usually attracted by most odorants tested (Fishilevich et al., 2005; Larsson et al., 2004). This fact may reflect the opportunistic foraging strategy of larvae. Since they have to develop rather quickly, they would just go toward whatever is smelly rather than evaluating the quality of potential food. Of course, not all the odorants are equally attractive since they tend to chemotax better to esters and alcohols than to aromatics (Fishilevich et al., 2005).

When do larvae have to rely on their olfactory system? If they were born on ample food, this sensory system might be unnecessary. The fact that natural selection spares larval neurons specialized for detecting and processing odor information implies that there are conditions when larvae need an olfactory system. This is further supported by the existence of behavioral polymorphisms that govern strategies of larval feeding. Polymorphisms in the gene *foraging* (Sokolowski, 1980), which encodes a guanylyl cyclase (Osborne et al., 1997),

correlate with either local or dispersed feeding. A dominant isoform of *foraging* with high enzymatic activity causes larvae to rove around the field even if they are fed and they are on food, a so-called “rover” state. A recessive isoform, on the other hand, causes larvae to stay where they are feeding, the so-called “sitter” state (Sokolowski, 1980). Therefore, rover larvae would crawl around even when food is locally abundant while sitters would sit. Rover larvae would be more adapted to patchy food resources, and the differential resource utilization is hypothesized to explain the persistence of both rover and sitter polymorphisms in wild fly populations (Fitzpatrick et al., 2007).

Thus the selective advantage of the larval olfactory system may only be apparent when these animals are forced to forage for food in environments of limiting resources. In this Chapter, I present several such conditions and compare the rate of successful metamorphosis among wild type and several olfactory mutants. While the conditions are still highly controlled and therefore artificial, my aim is to find the selective advantage of the olfactory system allowing animals to survive in these various harsher than normal environments.

5.2. Materials and methods

5.2.1. Fly stocks

Flies were raised on standard medium at the room temperature. The genotype of “wild type” flies is *w1118*; +; +. The genotype of “$Or83b^{-/-}$“ is *w1118*; +; $Or83b^{1}/Or83b^{2}$, which is obtained as the offspring from *w1118*; +; $Or83b^{1}/Or83b^{1}$ × *w1118*; +; $Or83b^{2}/Or83b^{2}$. The genotype of “*Or83b* functional” is *w1118*;

Or83b-Gal4/+; Or83b^{1}/ Or83b^{2}: UAS-Or83b, which is obtained as the offspring from *w1118*; +; *Or83b^{1}/Or83b^{1}* × *w1118: Or83b-Gal4; Or83b^{2}: UAS-Or83b/ Or83b^{2}: UAS-Or83b*. The genotype of "*Or42a* functional" is *w1118*; *Or42a-Gal4/+; Or83b^{1}/ Or83b^{2}: UAS-Or83b*, which is obtained as the offspring from *w1118*; +; *Or83b^{1}/Or83b^{1}* × *w1118: Or42a-Gal4; Or83b^{2}: UAS-Or83b/ Or83b^{2}: UAS-Or83b*.

5.2.2. Embryo collection and experimental materials

Adult flies were introduced to a cage with grape fruit agar plate in the evening of the day before collection of embryos. We define this day "0 day after egg laying (AEL)". The cage was placed in 25 degree, 70% relative humidity overnight. In the following day (1 day AEL), embryos laid on the plate were collected. Thus, the embryos used in the assays were 12 – 15 hours old.

We used the arena, the first food source and the second food source commonly in the three behavioral assays described below. The arena is a Petri dish (150 mm diameter, 15mm depth, Falcon) covered with 25 ml of 2.5% agarose. The lid was taped to the dish. For survival assay and competition assay, a small (3-4 mm diameter) hole was punched on the lid and covered with fine mesh. It was used to inject CO_2 as newly emerged flies were collected. The first food source was 100 mg of standard fly medium dispensed in a plastic screw cap (12 mm diameter, Sarstedt, Germany). The second food source was 100 mg of standard fly medium with 70mg of yeast paste on top dispensed in a plastic

screw cap. Unless otherwise mentioned, all the experiments were carried out at 25 ^{o}C, 70% relative humidity in the dark.

5.2.3. Survival assay

Either 10 or 50 fly embryos were introduced on the first food, which was subsequently placed at the center of an arena. On 3 days AEL, the second food source was introduced to the experimental group. It was placed 70mm away from the center of the arena. The control group received an empty screw cap at the same position. Starting 10 days AEL, newly emerged adults were collected by anesthetizing them with CO_2 injected from a small hole every day, and the number of adults was counted. The hole was covered with fine mesh to prevent flies from escaping. The experiment was terminated on 20 days AEL, when almost all the wild type adults had emerged. The number of emerged adults reached plateau by 20 days AEL as is shown in Figure 5.1B.

5.2.4. Migration assay

Five arenas with either 10 or 50 embryos were prepared in parallel in the same manner as in survival assay. On 3 days AEL, the second food was introduced. Starting 4 days AEL, one arena was used for an assay per day up to 8 days AEL. Each day, the first and second food sources were removed from the arena and transferred to a Petri dish. In the dish, the food was dissolved in water, and larvae in each food were counted. Larvae wandering on arena and pupae, if found, were also counted. The examined arenas were subsequently discarded,

since larvae and food were severely disturbed during count. The percentage of larvae on each section on N days AEL was calculated as (number of larvae on a section from all the experiments on N days AEL) / (sum of larvae and pupae in arena from all the experiments on N days AEL). The value therefore depends on the embryo mortality of each strain, which could be estimated by the total number of larvae and pupae found throughout the migration assay. The observed embryo mortality was 22% for wild type, 27% for *Or83b*$^{-/-}$, 18% for *Or83b* functional and 26% for *Or42a* functional. Although values are variable, we conclude that it does not significantly affect the outcome of the results. These values are also roughly consistent with the cumulative eclosion rate of survival assay in 10 embryos from the four strains. The tract of larvae on arena was photographed by contact print. An arena from day 5 was placed on Kodak BioMax MR film, and light was shed by an enlarger (Beseler Printmaker 67). The negative was scanned, and the image was inverted.

5.2.5. Competition assay

An equal number of embryos from two strains to be competed was simultaneously introduced to the first food source at the center of the arena. The number of embryos was either 5 each (10 in total), 25 each (50 in total) or 40 each (80 in total). On 3 days AEL, the second food source was introduced in the same manner as in survival assay. Starting 10 days AEL, newly eclosed adults were collected every day and were genotyped. For the competition between wild type and *Or83b*$^{-/-}$, *Or83b* functional or *Or42a* functional, the genotype of flies was

determined by the eye color. For the competition between *Or83b*$^{-/-}$ and *Or83b* functional, between *Or83b*$^{-/-}$ and *Or42a* functional and between *Or83b* functional and *Or42a* functional, the genotype of flies was determined by diagnostic PCR to individual flies. Briefly, flies were individually squished in 96-well PCR plate. Primer sets specific to *Or83b* knockout insertion (600 bp) and *UAS-Or83b* (500 bp) were used to discriminate *Or83b*$^{-/-}$ (1 DNA band) and *Or83b* functional (2 DNA bands). Primer sets specific to *Or83b* knockout insertion (600 bp) and *UAS-Or83b* (500 bp) were used to discriminate *Or83b*$^{-/-}$ (1 DNA band) and *Or42a* functional (2 DNA bands). Primer sets specific to *UAS-Or83b* and *Or42a-Gal4* (600 bp) were used to genotype flies from the competition assay between *Or83b* functional (1 DNA band) and *Or42a* functional (2 DNA bands). The number of newly emerged flies from the two strains was thus counted up to 20 days AEL, when the experiment was terminated.

Initially, experiments were carried out with intermittent illumination since the arenas were not covered. Later, experiments were carried out in the dark. We did not observe statistically significant differences between the results from the two conditions (Figure 5.8), and thus the data were pooled.

5.2.6. Data analysis

For survival and competition assays, cumulative eclosion rate on N days AEL was calculated as (number of adults eclosed by N days AEL) / (number of embryos initially introduced). Statistical analysis was performed with Microsoft Excel and XLSTAT software (Addinsoft).

5.2.7. Genotyping *foraging* polymorphism

We took advantage of recently reported single nucleotide polymorphism strongly linked to for^R and for^s alleles (Fitzpatrick et al., 2007). It is C (for^R) to T (for^s) substitution causing R390C amino acid polymorphism. We therefore designed two different primers such that the last nucleotide falls on the polymorphism site. One is for allele for^R (5'-TGA TCT GAA TGA AGC G-3', primer 1), and the other is for allele for^s (5'-TGA TCT GAA TGA AGC A-3', primer 2). Another primer (5'-CAA TTG AAC CAG GAT CC-3', primer 3) was located 366bp upstream of the polymorphism site. Flies from laboratory stock wild type, $Or83b^1/Or83b^1$ and $Or83b^2/Or83b^2$ were individually squished, which was used for PCR analysis with either primer 1 × primer 3 (detecting for^R) or primer 2 × primer 3 (detecting for^s).

5.3. Results

5.3.1. Wild type larvae in survival assay and migration assay

The survival assay (Figure 5.1A) is intended to discriminate foraging ability of *Or83b* null mutants from the wild type larvae. Both in the presence or absence of the second food, the cumulative eclosion rate of ten wild type embryos reached around 80%, and two values were not statistically significant (Figure 5.1B). One hundred milligrams of standard fly food therefore seems sufficient to support the development of ten wild type larvae. When 50 embryos were placed on 100 mg of food in the absence of the second food, on the other hand, the cumulative eclosion rate was only 14% at 20 days AEL (Figure 5.1B). This was improved to 73%, comparable to the rate achieved by ten embryos, when the second food

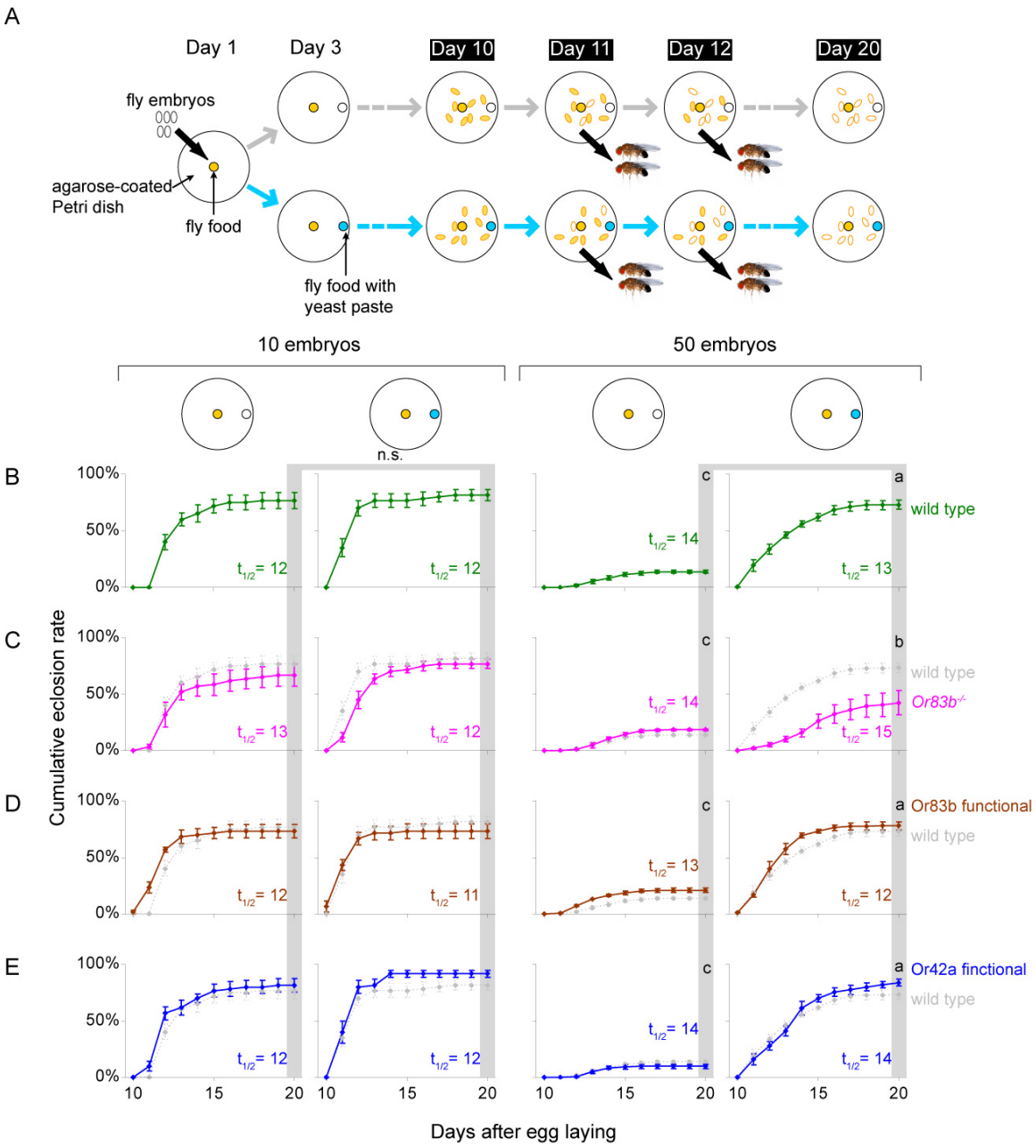

Figure 5.1: Anosmia causes compromised eclosion rate in survival assay

A) Schematic of experimental protocol of survival assay. Fixed number of embryos was deposited on fly food centered in the agarose-coated arena. The second food was given at 3 days after egg laying (AEL) to experimental groups (top) while empty can was given to control groups. Starting 10 days AEL, number of eclosed adults were counted day-by-day up to 20 days AEL. **B-E)** Cumulative eclosion rate of wild type **(B)**, *Or83b*$^{-/-}$ **(C)**, *Or83b* functional **(D)** and *Or42a* functional **(E)** are plotted against days AEL (mean ± S.E.M., n = 6). The number of initially deposited embryos is 10 (first two columns) or 50 (latter two columns), which are further divided by the absence (left) or presence (right) of the second food. In **C-E**, the data of wild type is superimposed in grey for reference. ANOVA and post-hoc Tukey HSD test (confidence interval: 95%) was applied to data from 10 embryos and 50 embryos, respectively. Alphabets denote significant groups, if applicable.

Figure 5.2: Functional olfactory system is necessary and sufficient to locate food patch in migration assay

A) Schematic of experimental protocol of migration assay. Embryos were deposited, and the second food was given in the same manner as in survival assay. Starting 4 days AEL, number of larvae found in the original (first) food, on arena and in the second food was counted. Five arenas were simultaneously set on 1 day AEL and one arena was used per day. **B-E)** Percentage distributions of wild type **(B)**, *Or83b*$^{-/-}$ **(C)**, *Or83b* functional **(D)** and *Or42a* functional **(E)** larvae are shown in 100% stack bars. Color keys are shown in **(A)**. Repeat number is shown below genotype. **(F)** Percentage of larvae on the second food on 5 days AEL (mean ± S.E.M.) in arenas with 10 embryos (left) and with 50 embryos (right). Alphabets denote significance groups among strains (ANOVA and post-hoc Tukey HSD test with a confidence interval of 95%). **(G,H)** Photographic images of tracks of larvae from wild type **(G)** and *Or83b*$^{-/-}$ **(H)** taken on 5 days AEL. Yellow circle indicates the position of the original (first) food, and cyan circle indicates the position of the second food.

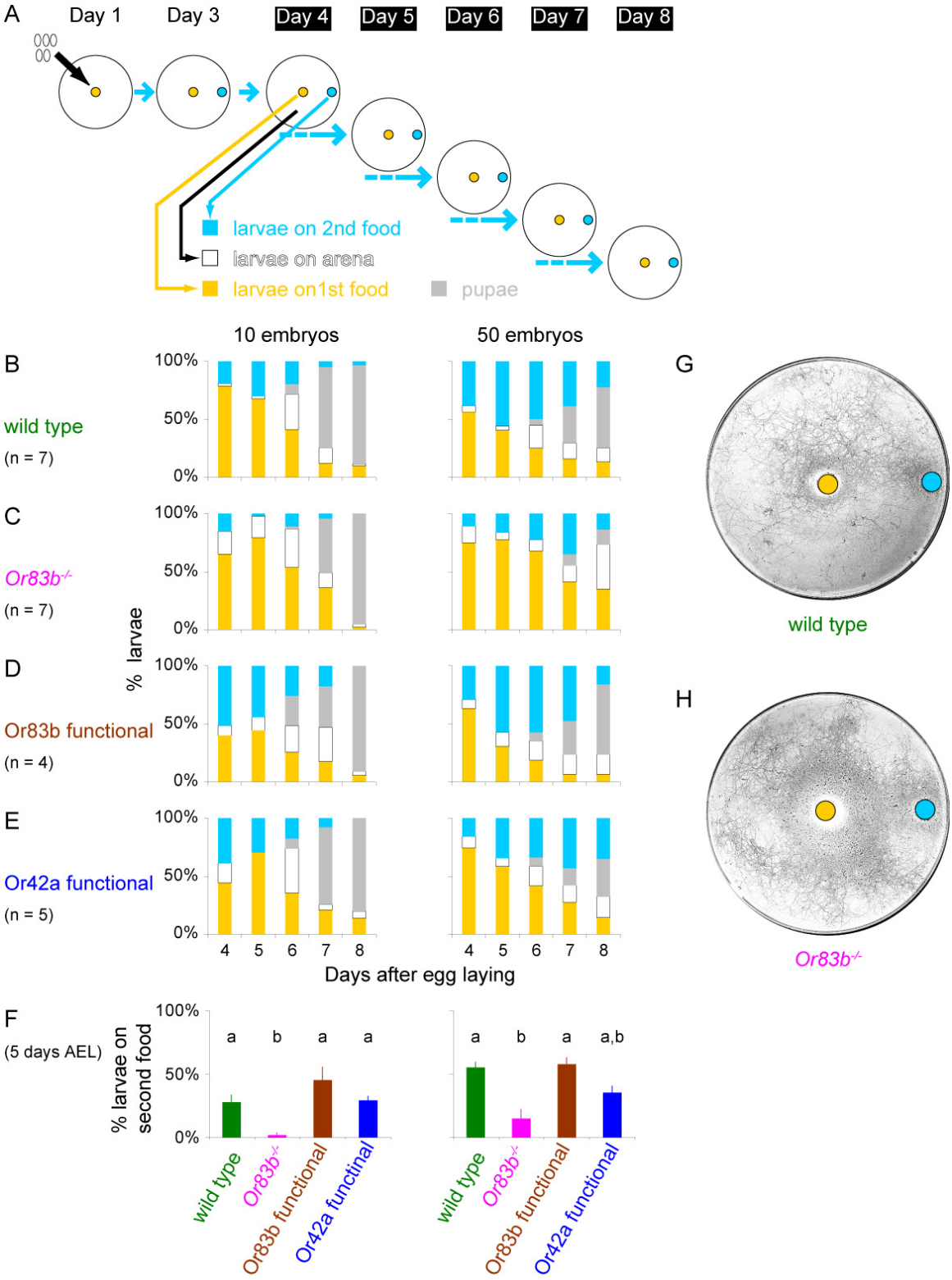
A
Day 1
Day 3
Day 4
Day 5
Day 6
Day 7
Day 8
larvae on 2nd food
larvae on arena
larvae on1st food
pupae
10 embryos
50 embryos
B
wild type
(n = 7)
C
Or83b-/-
(n = 7)
D
Or83b functional
(n = 4)
E
Or42a functional
(n = 5)
100%
50%
0%
% larvae
4 5 6 7 8
Days after egg laying
F
(5 days AEL)
% larvae on second food
a b a a
a b a a,b
wild type
Or83b-/-
Or83b functional
Or42a functional
G
wild type
H
Or83b-/-

represents supplemental nutrition necessary for larvae to achieve successful development into adulthood.

Do larvae actually feed on the second food supply? I directly monitored migration of larvae to the second food by a migration assay (Figure 5.2A). Larvae developing from 50 embryos actively migrated to the second food, in a migration that peaked at 5 days AEL: 56% of larvae moved from the first food to the second food (Figure 5.2B). Larvae from 10 embryos, on the other hand, did not migrate as much (Figure 5.2B). These results suggest that larvae need to make use of the second food when the initial feeding site is too crowded. This paradigm therefore presents a type of challenge that larvae do not face under normal laboratory conditions.

5.3.2. Performance of *Or83b* null mutants and "*OrX* functional" larvae

How do *Or83b*$^{-/-}$ manage this competitive environment? I tested ten or 50 embryos of *Or83b*$^{-/-}$ in both the survival assay and migration assay. Ten mutant embryos developed to adults in comparable rate as the wild type embryos regardless of the presence of the second food (Figure 5.1C). This result indicates that *Or83b*$^{-/-}$ have no major innate developmental handicap. As long as plenty of food is provided at the site they are born, the mutants can grow as well as wild type flies.

When the number of embryos is raised to 50, however, they could not reach the same cumulative eclosion rate even when the second food was given. On average, only 44% of embryos became adults by 20 days AEL (Figure 5.1C),

compared to 73% posted by the wild type embryos under the same condition. The difference of the two values is statistically significant. Therefore, patchy food could not support development of *Or83b*$^{-/-}$ as well as that of wild type.

I found that *Or83b*$^{-/-}$ larvae also failed to migrate to the second food as vigorously as the wild type larvae. At 5 days AEL, only 16% of mutant larvae from 50 embryos were found in the second food (Figure 5.2C). Throughout the five days when I examined the distribution of animals, the mutant larvae did not migrate very well, although a small proportion of larvae were found in the second food. While many wild type larvae start pupating from 6 days AEL, the vast majority of *Or83b*$^{-/-}$ larvae did not pupate by 8 days AEL (Figure 5.2C), possibly reflecting lagging development due to the lack of nutrition.

The poor migration of *Or83b* null mutant larvae is not due to decreased locomotion. I observed that they often actively wandering on arena and they left dense tracts (Figure 5.2H) similar to those left by the wild type larvae on the agar surface (Figure 5.2G). It appears therefore that the mutants left the first food and roved around the arena. Genotyping of the *foraging* locus of both wild type flies and *Or83b*$^{-/-}$ flies indicated that all strains used in these experiments are “rovers” (Figure 5.3). Therefore, we hypothesize that the lower cumulative eclosion rate in the survival assay is related to the anosmia of the mutant larvae.

However, the eclosion rate of 50 embryos of *Or83b*$^{-/-}$ in the presence of the second food was significantly better than in the absence of the second food (Figure 5.1C). They could be finding the second food source by random non-olfactory searching or they might be locating the second food through taste cues

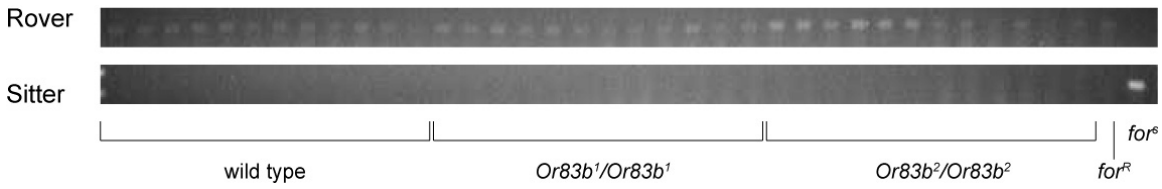

Figure 5.3: Laboratory flies carry *for*^{R} allele of *foraging*

Twelve adult flies (6 males and 6 females) of wild type, *Or83b*^{1}/ *Or83b*^{1} and *Or83b*^{2}/ *Or83b*^{2} were genotyped for *forager* allele with PCR using allele-specific primer sets ("rover" allele: top, "sitter" allele: bottom). One of each of *for*^{R} and *for*^{S} fly, respectively, were used as controls.

which could be left by the infusion of yeast scent by agar floor. Standard fly food contains high concentrations of propionic acid as an anti-fungal reagent, which could form taste gradient. I used food without propionic acid to address this concern. *Or83b*$^{-/-}$ from both 10 embryos and 50 embryos posted similar cumulative eclosion rate by 20 days AEL (Figure 5.4). The values are not statistically significant from the values when propionic acid was contained in the food. Therefore, we believe that these animals are using random searching to find the secondary food source.

To obtain further support that anosmia of *Or83b*$^{-/-}$ caused lower eclosion rate, I carried out control experiments with *Or83b* functional with the survival assay. *Or83b* functional larvae express *Or83b* protein in all the OSNs under the control of *Or83b*-Gal4 in otherwise *Or83b*$^{-/-}$, therefore representing the genetic rescue of the mutant. If anosmia caused the poor cumulative eclosion rate of 50

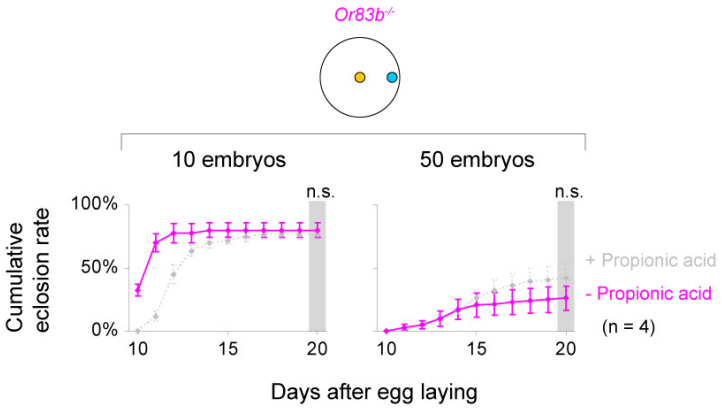

Figure 5.4: Propionic acid does not help *Or83*$^{-/-}$ larvae forage to the second food

Survival assay using food which does not contain propionic acid was carried out. Cumulative eclosion rates of *Or83b*$^{-/-}$ were plotted against days AEL (pink), and figures from equivalent experiment using standard food (with propionic acid) from Figure 5.1C were superimposed (grey). Statistical analysis was carried out on values from 20 days AEL (Student's t-test).

Or83b$^{-/-}$ embryos in the survival assay, genetic rescue of *Or83b* should rescue the phenotype.

The result was precisely what was expected. The cumulative eclosion rate of *Or83b* functional from 50 embryos with the second food was essentially the same as the value from the wild type (Figure 5.1D). The absence of the second food resulted in the same low cumulative eclosion rate, indicating that the genetic manipulation did not cause general enhancement of their development under malnutrition. Moreover, they migrated to the second food as robustly as the wild type (Figure 5.2D-F). Thus, the expression of the *Or83b* protein in all the OSNs is

sufficient for effective foraging and successful development under the patched distribution of food.

To what extent can an animal with a single functional OSN survive in these assays? In the survival assay the cumulative eclosion rate of *Or42a* functional larvae hatched from 50 embryos was virtually identical to the value of the wild type (Figure 5.1E) although they took one day longer to reach the half-maximum eclosion rate than the wild type (Figure 5.1E). They did migrate to the second food (Figure 5.2E), although the relative ratio of larvae found in the second food on 5 days AEL was not statistically significant from either of wild type or *Or83b*$^{-/-}$ (Figure 5.2F). Therefore, *Or42a* functional larvae behave very similar to the wild type, although there may be a small difference in the efficiency and developmental speed.

5.3.3. Selective advantage of the olfactory system

The poor cumulative eclosion rate of *Or83b*$^{-/-}$ in the challenging environment presented above suggests that the lack of the olfactory system can be a selective disadvantage. I next carried out a competition assay (Figure 5.5A) to further test this idea. Briefly, equal numbers of embryos from both wild type flies and *Or83b*$^{-/-}$ were introduced onto 100 mg of food. In the presence of the second food, eclosed adults of both strains were counted. This configuration would force individuals to compete, and any selective disadvantage of *Or83b*$^{-/-}$, if any, would result in decreased cumulative eclosion rate of this genotype.

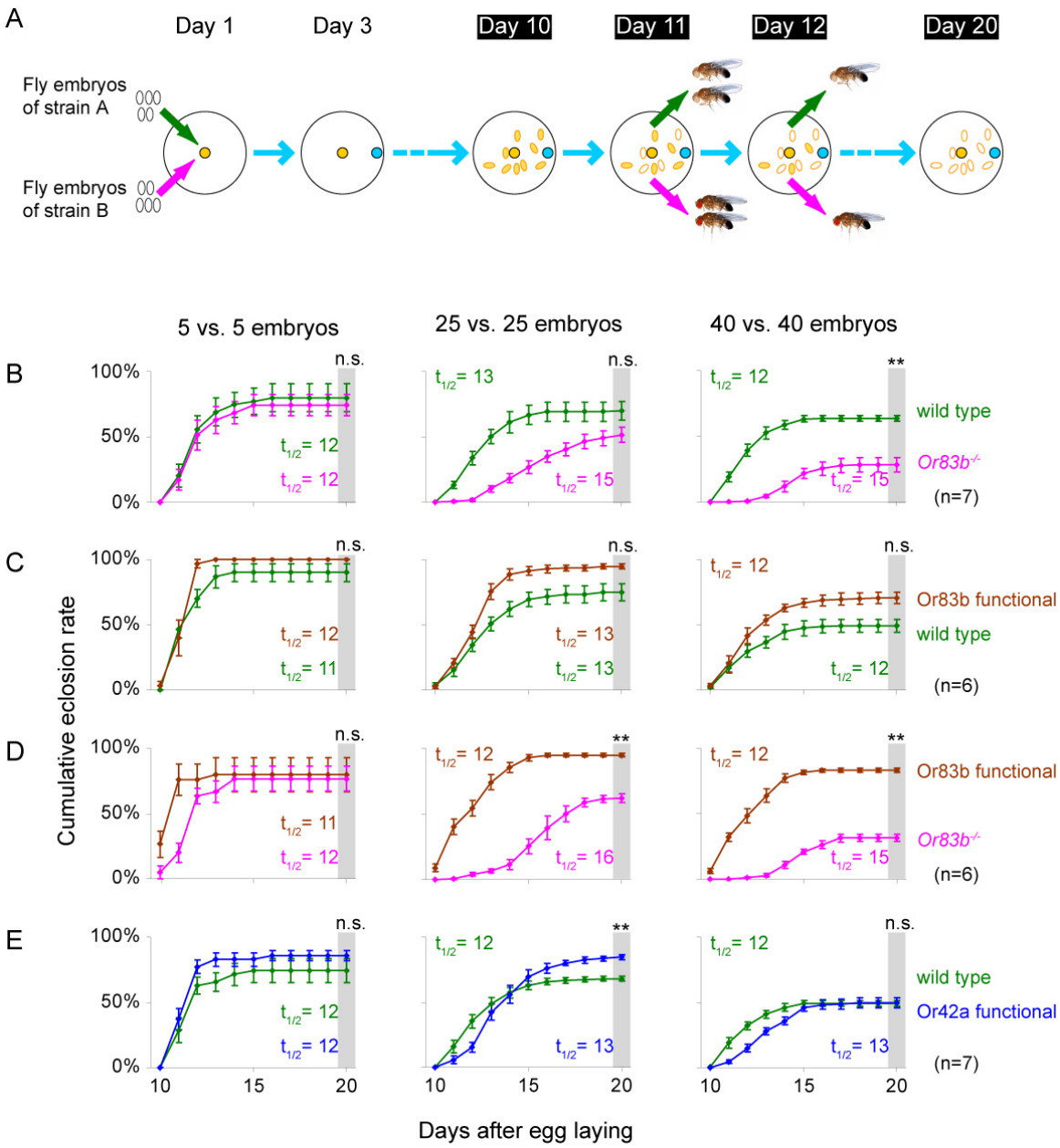

Figure 5.5: Competition assay reveals selective disadvantage of anosmic larvae

A) Schematic of experimental protocol of competition assay. Equal numbers of embryos from two fly strains were deposited on fly food centered in the agarose-coated arena. The second food was given at 3 days after egg laying (AEL). Starting 10 days AEL, numbers of eclosed adults were counted and genotyped day-by-day up to 20 days AEL. **B)** Cumulative eclosion rates from competition between wild type and *Or83b*$^{-/-}$ are plotted against days AEL (mean ± S.E.M.). **C-E** are plotted in the same manner. **C)** Competition between wild type and *Or83b* functional. **D)** Competition between *Or83b* functional and *Or83b*$^{-/-}$ **E)** Competition between wild type and *Or42a* functional. The number of embryos initially deposited is indicated at the top. Asterisks at 20 day AEL denote statistical significance (**: $P < 0.01$: Student's t-test. Bonferroni correction was applied to adjust p-value. **(B)**, **(C)**, **(D)**: factor = 6, **(E)**: factor = 4. Before the application of Bonferroni correction, the p-value from competition between 25 wild type and 25 *Or83b* functional is 0.0276, and the p-value from competition between 40 wild type and 40 *Or83b* functional is 0.0099).

When 5 embryos from both strains were introduced, both strains developed to adults with similar speed and rate, consistent with the results of the survival assay that 100 mg of food was sufficient for 10 embryos (Figure 5.5B, left). When 25 embryos each were introduced, however, *Or83b*$^{-/-}$ took markedly longer to develop to adulthood. Although the cumulative eclosion rate of the mutants at 20 days AEL was not statistically significant from that of the wild type, they took 2 more days to reach half maximum eclosion rate than wild type (Figure 5.5B, middle). This can be further illuminated by comparing distributions of eclosed adults of the two strains on each day. Eclosing patterns were significantly different between wild type and *Or83b*$^{-/-}$ from 25 embryos (Figure 5.6A) The difference became larger when 40 embryos each were introduced. Only 28% of *Or83b*$^{-/-}$ eclosed to adults by 20 days after egg laying (Figure 5.5B, right). Notably, the wild type showed only a small decrease of the eclosion rate as the density increased. Thus, *Or83b* null mutants were selectively eliminated in the competition with wild type larvae.

Again, *Or83b* functional restored the eclosion rate in the competition with wild type. In all the 3 conditions, the cumulative eclosion rate of *Or83b* functional was comparable to that of the wild type (Figure 5.5C). Eclosing patterns of the two were also the same (Figure 5.6B). Therefore, expression of *Or83b* proteins in OSNs is sufficient for effective competition with wild type larvae.

I applied this assay for competition between *Or83b*$^{-/-}$ and *Or83b* functional to address if the absence of *Or83b* protein in the OSNs is necessary for the poor performance of *Or83b*$^{-/-}$. As expected, the cumulative eclosion rate of *Or83b* null

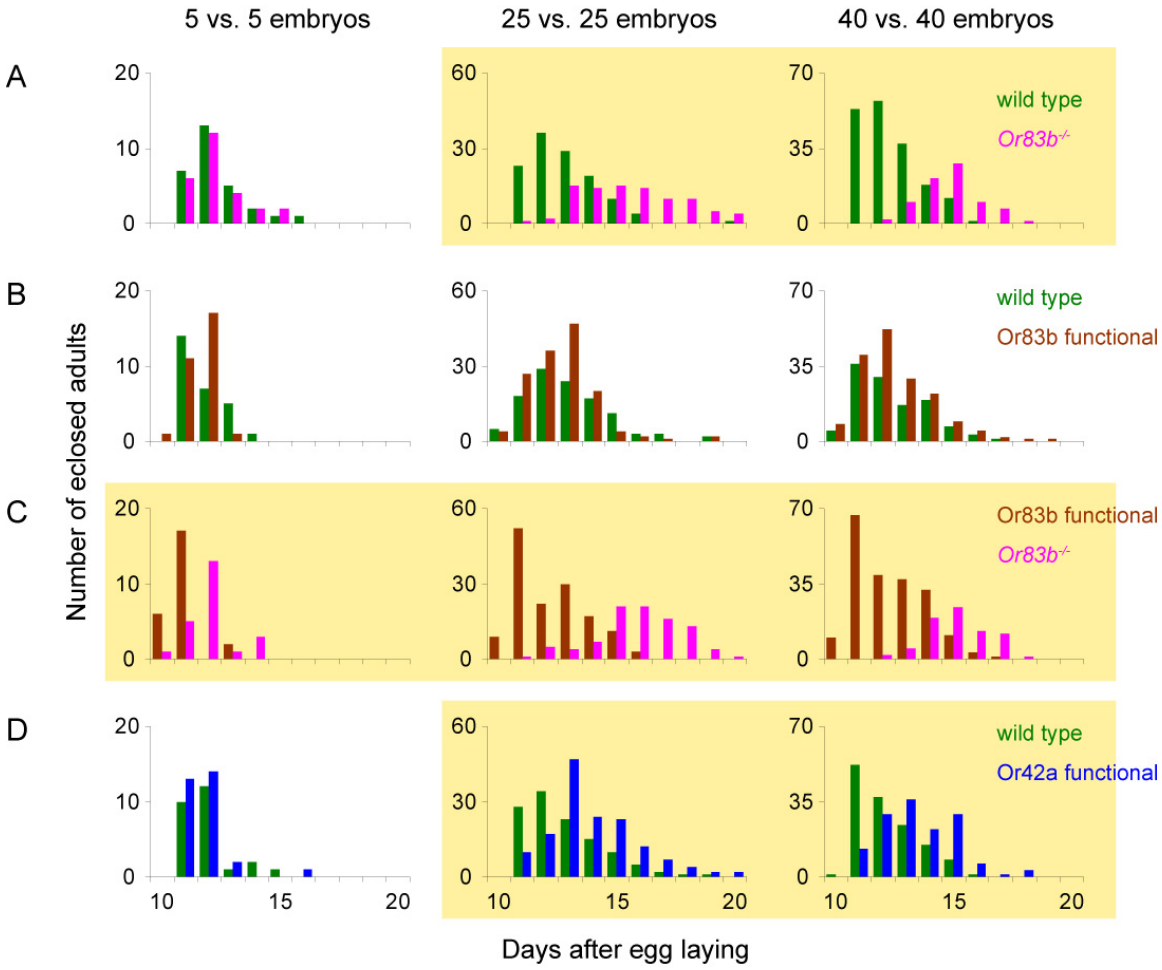

Figure 5.6: Delayed eclosion of *Or83b*$^{-/-}$ and *Or42a* functional in competition assay

The same data set in Figure 5.5 is represented as the total number of adults across all experiments eclosing on each day from 10 days AEL to 20 days AEL from all combinations. **A)** Competition between wild type and *Or83b*$^{-/-}$. **B)** Competition between wild type and *Or83b* functional. **C)** Competition between *Or83b*$^{-/-}$ and *Or83b* functional. **D)** Competition between wild type and *Or42a* functional. Yellow background indicates statistically significant difference between the two strains ($P < 0.01$, Kolmogorov-Smirnov test).

mutants was significantly lower than the value of *Or83b* functional when 25 or 40 embryos each were introduced (Figure 5.5D). Thus, a functional olfactory system

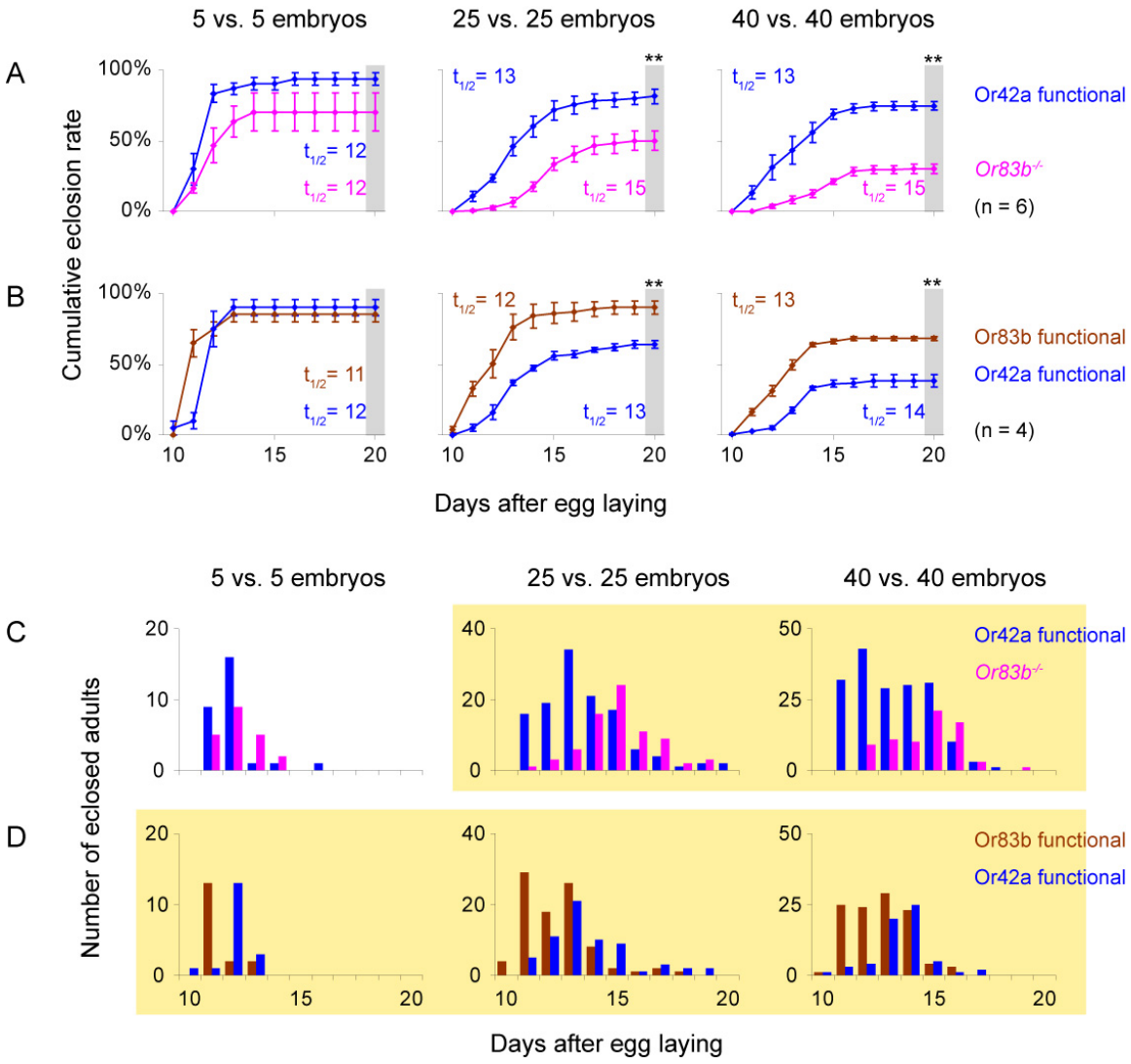

Figure 5.7: *Or42a* functional larvae are handicapped, but are more competitive than *Or83b*$^{-/-}$

A,B) The results of competitive assay are plotted as cumulative eclosion rate as in Figure 5.5. **A)** The result of competition assay between *Or83b*$^{-/-}$ and *Or42a* functional. **B)** The result of competitive assay between *Or83b* functional and *Or42a* functional. **: $P < 0.01$, Student's t-test. **C,D)** The same data set as in A and B is represented as the number of eclosed adults as in Figure 5.6. **C)** Competition between *Or83b*$^{-/-}$ and *Or42a* functional. **D)** Competition between *Or83b* functional and *Or42a* functional. Yellow background indicates statistically significant difference between the two strains ($P < 0.01$, Kolmogorov-Smirnov test).

is both necessary and sufficient for these animals to develop successfully under the competitive environment with the wild type.

I also tested *Or42a* functional in the competitive assay. When they were placed together with wild type embryos, their cumulative rate was comparable from the rate of wild type (Figure 5.5E). However, they took longer to reach half maximum eclosion rate than the wild type larvae. This is similar to the result of survival assay, and manifests a significant difference of eclosion pattern from the wild type in higher density (Figure 5.6D). When *Or83b* functional was introduced together with *Or42a* functional, the eclosion of *Or42a* functional was reduced compared to the *Or83b* functional larvae as the density increased (Figure 5.7B). *Or42a* functional developed better than $Or83b^{-/-}$ (Figure 5.7A), but still required one day more to reach the half maximum eclosion rate than the wild type when they competed with the *Or83b* null mutants. This difference can be clearly visualized when the number of eclosed adult is plotted day by day. The peak of *Or42a* functional eclosion is shifted one or two days later than the wild type (Figure 5.6D) or *Or83b* functional competitors (Figure 5.7D). As a result, the distribution pattern of eclosed *Or42a* functional is significantly different from that of the wild type or *Or83b* rescue competitors when 25 or 40 embryos each were introduced. Therefore, while larvae with one functional *Or42a*-expressing OSN are unexpectedly competitive, they perform less well when compared to larvae with 21 functional OSNs.

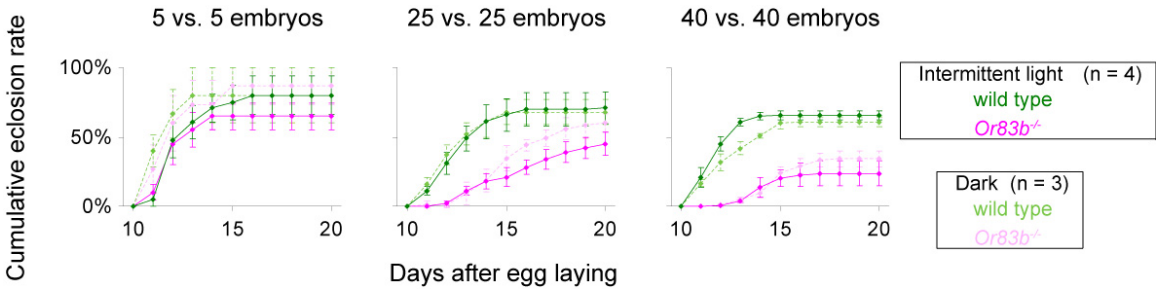

Figure 5.8: Intermittent illumination does not influence the outcome of competition assay

The results of competition assay between wild type and *Or83b*$^{-/-}$ in the darkness (lighter colors) and under intermittent illumination (darker colors) are plotted as Figure 5.5. Cumulative eclosion rates of wild type or *Or83b*$^{-/-}$ between the two conditions are not statistically significant under any embryo density ($P > 0.05$, Student's t-test).

5.4. Discussion

As far as I am aware, this is the first attempt to illuminate the selective advantage of the olfactory system. The result seems consistent with the popular notion that the olfactory system plays an important role in successful development.

5.4.1. Significance of the olfactory system on the survival of larvae

Even though the paradigm I employed here is highly artificial, the environment is nonetheless more challenging than standard laboratory condition. It is because larvae must reach the second food for sufficient nutrition for completing development when there are too many embryos on the initial food source. Yeast paste on the second food must be providing useful olfactory cue about the location of the second food. Thus, I interpret that the *Or83b* null mutants were

unable to locate where the additional food was, at least as efficiently as the wild type larvae, when they needed it. This resulted in poor eclosion rate both in the presence or absence of competitors.

It is also interesting that *Or42a*-expressing OSN can significantly restore the foraging ability in *Or83b*$^{-/-}$. So far, it is unclear what odorants the OSN is sensing in this experiment. *Or42a* is tuned to respond to many odorants (see Figure 3.2 and Kreher et al., 2005), and *Or42a* functional larvae can chemotax to diverse odorants (Fishilevich et al., 2005). Results from the competition assay are suggestive. Competition is often discussed in the context of interspecies interaction, such as a predator and prey. However, intraspecies competition also occurs. At least for larvae, the olfactory system plays a major role in the intraspecies competition over limiting food. How often such competition happens in nature is unknown. The availability and condition of rotten fruits can change rapidly. While it is unlikely that *Drosophila* larvae must “travel” for a long distance, it is certainly possible that they rove in search of better microenvironment. Their olfactory system will be a powerful tool to locate the best available feeding site. It is therefore of great interest for future research to monitor the behavior of these animals in their natural environment.

6. Concluding Remarks and Future Directions

Although *Drosophila* larvae possess a small olfactory organ and correspondingly simple olfactory circuit, they can serve as invaluable model organism for obtaining general insights into how this sensory system encodes odor information. Furthermore, it is possible to address the behavioral significance of the individual neuronal component of the olfactory circuit. The neuronal process in which the sensory information is converted to the motor output is an exciting topic in the field of neuroscience.

Studies on the olfactory system have lagged behind the other sensory systems such as the visual, auditory or somatosensory systems. The complex and often mysterious nature of odorants defied precise experimental controls, and the molecular identity and connectivity of the neurons in the olfactory circuit had been long unknown. The gap is closing rapidly, however, with explosive progress in describing the neuroanatomy and physiology of the olfactory system.

This thesis describes several fundamental aspects of the organization of the larval olfactory system. The isolation of the larval OR repertoire and the characterization of the larval odor response profiles are invaluable pieces of information to study this exceptionally tractable olfactory system of *Drosophila* larvae. Genetically defined populations of projection neurons and local interneurons make it possible to visualize the olfactory circuit beyond peripheral OSNs. Behavioral data strongly suggests that larvae utilize an ensemble of at least three OSNs to chemotax to ethyl butyrate, one of major components of fruit

odor, and calcium imaging allowed the visualization of neuronal components involved in integration of the inputs.

My work studying the selective advantage of the olfactory system under competitive condition has important implications for the rest of the thesis. Natural selection must have sculpted the fittest organisms. Thus the olfactory system of *Drosophila* larva appears to have an indispensable role in the development of this animal. Although the experimental conditions used in my study are clearly artificial, these were sufficient to demonstrate that there is a condition which necessitates the olfactory system. It would be interesting to study the ecology of *Drosophila melanogaster* and better simulate the composition of microenvironments through which they navigate (Keller, 2007).

The ubiquity of *Drosophila melanogaster* may be derived from wide receptive range of their olfactory system. *Drosophila melanogaster* has several closely related species. Among them, *Drosophila sechellia* specifically oviposits on the fruit of *Morinda citrifolia* (noni fruit). Reflecting this specialization, adult *D. sechellia* have many more *Or22a*-expressing OSN possibly at the expense of other classes of OSNs (Dekker et al., 2006; Stensmyr et al., 2003a). This amplification of one OSN class is correlated with elevated physiological and behavioral sensitivity of this species to methyl hexanoate, a major component of noni fruit odor (Dekker et al., 2006). Thus, it appears that *D. sechellia* organizes its olfactory system for narrower tuning to a specific host. *D. melanogaster*, on the other hand, flourishes near human habitats with a generalist olfactory system compared to its more specialized sister species. It will be interesting to

characterize larval OR repertoires in the other 12 *Drosophila* species whose genome sequences were recently decoded (*Drosophila* 12 Genomes Consortium, 2007), and to correlate odor response profiles with the known habitats of these fly species. Such knowledge may bring a hint on what odorants *Drosophila* melanogaster larvae detects through aromatic-sensitive Class 2 receptors. It is possible that these ORs are conserved among larvae for detection of common odorants such as yeast by-products. Any *Drosophila melanogaster*-specific ORs, on the other hand, may illuminate their specific niche requirements. *Drosophila melanogaster*'s preference of yeast species, if it exists as was reported in larvae of other *Drosophila* species (Cooper, 1960; Fogleman et al., 1981; Lindsay, 1958), may provide an alternative approach to identify ecologically relevant cues from their natural habitat and olfactory environment.

I used ethyl butyrate to dissect the larval olfactory circuit. Monitoring three different neuronal components suggests the functional significance of each. As was stated in Section 1.5, however, odors seldom exist as pure compound in nature. "Natural" stimuli for the olfactory system are almost always a mixture of many odorant molecules. This is similar to the case in visual system or auditory system, for example, in which light and sounds come in composite of many wavelengths and amplitudes. In case of light, these heterogeneous stimuli have even more complex spatial pattern. As was reviewed in Section 1.1, the visual system of vertebrates is organized to be sensitive to contrast rather than a uniform stimulus. Therefore, the true capacity of a sensory organ – and what really it is tuned for – can be revealed by complex yet natural stimuli. Processing

of odor mixtures at the neuronal level, however, has become the focus of research only recently (Lei et al., 2006; Tabor et al., 2004; Yoshida and Mori, 2007; Zou and Buck, 2006). In many experiments, binary mixtures of odorants were used, which is still a significant decrease of complexity from natural odors. In a rare test of more naturalistic odor samples to mouse olfactory bulb (Lin et al., 2006), Lawrence Katz and colleagues argue that an odor mixture is processed as a linear summation of each of the components.

After examination of several neuronal components, I am curious if the observed phenomenon is due to the lateral processing. It is possible, for instance, that increasing noise level created by mixture of odorants is canceled out by gating inhibition mediated by local interneurons. Thus, glomerular representations of mixture may appear similar to the sum of individual components because of active processing at the olfactory bulb, not simply because there is no interaction between OSN inputs. Since the effect of single OSNs on projection neurons or local interneurons can be measured in larvae, it will be of great interest to address how an odor mixture influences the activity of the olfactory circuit. My personal experience in a fly laboratory for the past 5 years tells me that flies are more attracted by natural food odors such as salad dressing, coffee, pizza, and so on than pure chemicals. Odor mixtures may therefore have a special appeal to flies.

A popular idea is that a mixture of odorants has quality distinct from individual components. Humans may be unable to discriminate more than four odorants in the mixture, even if each of them has a different perceptual quality

(Livermore and Laing, 1998). This suggests that the combination of activated OSNs produces a novel perceptual quality, and argues against olfactory labeled-line model at the cognitive level. Several observations suggest that neurons in higher processing center can be activated more efficiently by a mixture than any single component (Lei et al., 2006; Yoshida and Mori, 2007; Zou and Buck, 2006), or inhibited strongly while individual components do not inhibit the neuron (Yoshida and Mori, 2007). It is certainly possible that cortical neurons simultaneously receive input from multiple classes of M/T cells. The innervation patterns of Kenyon cells in the insect mushroom body appear to be suited for this type of integration. Kenyon cells sensitive to particular concentration of an odor have been reported (Perez-Orive et al., 2002; Wang et al., 2004a): neither lower nor higher concentration activates them. Although this is different from mixture activation, Kenyon cells may be also tuned to an olfactory receptive range that is not present in OSNs or projection neurons. Taken together, higher-order neurons may provide the neuronal substrate to encode a distinct perceptual value to an odor.

It is tempting to speculate that the “complex” receptive ranges of higher order neurons are generated by progressive integration and processing of odorant information. However, several lines of observation suggest that OSNs can perform rather complex integration of mixture (Duchamp-Viret et al., 2003; Oka et al., 2004), just as retinal ganglion cells or polymodal noticeptive neurons can encode compound sensory signals. Some cockroach OSNs can respond to a change of odor concentration, not necessarily the presence or absence of an

odorant (Tichy et al., 2005). Thus, a degree of information processing may occur at the very periphery of the olfactory system, which makes one wonder if the complex receptive ranges observed in the cortex or in the mushroom body are merely a reflection of complex responses in peripheral OSNs.

I have been unable to apply calcium imaging to the larval Kenyon cells (data not shown). However, once this becomes possible, the larval olfactory system can provide a basic platform to study where the complex receptive range of an olfactory neuron originates. As I pointed out above, a major challenge is how to define “complex” stimuli in a behaviorally relevant manner. Yoshida and Mori (Yoshida and Mori, 2007) advocate that any food smell can be characterized by a combination of 14 chemical groups, each of which has distinct chemical structure and perceptual quality. In other words, there may be only as many as 14 dimensions in the human olfactory world. If that is indeed the case, the olfactory world of larvae can be even less – maybe few enough to model the perceptual odor space of larvae.

How do animals “decide” to proceed toward the odor source? Sensory input must be somehow converted to motor output, but the neuronal process still defies detailed molecular and cellular research. Since larval motor neurons have been extensively studied, both anatomically and physiologically, larval chemotaxis behavior allows future investigators to link the processing of sensory input to motor output. Is there a “Go” or “No Go” neuron in the brain, which dictates what larvae do in response to olfactory stimuli? How is it combined with other sensory modalities such as taste or light? Are there any factors influencing

the behavioral output, such as circadian rhythm or hunger state? These are all technically and intellectually challenging questions, but we may mark a first step by examining the *Drosophila larva*, a simple yet increasingly useful model organism for behavioral neuroscience.

Publications

Peer-Reviewed Articles

Fishilevich, E., Domingos, A.I., **Asahina, K.**, Naef, F., Vosshall, L.B. and Louis, M. (2005). Chemotaxis Behavior Mediated by Single Larval Olfactory Neurons in *Drosophila*. *Current Biology 15*, 2086-2096.

Asahina, K.*, Louis, M.*, Piccinotti, S. and Vosshall, L.B. (2008) A Circuit Supporting the Perception of Odor Concentration. In preparation for submission to Cell. *equal contribution

Asahina, K., Pavlenkovich, V. and Vosshall, L.B. (2008) The Selective Advantage of Olfaction in a Competitive Environment. In preparation for submission to Current Biology.

Review Article

Asahina, K. and Benton, R. (2007) Smell and Taste on a High: Symposium on Chemical Senses: from Genes to Perception. *EMBO Report 8*, 634-638

References

Abbott, L. F., and Luo, S. X. (2007). A step toward optimal coding in olfaction. Nat Neurosci *10*, 1342-1343.

Abbott, L. F., and Regehr, W. G. (2004). Synaptic computation. Nature *431*, 796-803.

Abraham, N. M., Spors, H., Carleton, A., Margrie, T. W., Kuner, T., and Schaefer, A. T. (2004). Maintaining accuracy at the expense of speed: stimulus similarity defines odor discrimination time in mice. Neuron *44*, 865-876.

Aceves-Pina, E. O., and Quinn, W. G. (1979). Learning in Normal and Mutant *Drosophila* Larvae. Science *206*, 93-96.

Ache, B. W., and Young, J. M. (2005). Olfaction: diverse species, conserved principles. Neuron *48*, 417-430.

Adler, E., Hoon, M. A., Mueller, K. L., Chandrashekar, J., Ryba, N. J., and Zuker, C. S. (2000). A novel family of mammalian taste receptors. Cell *100*, 693-702.

Arevian, A. C., Kapoor, V., and Urban, N. N. (2008). Activity-dependent gating of lateral inhibition in the mouse olfactory bulb. Nat Neurosci *11*, 80-87.

Augustine, G. J., Santamaria, F., and Tanaka, K. (2003). Local calcium signaling in neurons. Neuron *40*, 331-346.

Aungst, J. L., Heyward, P. M., Puche, A. C., Karnup, S. V., Hayar, A., Szabo, G., and Shipley, M. T. (2003). Centre-surround inhibition among olfactory bulb glomeruli. Nature *426*, 623-629.

Bandell, M., Story, G. M., Hwang, S. W., Viswanath, V., Eid, S. R., Petrus, M. J., Earley, T. J., and Patapoutian, A. (2004). Noxious cold ion channel TRPA1 is activated by pungent compounds and bradykinin. Neuron *41*, 849-857.

Bargmann, C. I. (2006). Comparative chemosensation from receptors to ecology. Nature *444*, 295-301.

Benton, R., Sachse, S., Michnick, S. W., and Vosshall, L. B. (2006). Atypical membrane topology and heteromeric function of *Drosophila* odorant receptors in vivo. PLoS Biol *4*, e20.

Benton, R., Vannice, K. S., and Vosshall, L. B. (2007). An essential role for a CD36-related receptor in pheromone detection in *Drosophila*. Nature *450*, 289-293.

Berg, B. G., Almaas, T. J., Bjaalie, J. G., and Mustaparta, H. (2005). Projections of male-specific receptor neurons in the antennal lobe of the Oriental tobacco budworm moth, *Helicoverpa assulta*: a unique glomerular organization among related species. J Comp Neurol *486*, 209-220.

Bhandawat, V., Olsen, S. R., Gouwens, N. W., Schlief, M. L., and Wilson, R. I. (2007). Sensory processing in the *Drosophila* antennal lobe increases reliability and separability of ensemble odor representations. Nat Neurosci *10*, 1474-1482.

Bohbot, J., Pitts, R. J., Kwon, H. W., Rutzler, M., Robertson, H. M., and Zwiebel, L. J. (2007). Molecular characterization of the *Aedes aegypti* odorant receptor gene family. Insect Mol Biol *16*, 525-537.

Boyle, J., and Cobb, M. (2005). Olfactory coding in *Drosophila* larvae investigated by cross-adaptation. J Exp Biol *208*, 3483-3491.

Bozza, T., Feinstein, P., Zheng, C., and Mombaerts, P. (2002). Odorant receptor expression defines functional units in the mouse olfactory system. J Neurosci *22*, 3033-3043.

Bozza, T., McGann, J. P., Mombaerts, P., and Wachowiak, M. (2004). *In vivo* imaging of neuronal activity by targeted expression of a genetically encoded probe in the mouse. Neuron *42*, 9-21.

Brennan, P. A., and Zufall, F. (2006). Pheromonal communication in vertebrates. Nature *444*, 308-315.

Bronstein, J. L., Alarcon, R., and Geber, M. (2006). The evolution of plant-insect mutualisms. New Phytol *172*, 412-428.

Buck, L., and Axel, R. (1991). A novel multigene family may encode odorant receptors: a molecular basis for odor recognition. Cell *65*, 175-187.

Cant, N. B., and Benson, C. G. (2003). Parallel auditory pathways: projection patterns of the different neuronal populations in the dorsal and ventral cochlear nuclei. Brain Res Bull *60*, 457-474.

Carr, W. E., Gleeson, R. A., and Trapido-Rosenthal, H. G. (1990). The role of perireceptor events in chemosensory processes. Trends Neurosci *13*, 212-215.

Caterina, M. J., Rosen, T. A., Tominaga, M., Brake, A. J., and Julius, D. (1999). A capsaicin-receptor homologue with a high threshold for noxious heat. Nature *398*, 436-441.

Caterina, M. J., Schumacher, M. A., Tominaga, M., Rosen, T. A., Levine, J. D., and Julius, D. (1997). The capsaicin receptor: a heat-activated ion channel in the pain pathway. Nature *389*, 816-824.

Chan, D. K., and Hudspeth, A. J. (2005). Ca^{2+} current-driven nonlinear amplification by the mammalian cochlea *in vitro*. Nat Neurosci *8*, 149-155.

Chandrashekar, J., Hoon, M. A., Ryba, N. J., and Zuker, C. S. (2006). The receptors and cells for mammalian taste. Nature *444*, 288-294.

Chandrashekar, J., Mueller, K. L., Hoon, M. A., Adler, E., Feng, L., Guo, W., Zuker, C. S., and Ryba, N. J. (2000). T2Rs function as bitter taste receptors. Cell *100*, 703-711.

Christensen, A. P., and Corey, D. P. (2007). TRP channels in mechanosensation: direct or indirect activation? Nat Rev Neurosci *8*, 510-521.

Christensen, T. A., and Hildebrand, J. G. (1987). Male-specific, sex pheromone-selective projection neurons in the antennal lobes of the moth *Manduca sexta*. J Comp Physiol [A] *160*, 553-569.

Christensen, T. A., Waldrop, B. R., Harrow, I. D., and Hildebrand, J. G. (1993). Local interneurons and information processing in the olfactory glomeruli of the moth *Manduca sexta*. J Comp Physiol [A] *173*, 385-399.

Chyb, S., Dahanukar, A., Wickens, A., and Carlson, J. R. (2003). *Drosophila Gr5a* encodes a taste receptor tuned to trehalose. Proc Natl Acad Sci U S A *100 Suppl 2*, 14526-14530.

Clyne, P. J., Warr, C. G., Freeman, M. R., Lessing, D., Kim, J., and Carlson, J. R. (1999). A novel family of divergent seven-transmembrane proteins: candidate odorant receptors in *Drosophila*. Neuron *22*, 327-338.

Cobb, M. (1999). What and how do maggots smell? Biological Review *74*, 425-459.

Cobb, M., and Domain, I. (2000). Olfactory coding in a simple system: adaptation in *Drosophila* larvae. Proc Biol Sci *267*, 2119-2125.

Cooper, D. M. (1960). Food preference of larval and adult *Drosophila*. Evolution *14*, 41-55.

Couto, A., Alenius, M., and Dickson, B. J. (2005). Molecular, anatomical, and functional organization of the *Drosophila* olfactory system. Curr Biol *15*, 1535-1547.

Crane, P. R., Friis, E. M., Pedersen, K. R. (1995). The origin and early diversification of angiosperms. Nature *374*, 27-33.

Dacey, D. M., Lee, B. B., Stafford, D. K., Pokorny, J., and Smith, V. C. (1996). Horizontal cells of the primate retina: cone specificity without spectral opponency. Science *271*, 656-659.

Dallos, P. (1992). The active cochlea. J Neurosci *12*, 4575-4585.

de Bruyne, M., Clyne, P. J., and Carlson, J. R. (1999). Odor coding in a model olfactory organ: the *Drosophila* maxillary palp. J Neurosci *19*, 4520-4532.

de Bruyne, M., Foster, K., and Carlson, J. R. (2001). Odor coding in the *Drosophila* antenna. Neuron *30*, 537-552.

Dekker, T., Ibba, I., Siju, K. P., Stensmyr, M. C., and Hansson, B. S. (2006). Olfactory shifts parallel superspecialism for toxic fruit in *Drosophila melanogaster* sibling, *D. sechellia*. Curr Biol *16*, 101-109.

Dobritsa, A. A., van der Goes van Naters, W., Warr, C. G., Steinbrecht, R. A., and Carlson, J. R. (2003). Integrating the molecular and cellular basis of odor coding in the *Drosophila* antenna. Neuron *37*, 827-841.

Drosophila 12 Genomes Consortium. (2007). Evolution of genes and genomes on the *Drosophila* phylogeny. Nature *450*, 203-218.

Duchamp-Viret, P., Duchamp, A., and Chaput, M. A. (2003). Single olfactory sensory neurons simultaneously integrate the components of an odour mixture. Eur J Neurosci *18*, 2690-2696.

Elmore, T., Ignell, R., Carlson, J. R., and Smith, D. P. (2003). Targeted mutation of a *Drosophila* odor receptor defines receptor requirement in a novel class of sensillum. J Neurosci *23*, 9906-9912.

Estes, P. S., Ho, G. L., Narayanan, R., and Ramaswami, M. (2000). Synaptic localization and restricted diffusion of a *Drosophila* neuronal synaptobrevin--green fluorescent protein chimera *in vivo*. J Neurogenet *13*, 233-255.

Euler, T., Detwiler, P. B., and Denk, W. (2002). Directionally selective calcium signals in dendrites of starburst amacrine cells. Nature *418*, 845-852.

Fiala, A., Spall, T., Diegelmann, S., Eisermann, B., Sachse, S., Devaud, J. M., Buchner, E., and Galizia, C. G. (2002). Genetically expressed cameleon in *Drosophila melanogaster* is used to visualize olfactory information in projection neurons. Curr Biol *12*, 1877-1884.

Fischler, W., Kong, P., Marella, S., and Scott, K. (2007). The detection of carbonation by the *Drosophila* gustatory system. Nature *448*, 1054-1057.

Fishilevich, E., Domingos, A. I., Asahina, K., Naef, F., Vosshall, L. B., and Louis, M. (2005). Chemotaxis behavior mediated by single larval olfactory neurons in *Drosophila*. Curr Biol *15*, 2086-2096.

Fishilevich, E., and Vosshall, L. B. (2005). Genetic and functional subdivision of the *Drosophila* antennal lobe. Curr Biol *15*, 1548-1553.

Fitzpatrick, M. J., Feder, E., Rowe, L., and Sokolowski, M. B. (2007). Maintaining a behaviour polymorphism by frequency-dependent selection on a single gene. Nature *447*, 210-212.

Fogleman, J. C., Starmer, W. T., and Heed, W. B. (1981). Larval selectivity for yeast species by *Drosophila mojavensis* in natural substrates. Proc Natl Acad Sci U S A *78*, 4435-4439.

Fonta, C., Sun, X.-J., Masson, C (1993). Morphology and spatial distribution of bee lobe interneurons responsive to odours. Chem Senses *18*, 101-119.

Fried, S. I., Munch, T. A., and Werblin, F. S. (2002). Mechanisms and circuitry underlying directional selectivity in the retina. Nature *420*, 411-414.

Friedrich, R. W., and Korsching, S. I. (1997). Combinatorial and chemotopic odorant coding in the zebrafish olfactory bulb visualized by optical imaging. Neuron *18*, 737-752.

Friedrich, R. W., and Laurent, G. (2001). Dynamic optimization of odor representations by slow temporal patterning of mitral cell activity. Science *291*, 889-894.

Fuss, S. H., Omura, M., and Mombaerts, P. (2007). Local and *cis* effects of the H element on expression of odorant receptor genes in mouse. Cell *130*, 373-384.

Galizia, C. G., McIlwrath, S. L., and Menzel, R. (1999a). A digital three-dimensional atlas of the honeybee antennal lobe based on optical sections acquired by confocal microscopy. Cell Tissue Res *295*, 383-394.

Galizia, C. G., Sachse, S., and Mustaparta, H. (2000). Calcium responses to pheromones and plant odours in the antennal lobe of the male and female moth *Heliothis virescens*. J Comp Physiol [A] *186*, 1049-1063.

Galizia, C. G., Sachse, S., Rappert, A., and Menzel, R. (1999b). The glomerular code for odor representation is species specific in the honeybee *Apis mellifera*. Nat Neurosci *2*, 473-478.

Gao, Q., and Chess, A. (1999). Identification of candidate *Drosophila* olfactory receptors from genomic DNA sequence. Genomics *60*, 31-39.

Gao, Q., Yuan, B., and Chess, A. (2000). Convergent projections of *Drosophila* olfactory neurons to specific glomeruli in the antennal lobe. Nat Neurosci *3*, 780-785.

Gardner, E. P., Martin, J. H., Jessell, T. M. (2000). The bodily senses. In Principles of Neural Science, E. R. Kandel, Schwartz, J. H., Jessell, T. M., ed. (New York, McGraw-Hill), pp. 430-450.

Gegenfurtner, K. R., and Kiper, D. C. (2003). Color vision. Annu Rev Neurosci *26*, 181-206.

Gong, Z., Son, W., Chung, Y. D., Kim, J., Shin, D. W., McClung, C. A., Lee, Y., Lee, H. W., Chang, D. J., Kaang, B. K.*, et al.* (2004). Two interdependent TRPV channel subunits, *inactive* and *Nanchung*, mediate hearing in *Drosophila*. J Neurosci *24*, 9059-9066.

Ha, T. S., and Smith, D. P. (2006). A pheromone receptor mediates 11-*cis*-vaccenyl acetate-induced responses in *Drosophila*. J Neurosci *26*, 8727-8733.

Halfon, M. S., Gisselbrecht, S., Lu, J., Estrada, B., Keshishian, H., and Michelson, A. M. (2002). New fluorescent protein reporters for use with the *Drosophila* Gal4 expression system and for vital detection of balancer chromosomes. Genesis *34*, 135-138.

Hallem, E. A., and Carlson, J. R. (2006). Coding of odors by a receptor repertoire. Cell *125*, 143-160.

Hallem, E. A., Ho, M. G., and Carlson, J. R. (2004). The molecular basis of odor coding in the *Drosophila* antenna. Cell *117*, 965-979.

Hart, K., and Bienz, M. (1996). A test for cell autonomy, based on di-cistronic messenger translation. Development *122*, 747-751.

Heimbeck, G., Bugnon, V., Gendre, N., Haberlin, C., and Stocker, R. F. (1999). Smell and taste perception in *Drosophila melanogaster* larva: toxin expression studies in chemosensory neurons. J Neurosci *19*, 6599-6609.

Hildebrand, J. G., and Shepherd, G. M. (1997). Mechanisms of olfactory discrimination: converging evidence for common principles across phyla. Annu Rev Neurosci *20*, 595-631.

Hill, C. A., Fox, A. N., Pitts, R. J., Kent, L. B., Tan, P. L., Chrystal, M. A., Cravchik, A., Collins, F. H., Robertson, H. M., and Zwiebel, L. J. (2002). G protein-coupled receptors in *Anopheles gambiae*. Science *298*, 176-178.

Huang, A. L., Chen, X., Hoon, M. A., Chandrashekar, J., Guo, W., Trankner, D., Ryba, N. J., and Zuker, C. S. (2006). The cells and logic for mammalian sour taste detection. Nature *442*, 934-938.

Hudspeth, A. J. (1989). How the ear's works work. Nature *341*, 397-404.

Hudspeth, A. J. (2000). Hearing. In The Principles of Neural Science, E. R. Kandel, Schwartz, J. H., Jessell, T. M., ed. (New York, McGraw-Hill), pp. 590-613.

Inoshita, T., and Tanimura, T. (2006). Cellular identification of water gustatory receptor neurons and their central projection pattern in *Drosophila*. Proc Natl Acad Sci U S A *103*, 1094-1099.

Isaacson, J. S., and Strowbridge, B. W. (1998). Olfactory reciprocal synapses: dendritic signaling in the CNS. Neuron *20*, 749-761.

Ishimaru, Y., Inada, H., Kubota, M., Zhuang, H., Tominaga, M., and Matsunami, H. (2006). Transient receptor potential family members PKD1L3 and PKD2L1 form a candidate sour taste receptor. Proc Natl Acad Sci U S A *103*, 12569-12574.

Jefferis, G. S., Potter, C. J., Chan, A. M., Marin, E. C., Rohlfing, T., Maurer, C. R., Jr., and Luo, L. (2007). Comprehensive maps of *Drosophila* higher olfactory centers: spatially segregated fruit and pheromone representation. Cell *128*, 1187-1203.

Johnson, K. O., Hsiao, S. S., and Yoshioka, T. (2002). Neural coding and the basic law of psychophysics. Neuroscientist *8*, 111-121.

Jones, W. D., Cayirlioglu, P., Kadow, I. G., and Vosshall, L. B. (2007). Two chemosensory receptors together mediate carbon dioxide detection in *Drosophila*. Nature *445*, 86-90.

Jones, W. D., Nguyen, T. A., Kloss, B., Lee, K. J., and Vosshall, L. B. (2005). Functional conservation of an insect odorant receptor gene across 250 million years of evolution. Curr Biol *15*, R119-121.

Jordt, S. E., Bautista, D. M., Chuang, H. H., McKemy, D. D., Zygmunt, P. M., Hogestatt, E. D., Meng, I. D., and Julius, D. (2004). Mustard oils and cannabinoids excite sensory nerve fibres through the TRP channel ANKTM1. Nature *427*, 260-265.

Jorerges, J., Kuttner, A., Galizia, C. G., Menzel, R. (1997). Representations of odours and odour mixtures visualized in the honeybee brain. Nature *387*, 285-288.

Julius, D., and Basbaum, A. I. (2001). Molecular mechanisms of nociception. Nature *413*, 203-210.

Katada, S., Hirokawa, T., Oka, Y., Suwa, M., and Touhara, K. (2005). Structural basis for a broad but selective ligand spectrum of a mouse olfactory receptor: mapping the odorant-binding site. J Neurosci *25*, 1806-1815.

Keen, E. C., and Hudspeth, A. J. (2006). Transfer characteristics of the hair cell's afferent synapse. Proc Natl Acad Sci U S A *103*, 5537-5542.

Keller, A. (2007). *Drosophila melanogaster*'s history as a human commensal. Curr Biol *17*, R77-81.

Kim, J., Chung, Y. D., Park, D. Y., Choi, S., Shin, D. W., Soh, H., Lee, H. W., Son, W., Yim, J., Park, C. S.*, et al.* (2003). A TRPV family ion channel required for hearing in *Drosophila*. Nature *424*, 81-84.

Kreher, S. A., Kwon, J. Y., and Carlson, J. R. (2005). The molecular basis of odor coding in the *Drosophila* larva. Neuron *46*, 445-456.

Kurtovic, A., Widmer, A., and Dickson, B. J. (2007). A single class of olfactory neurons mediates behavioural responses to a *Drosophila* sex pheromone. Nature *446*, 542-546.

Kwon, H. W., Lu, T., Rutzler, M., and Zwiebel, L. J. (2006). Olfactory responses in a gustatory organ of the malaria vector mosquito *Anopheles gambiae*. Proc Natl Acad Sci U S A *103*, 13526-13531.

Kwon, J. Y., Dahanukar, A., Weiss, L. A., and Carlson, J. R. (2007). The molecular basis of CO_2 reception in *Drosophila*. Proc Natl Acad Sci U S A *104*, 3574-3578.

Laissue, P. P., Reiter, C., Hiesinger, P. R., Halter, S., Fischbach, K. F., and Stocker, R. F. (1999). Three-dimensional reconstruction of the antennal lobe in *Drosophila melanogaster*. J Comp Neurol *405*, 543-552.

Larsson, M. C., Domingos, A. I., Jones, W. D., Chiappe, M. E., Amrein, H., and Vosshall, L. B. (2004). *Or83b* encodes a broadly expressed odorant receptor essential for *Drosophila* olfaction. Neuron *43*, 703-714.

Lee, S., and Zhou, Z. J. (2006). The synaptic mechanism of direction selectivity in distal processes of starburst amacrine cells. Neuron *51*, 787-799.

Lei, H., Mooney, R., and Katz, L. C. (2006). Synaptic integration of olfactory information in mouse anterior olfactory nucleus. J Neurosci *26*, 12023-12032.

Liberles, S. D., and Buck, L. B. (2006). A second class of chemosensory receptors in the olfactory epithelium. Nature *442*, 645-650.

Lin, D. Y., Shea, S. D., and Katz, L. C. (2006). Representation of natural stimuli in the rodent main olfactory bulb. Neuron *50*, 937-949.

Lin, H. H., Lai, J. S., Chin, A. L., Chen, Y. C., and Chiang, A. S. (2007). A map of olfactory representation in the *Drosophila* mushroom body. Cell *128*, 1205-1217.

Lindsay, S. L. (1958). Food preference of *Drosophila* larvae. The American Naturalist *92*, 279-285.

Livermore, A., and Laing, D. G. (1998). The influence of odor type on the discrimination and identification of odorants in multicomponent odor mixtures. Physiol Behav *65*, 311-320.

Lomvardas, S., Barnea, G., Pisapia, D. J., Mendelsohn, M., Kirkland, J., and Axel, R. (2006). Interchromosomal interactions and olfactory receptor choice. Cell *126*, 403-413.

Louis, M., Huber, T., Benton, R., Sakmar, T. P., and Vosshall, L. B. (2008). Bilateral olfactory sensory input enhances chemotaxis behavior. Nat Neurosci *11*, 187-199.

Lumpkin, E. A., and Caterina, M. J. (2007). Mechanisms of sensory transduction in the skin. Nature *445*, 858-865.

Lundin, C., Kall, L., Kreher, S. A., Kapp, K., Sonnhammer, E. L., Carlson, J. R., Heijne, G., and Nilsson, I. (2007). Membrane topology of the Drosophila OR83b odorant receptor. FEBS Lett *581*, 5601-5604.

Luo, M., and Katz, L. C. (2001). Response correlation maps of neurons in the mammalian olfactory bulb. Neuron *32*, 1165-1179.

Malnic, B., Hirono, J., Sato, T., and Buck, L. B. (1999). Combinatorial receptor codes for odors. Cell *96*, 713-723.

Man, O., Gilad, Y., and Lancet, D. (2004). Prediction of the odorant binding site of olfactory receptor proteins by human-mouse comparisons. Protein Sci *13*, 240-254.

Marella, S., Fischler, W., Kong, P., Asgarian, S., Rueckert, E., and Scott, K. (2006). Imaging taste responses in the fly brain reveals a functional map of taste category and behavior. Neuron *49*, 285-295.

Marin, E. C., Jefferis, G. S., Komiyama, T., Zhu, H., and Luo, L. (2002). Representation of the glomerular olfactory map in the *Drosophila* brain. Cell *109*, 243-255.

Marin, E. C., Watts, R. J., Tanaka, N. K., Ito, K., and Luo, L. (2005). Developmentally programmed remodeling of the *Drosophila* olfactory circuit. Development *132*, 725-737.

McKemy, D. D., Neuhausser, W. M., and Julius, D. (2002). Identification of a cold receptor reveals a general role for TRP channels in thermosensation. Nature *416*, 52-58.

Meisami, E., and Bhatnagar, K. P. (1998). Structure and diversity in mammalian accessory olfactory bulb. Microsc Res Tech *43*, 476-499.

Meister, M., and Bonhoeffer, T. (2001). Tuning and topography in an odor map on the rat olfactory bulb. J Neurosci *21*, 1351-1360.

Melzack, R., and Wall, P. D. (1965). Pain mechanisms: a new theory. Science *150*, 971-979.

Mombaerts, P. (1999). Seven-transmembrane proteins as odorant and chemosensory receptors. Science *286*, 707-711.

Mombaerts, P. (2004). Genes and ligands for odorant, vomeronasal and taste receptors. Nat Rev Neurosci *5*, 263-278.

Mombaerts, P., Wang, F., Dulac, C., Chao, S. K., Nemes, A., Mendelsohn, M., Edmondson, J., and Axel, R. (1996). Visualizing an olfactory sensory map. Cell *87*, 675-686.

Mori, K., Mataga, N., and Imamura, K. (1992). Differential specificities of single mitral cells in rabbit olfactory bulb for a homologous series of fatty acid odor molecules. J Neurophysiol *67*, 786-789.

Mueller, K. L., Hoon, M. A., Erlenbach, I., Chandrashekar, J., Zuker, C. S., and Ryba, N. J. (2005). The receptors and coding logic for bitter taste. Nature *434*, 225-229.

Murphy, G. J., Darcy, D. P., and Isaacson, J. S. (2005). Intraglomerular inhibition: signaling mechanisms of an olfactory microcircuit. Nat Neurosci *8*, 354-364.

Nakagawa, T., Sakurai, T., Nishioka, T., and Touhara, K. (2005). Insect sex-pheromone signals mediated by specific combinations of olfactory receptors. Science *307*, 1638-1642.

Nakai, J., Ohkura, M., and Imoto, K. (2001). A high signal-to-noise Ca^{2+} probe composed of a single green fluorescent protein. Nat Biotechnol *19*, 137-141.

Nakanishi, S. (1992). Molecular diversity of glutamate receptors and implications for brain function. Science *258*, 597-603.

Nelson, G., Chandrashekar, J., Hoon, M. A., Feng, L., Zhao, G., Ryba, N. J., and Zuker, C. S. (2002). An amino-acid taste receptor. Nature *416*, 199-202.

Nelson, G., Hoon, M. A., Chandrashekar, J., Zhang, Y., Ryba, N. J., and Zuker, C. S. (2001). Mammalian sweet taste receptors. Cell *106*, 381-390.

Neuhaus, E. M., Gisselmann, G., Zhang, W., Dooley, R., Stortkuhl, K., and Hatt, H. (2005). Odorant receptor heterodimerization in the olfactory system of *Drosophila melanogaster*. Nat Neurosci *8*, 15-17.

Ng, M., Roorda, R. D., Lima, S. Q., Zemelman, B. V., Morcillo, P., and Miesenbock, G. (2002). Transmission of olfactory information between three populations of neurons in the antennal lobe of the fly. Neuron *36*, 463-474.

Niimura, Y., and Nei, M. (2003). Evolution of olfactory receptor genes in the human genome. Proc Natl Acad Sci U S A *100*, 12235-12240.

Nobili, R., Mammano, F., and Ashmore, J. (1998). How well do we understand the cochlea? Trends Neurosci *21*, 159-167.

Ohkura, M., Matsuzaki, M., Kasai, H., Imoto, K., and Nakai, J. (2005). Genetically encoded bright Ca^{2+} probe applicable for dynamic Ca^{2+} imaging of dendritic spines. Anal Chem *77*, 5861-5869.

Oka, Y., Katada, S., Omura, M., Suwa, M., Yoshihara, Y., and Touhara, K. (2006). Odorant receptor map in the mouse olfactory bulb: *in vivo* sensitivity and specificity of receptor-defined glomeruli. Neuron *52*, 857-869.

Oka, Y., Omura, M., Kataoka, H., and Touhara, K. (2004). Olfactory receptor antagonism between odorants. Embo J *23*, 120-126.

Olsen, S. R., Bhandawat, V., and Wilson, R. I. (2007). Excitatory interactions between olfactory processing channels in the *Drosophila* antennal lobe. Neuron *54*, 89-103.

Oppliger, F. Y., P, M. G., and Vlimant, M. (2000). Neurophysiological and behavioural evidence for an olfactory function for the dorsal organ and a gustatory one for the terminal organ in *Drosophila melanogaster* larvae. J Insect Physiol *46*, 135-144.

Osborne, K. A., Robichon, A., Burgess, E., Butland, S., Shaw, R. A., Coulthard, A., Pereira, H. S., Greenspan, R. J., and Sokolowski, M. B. (1997). Natural behavior polymorphism due to a cGMP-dependent protein kinase of *Drosophila*. Science *277*, 834-836.

Peier, A. M., Moqrich, A., Hergarden, A. C., Reeve, A. J., Andersson, D. A., Story, G. M., Earley, T. J., Dragoni, I., McIntyre, P., Bevan, S., and Patapoutian, A. (2002). A TRP channel that senses cold stimuli and menthol. Cell *108*, 705-715.

Pelz, D., Roeske, T., Syed, Z., de Bruyne, M., and Galizia, C. G. (2006). The molecular receptive range of an olfactory receptor *in vivo* (*Drosophila melanogaster Or22a*). J Neurobiol *66*, 1544-1563.

Perez-Orive, J., Mazor, O., Turner, G. C., Cassenaer, S., Wilson, R. I., and Laurent, G. (2002). Oscillations and sparsening of odor representations in the mushroom body. Science *297*, 359-365.

Phaff, H. J., Miller, M. W., Recca, J. A., Shifrine, M., Mark, E. M. (1956). Studies on the ecology of *Drosophila* in the Yosemite region of California. II. Yeasts found in the alimentary canal of *Drosophila*. Ecology *37*, 533-538.

Pologruto, T. A., Yasuda, R., and Svoboda, K. (2004). Monitoring neural activity and [Ca^{2+}] with genetically encoded Ca^{2+} indicators. J Neurosci *24*, 9572-9579.

Python, F., and Stocker, R. F. (2002). Adult-like complexity of the larval antennal lobe of *D. melanogaster* despite markedly low numbers of odorant receptor neurons. J Comp Neurol *445*, 374-387.

Ramaekers, A., Magnenat, E., Marin, E. C., Gendre, N., Jefferis, G. S., Luo, L., and Stocker, R. F. (2005). Glomerular maps without cellular redundancy at successive levels of the *Drosophila* larval olfactory circuit. Curr Biol *15*, 982-992.

Raphael, Y., and Altschuler, R. A. (2003). Structure and innervation of the cochlea. Brain Res Bull *60*, 397-422.

Ray, A., van Naters, W. G., Shiraiwa, T., and Carlson, J. R. (2007). Mechanisms of odor receptor gene choice in *Drosophila*. Neuron *53*, 353-369.

Reid, C. A., Bekkers, J. M., and Clements, J. D. (2003). Presynaptic Ca^{2+} channels: a functional patchwork. Trends Neurosci *26*, 683-687.

Rinberg, D., Koulakov, A., and Gelperin, A. (2006). Speed-accuracy tradeoff in olfaction. Neuron *51*, 351-358.

Rizo, J., Chen, X., and Arac, D. (2006). Unraveling the mechanisms of synaptotagmin and SNARE function in neurotransmitter release. Trends Cell Biol *16*, 339-350.

Robertson, H. M., and Wanner, K. W. (2006). The chemoreceptor superfamily in the honey bee, *Apis mellifera*: expansion of the odorant, but not gustatory, receptor family. Genome Res *16*, 1395-1403.

Robertson, H. M., Warr, C. G., and Carlson, J. R. (2003). Molecular evolution of the insect chemoreceptor gene superfamily in *Drosophila melanogaster*. Proc Natl Acad Sci U S A *100 Suppl 2*, 14537-14542.

Rosenzweig, M., Brennan, K. M., Tayler, T. D., Phelps, P. O., Patapoutian, A., and Garrity, P. A. (2005). The *Drosophila* ortholog of vertebrate TRPA1 regulates thermotaxis. Genes Dev *19*, 419-424.

Rubin, B. D., and Katz, L. C. (1999). Optical imaging of odorant representations in the mammalian olfactory bulb. Neuron *23*, 499-511.

Sachse, S., and Galizia, C. G. (2002). Role of inhibition for temporal and spatial odor representation in olfactory output neurons: a calcium imaging study. J Neurophysiol *87*, 1106-1117.

Sachse, S., Rueckert, E., Keller, A., Okada, R., Tanaka, N. K., Ito, K., and Vosshall, L. B. (2007). Activity-dependent plasticity in an olfactory circuit. Neuron *56*, 838-850.

Saito, H., Kubota, M., Roberts, R. W., Chi, Q., and Matsunami, H. (2004). RTP family members induce functional expression of mammalian odorant receptors. Cell *119*, 679-691.

Sakai, M., and Suga, N. (2001). Plasticity of the cochleotopic (frequency) map in specialized and nonspecialized auditory cortices. Proc Natl Acad Sci U S A *98*, 3507-3512.

Sato, K., Pellegrino, M., Nakagawa, T., Nakagawa, T., Vosshall, L.B., Touhara, K. (2008). Insect olfactory receptors are heteromeric ligand-gated channels. Nature *in press*.

Sato, T., Hirono, J., Tonoike, M., and Takebayashi, M. (1994). Tuning specificities to aliphatic odorants in mouse olfactory receptor neurons and their local distribution. J Neurophysiol *72*, 2980-2989.

Scherer, S., Stocker, R. F., and Gerber, B. (2003). Olfactory learning in individually assayed *Drosophila* larvae. Learn Mem *10*, 217-225.

Schlief, M. L., and Wilson, R. I. (2007). Olfactory processing and behavior downstream from highly selective receptor neurons. Nat Neurosci *10*, 623-630.

Schoppa, N. E., and Urban, N. N. (2003). Dendritic processing within olfactory bulb circuits. Trends Neurosci *26*, 501-506.

Schroll, C., Riemensperger, T., Bucher, D., Ehmer, J., Voller, T., Erbguth, K., Gerber, B., Hendel, T., Nagel, G., Buchner, E., and Fiala, A. (2006). Light-induced activation of distinct modulatory neurons triggers appetitive or aversive learning in *Drosophila* larvae. Curr Biol *16*, 1741-1747.

Scott, K. (2005). Taste recognition: food for thought. Neuron *48*, 455-464.

Scott, K., Brady, R., Jr., Cravchik, A., Morozov, P., Rzhetsky, A., Zuker, C., and Axel, R. (2001). A chemosensory gene family encoding candidate gustatory and olfactory receptors in *Drosophila*. Cell *104*, 661-673.

Serizawa, S., Miyamichi, K., Nakatani, H., Suzuki, M., Saito, M., Yoshihara, Y., and Sakano, H. (2003). Negative feedback regulation ensures the one receptor-one olfactory neuron rule in mouse. Science *302*, 2088-2094.

Shaner, N. C., Campbell, R. E., Steinbach, P. A., Giepmans, B. N., Palmer, A. E., and Tsien, R. Y. (2004). Improved monomeric red, orange and yellow fluorescent proteins derived from *Discosoma sp.* red fluorescent protein. Nat Biotechnol *22*, 1567-1572.

Shang, Y., Claridge-Chang, A., Sjulson, L., Pypaert, M., and Miesenbock, G. (2007). Excitatory local circuits and their implications for olfactory processing in the fly antennal lobe. Cell *128*, 601-612.

Shepherd, G. M. (1972). Synaptic organization of the mammalian olfactory bulb. Physiol Rev *52*, 864-917.

Shepherd, G. M., Chen, W. R., Willhite, D., Migliore, M., and Greer, C. A. (2007). The olfactory granule cell: from classical enigma to central role in olfactory processing. Brain Res Rev *55*, 373-382.

Sicard, G., and Holley, A. (1984). Receptor cell responses to odorants: similarities and differences among odorants. Brain Res *292*, 283-296.

Sidi, S., Friedrich, R. W., and Nicolson, T. (2003). *NompC* TRP channel required for vertebrate sensory hair cell mechanotransduction. Science *301*, 96-99.

Silbering, A. F., and Galizia, C. G. (2007). Processing of odor mixtures in the *Drosophila* antennal lobe reveals both global inhibition and glomerulus-specific interactions. J Neurosci *27*, 11966-11977.

Sincich, L. C., and Horton, J. C. (2005). The circuitry of V1 and V2: integration of color, form, and motion. Annu Rev Neurosci *28*, 303-326.

Singh, R. N. a. S. K. (1984). Fine structure of the sensory organs of *Drosophila melanogaster* meigen larva (*Diptera: Drosophilidae*). International Journal of Insect Morphology and Embryology *13*, 255-273.

Sokolowski, M. B. (1980). Foraging strategies of *Drosophila melanogaster*: a chromosomal analysis. Behav Genet *10*, 291-302.

Stensmyr, M. C., Dekker, T., and Hansson, B. S. (2003a). Evolution of the olfactory code in the *Drosophila melanogaster* subgroup. Proc Biol Sci *270*, 2333-2340.

Stensmyr, M. C., Giordano, E., Balloi, A., Angioy, A. M., and Hansson, B. S. (2003b). Novel natural ligands for *Drosophila* olfactory receptor neurones. J Exp Biol *206*, 715-724.

Stephenson, F. A. (1988). Understanding the $GABA_A$ receptor: a chemically gated ion channel. Biochem J *249*, 21-32.

Stocker, R. F. (1994). The organization of the chemosensory system in *Drosophila melanogaster*: a review. Cell Tissue Res *275*, 3-26.

Stocker, R. F., Heimbeck, G., Gendre, N., and de Belle, J. S. (1997). Neuroblast ablation in *Drosophila* P[GAL4] lines reveals origins of olfactory interneurons. J Neurobiol *32*, 443-456.

Stocker, R. F., Lienhard, M. C., Borst, A., and Fischbach, K. F. (1990). Neuronal architecture of the antennal lobe in *Drosophila melanogaster*. Cell Tissue Res *262*, 9-34.

Stockinger, P., Kvitsiani, D., Rotkopf, S., Tirian, L., and Dickson, B. J. (2005). Neural circuitry that governs *Drosophila* male courtship behavior. Cell *121*, 795-807.

Story, G. M., Peier, A. M., Reeve, A. J., Eid, S. R., Mosbacher, J., Hricik, T. R., Earley, T. J., Hergarden, A. C., Andersson, D. A., Hwang, S. W.*, et al.* (2003). ANKTM1, a TRP-like channel expressed in nociceptive neurons, is activated by cold temperatures. Cell *112*, 819-829.

Sudhof, T. C. (1995). The synaptic vesicle cycle: a cascade of protein-protein interactions. Nature *375*, 645-653.

Suh, G. S., Ben-Tabou de Leon, S., Tanimoto, H., Fiala, A., Benzer, S., and Anderson, D. J. (2007). Light activation of an innate olfactory avoidance response in *Drosophila*. Curr Biol *17*, 905-908.

Suh, G. S., Wong, A. M., Hergarden, A. C., Wang, J. W., Simon, A. F., Benzer, S., Axel, R., and Anderson, D. J. (2004). A single population of olfactory sensory neurons mediates an innate avoidance behaviour in *Drosophila*. Nature *431*, 854-859.

Tabor, R., Yaksi, E., Weislogel, J. M., and Friedrich, R. W. (2004). Processing of odor mixtures in the zebrafish olfactory bulb. J Neurosci *24*, 6611-6620.

Tanaka, N. K., Awasaki, T., Shimada, T., and Ito, K. (2004). Integration of chemosensory pathways in the *Drosophila* second-order olfactory centers. Curr Biol *14*, 449-457.

Taylor, W. R., He, S., Levick, W. R., and Vaney, D. I. (2000). Dendritic computation of direction selectivity by retinal ganglion cells. Science *289*, 2347-2350.

Terakita, A. (2005). The opsins. Genome Biol *6*, 213.

Thorne, N., Chromey, C., Bray, S., and Amrein, H. (2004). Taste perception and coding in *Drosophila*. Curr Biol *14*, 1065-1079.

Tichy, H., Hinterwirth, A., and Gingl, E. (2005). Olfactory receptors on the cockroach antenna signal odour ON and odour OFF by excitation. Eur J Neurosci *22*, 3147-3160.

Tissot, M., Gendre, N., Hawken, A., Stortkuhl, K. F., and Stocker, R. F. (1997). Larval chemosensory projections and invasion of adult afferents in the antennal lobe of *Drosophila*. J Neurobiol *32*, 281-297.

Tissot, M., and Stocker, R. F. (2000). Metamorphosis in drosophila and other insects: the fate of neurons throughout the stages. Prog Neurobiol *62*, 89-111.

Touhara, K., Sengoku, S., Inaki, K., Tsuboi, A., Hirono, J., Sato, T., Sakano, H., and Haga, T. (1999). Functional identification and reconstitution of an odorant receptor in single olfactory neurons. Proc Natl Acad Sci U S A *96*, 4040-4045.

Uchida, N., and Mainen, Z. F. (2003). Speed and accuracy of olfactory discrimination in the rat. Nat Neurosci *6*, 1224-1229.

Uchida, N., Takahashi, Y. K., Tanifuji, M., and Mori, K. (2000). Odor maps in the mammalian olfactory bulb: domain organization and odorant structural features. Nat Neurosci *3*, 1035-1043.

van der Goes van Naters, W., and Carlson, J. R. (2007). Receptors and neurons for fly odors in *Drosophila*. Curr Biol *17*, 606-612.

Vosshall, L. B., Amrein, H., Morozov, P. S., Rzhetsky, A., and Axel, R. (1999). A spatial map of olfactory receptor expression in the *Drosophila* antenna. Cell *96*, 725-736.

Vosshall, L. B., and Stocker, R. F. (2007). Molecular architecture of smell and taste in *Drosophila*. Annu Rev Neurosci *30*, 505-533.

Vosshall, L. B., Wong, A. M., and Axel, R. (2000). An olfactory sensory map in the fly brain. Cell *102*, 147-159.

Wachowiak, M., and Cohen, L. B. (2001). Representation of odorants by receptor neuron input to the mouse olfactory bulb. Neuron *32*, 723-735.

Walker, R. G., Willingham, A. T., and Zuker, C. S. (2000). A *Drosophila* mechanosensory transduction channel. Science *287*, 2229-2234.

Wang, H., and Woolf, C. J. (2005). Pain TRPs. Neuron *46*, 9-12.

Wang, J. W., Wong, A. M., Flores, J., Vosshall, L. B., and Axel, R. (2003). Two-photon calcium imaging reveals an odor-evoked map of activity in the fly brain. Cell *112*, 271-282.

Wang, Y., Guo, H. F., Pologruto, T. A., Hannan, F., Hakker, I., Svoboda, K., and Zhong, Y. (2004a). Stereotyped odor-evoked activity in the mushroom body of *Drosophila* revealed by green fluorescent protein-based Ca^{2+} imaging. J Neurosci *24*, 6507-6514.

Wang, Z., Singhvi, A., Kong, P., and Scott, K. (2004b). Taste representations in the *Drosophila* brain. Cell *117*, 981-991.

Whittaker, R. H., and Feeny, P. P. (1971). Allelochemics: chemical interactions between species. Science *171*, 757-770.

Wilson, R. I., and Laurent, G. (2005). Role of GABAergic inhibition in shaping odor-evoked spatiotemporal patterns in the *Drosophila* antennal lobe. J Neurosci *25*, 9069-9079.

Wilson, R. I., Turner, G. C., and Laurent, G. (2004). Transformation of olfactory representations in the *Drosophila* antennal lobe. Science *303*, 366-370.

Wistrand, M., Kall, L., and Sonnhammer, E. L. (2006). A general model of G protein-coupled receptor sequences and its application to detect remote homologs. Protein Sci *15*, 509-521.

Wong, A. M., Wang, J. W., and Axel, R. (2002). Spatial representation of the glomerular map in the *Drosophila* protocerebrum. Cell *109*, 229-241.

Xu, P., Atkinson, R., Jones, D. N., and Smith, D. P. (2005). *Drosophila* OBP LUSH is required for activity of pheromone-sensitive neurons. Neuron *45*, 193-200.

Yao, C. A., Ignell, R., and Carlson, J. R. (2005). Chemosensory coding by neurons in the coeloconic sensilla of the *Drosophila* antenna. J Neurosci *25*, 8359-8367.

Yokoi, M., Mori, K., and Nakanishi, S. (1995). Refinement of odor molecule tuning by dendrodendritic synaptic inhibition in the olfactory bulb. Proc Natl Acad Sci U S A *92*, 3371-3375.

Yoshida, I., and Mori, K. (2007). Odorant category profile selectivity of olfactory cortex neurons. J Neurosci *27*, 9105-9114.

Yu, D., Baird, G. S., Tsien, R. Y., and Davis, R. L. (2003). Detection of calcium transients in *Drosophila* mushroom body neurons with camgaroo reporters. J Neurosci *23*, 64-72.

Yu, D., Keene, A. C., Srivatsan, A., Waddell, S., and Davis, R. L. (2005). *Drosophila* DPM neurons form a delayed and branch-specific memory trace after olfactory classical conditioning. Cell *123*, 945-957.

Zhang, X., and Firestein, S. (2002). The olfactory receptor gene superfamily of the mouse. Nat Neurosci *5*, 124-133.

Zhao, G. Q., Zhang, Y., Hoon, M. A., Chandrashekar, J., Erlenbach, I., Ryba, N. J., and Zuker, C. S. (2003). The receptors for mammalian sweet and umami taste. Cell *115*, 255-266.

Zhuang, H., and Matsunami, H. (2007). Synergism of accessory factors in functional expression of mammalian odorant receptors. J Biol Chem *282*, 15284-15293.

Zou, Z., and Buck, L. B. (2006). Combinatorial effects of odorant mixes in olfactory cortex. Science *311*, 1477-1481.

Zufall, F., Firestein, S., and Shepherd, G. M. (1994). Cyclic nucleotide-gated ion channels and sensory transduction in olfactory receptor neurons. Annu Rev Biophys Biomol Struct *23*, 577-607.